AD-A189 652 DAMAGE MODELS FOR DELAMINATION AND TRANSVERSE FRACTURE 1/1
(U) TEXAS A AND M UNIV COLLEGE STATION MECHANICS AND
MATERIALS CE R A SCHAPERY ET AL AUG 87
UNCLASSIFIED MM-5034-87-11 AFOSR-TR-88-0129 F/G 11/4 NL

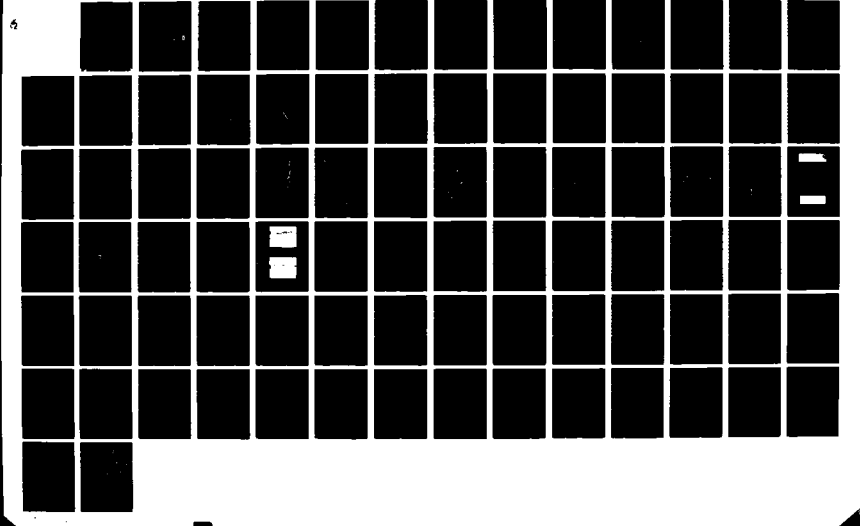

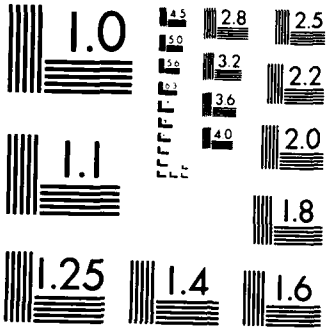

MICROCOPY RESOLUTION TEST CHART
NATIONAL BUREAU OF STANDARDS-1963-A

(2)

Mechanics and Materials Center
TEXAS A&M UNIVERSITY
College Station, Texas

AFOSR-TR- 88-0129

DAMAGE MODELS FOR DELAMINATION AND TRANSVERSE FRACTURE

FINAL TECHNICAL REPORT

R.A. SCHAPERY
D.P. GOETZ
M.J. LAMBORN

AIR FORCE OFFICE OF SCIENTIFIC RESEARCH
OFFICE OF AEROSPACE RESEARCH
UNITED STATES AIR FORCE
GRANT NO. AFOSR-84-0068

MM 5034-87-11

AUGUST 1987

unclassified

SECURITY CLASSIFICATION OF THIS PAGE

JAN 1988 1 2

REPORT DOCUMENTATION PAGE

1a. REPORT SECURITY CLASSIFICATION: unclassified	1b. RESTRICTIVE MARKINGS
2a. SECURITY CLASSIFICATION AUTHORITY	3. DISTRIBUTION/AVAILABILITY OF REPORT: unlimited
2b. DECLASSIFICATION/DOWNGRADING SCHEDULE	
4. PERFORMING ORGANIZATION REPORT NUMBER(S): MM-5034-87-11	5. MONITORING ORGANIZATION REPORT NUMBER(S): AFOSR-TR- 88-0129
6a. NAME OF PERFORMING ORGANIZATION: Mechanics and Materials Center, Texas A&M University; 6b. OFFICE SYMBOL (If applicable):	7a. NAME OF MONITORING ORGANIZATION: AFOSR/NA
6c. ADDRESS (City, State and ZIP Code): College Station, TX 77843	7b. ADDRESS (City, State and ZIP Code): Building 410, Bolling AFB, DC 20332-6448
8a. NAME OF FUNDING/SPONSORING ORGANIZATION: AFOSR; 8b. OFFICE SYMBOL (If applicable): NA	9. PROCUREMENT INSTRUMENT IDENTIFICATION NUMBER: Grant No. AFOSR-84-0068
8c. ADDRESS (City, State and ZIP Code): Building 410, Bolling AFB, DC 20332-6448	10. SOURCE OF FUNDING NOS.

PROGRAM ELEMENT NO.	PROJECT NO.	TASK NO.	WORK UNIT NO.
61102F	2302	B2	

11. TITLE (Include Security Classification): Damage Models for Delamination and Transverse Fracture ~~in Fibrous Composites~~

12. PERSONAL AUTHOR(S): R.A. Schapery, M.J. Lamborn, D.P. Goetz

13a. TYPE OF REPORT	13b. TIME COVERED	14. DATE OF REPORT (Yr., Mo., Day)	15. PAGE COUNT
Final	FROM 2/15/84 TO 6/14/87	August 1987	79

16. SUPPLEMENTARY NOTATION

17. COSATI CODES		
FIELD	GROUP	SUB. GR.

18. SUBJECT TERMS (Continue on reverse if necessary and identify by block number): Composites, Damage, Delamination, Fracture, ~~of Composites~~, Fiber Reinforced Plastic

19. ABSTRACT (Continue on reverse if necessary and identify by block number)

Theoretical and experimental work on the deformation and fracture of fibrous composites with distributed damage is described. Emphasis is on establishing the existence of potentials analogous to strain energy and on using these so-called work potentials in deformation and fracture studies. The difference between changing damage and constant damage processes is accounetd for by using multivalued work potentials. Discussed first are investigations of flat rectangular bar specimens and thin-walled tubes under axial and torsional loading. The limited amount of experimental data presently available on angle-ply laminates confirms the existence of a potential even when there are large increases in microcracking. Next, path independence of the J integral is discussed. A study is then described in which the J integral is used to determine fracture energy for delamination in double-cantilevered beam specimens, some of which have a large percentage of off-axis fibers; the results are compared with fracture energies found by standard methods (which do not account for effects of distributed damage). The Appendix contains reprints of papers published during the final project year and the abstracts of two Ph.D. dissertations

20. DISTRIBUTION/AVAILABILITY OF ABSTRACT	21. ABSTRACT SECURITY CLASSIFICATION
UNCLASSIFIED/UNLIMITED ☐ SAME AS RPT. ☐ DTIC USERS ☐	

22a. NAME OF RESPONSIBLE INDIVIDUAL	22b. TELEPHONE NUMBER (Include Area Code)	22c. OFFICE SYMBOL
Major George Haritos	(202) 767-0463	NA

DD FORM 1473, 83 APR EDITION OF 1 JAN 73 IS OBSOLETE.

unclassified

SECURITY CLASSIFICATION OF THIS PA

(Key)

TABLE OF CONTENTS

I. RESEARCH OBJECTIVES

The overall objective of the research is to develop and verify mathematical models of delamination and transverse fracture which account for local (crack tip) and global damage distributions. One specific objective is to demonstrate theoretically and experimentally that "work potentials" (which are analogous to strain energy) exist for composites with constant and changing damage and with viscoelastic behavior; validity of the very useful J integral theory of fracture analysis depends on the existence of work potentials. The second specific objective is to develop and verify methods of analysis for predicting crack growth in elastic and viscoelastic composites with distributed damage using, when applicable, the J integral.

II. RESEARCH SUMMARY

1. Overview

Methods of deformation and fracture characterization and prediction are simplified when strain energy-like potentials based on mechanical work can be used, as described in the first paper in the Appendix, "Deformation and Fracture Characterization of Inelastic Composite Materials Using Potentials". With these so-called work potentials, important theoretical and experimental methods using the J integral and energy release rate (originally developed for fracture of elastic media and fracture initiation in metals with plastic deformations) may be extended to fracture initiation and crack propagation in monolithic and composite materials.

Section 2 is concerned primarily with a study of rectangular angle-ply bars under combined axial and torsional deformation. This investigation is by Mark Lamborn, a Ph.D. student, and it deals with (i) the existence and then determination of a work potential for specimens with significant amounts of distributed damage and (ii) characterization and prediction of delamination

when distributed damage and the mode III (antiplane) component of energy release rate are relatively large. Experimental studies to-date on a composite with brittle resin (Hercules AS4/3502), as reported in the first paper in the Appendix, and on a composite with rubber-toughened resin (Hexcel T2CT145/F155), as reported in Section 2, show that a work potential exists with proportional axial and torsional deformation. On the basis of the theory, we expect a work potential to exist over many sets of non-proportional deformation histories; some experimental work planned for the near term on a new AFOSR grant will be concerned with non-proportional deformation.

Also summarized in Section 2 is work on cyclic axial-torsional loading of tubes by another Ph.D. student, Richard Tonda. Here, the objective is to develop a method for removing from experimental data effects of visco-elasticity on hysteresis and stiffness so that effects of distributed damage growth may be more readily studied.

A numerical investigation of crack growth initiation and continuing crack growth in inelastic media is summarized in Section 3; this work was done by Randall Weatherby, a Ph.D. student. A multivalued work potential is used to characterize material behavior. Path independence of the J integral is then studied and shown to be consistent with theory developed on an earlier AFOSR grant.

Finally, in Section 4 a delamination study by Douglas Goetz, a Ph.D. student, is described. Mode I delamination of laminates with multiple fiber orientations is investigated, and the usefulness of the J integral as a fracture characterizing parameter is demonstrated.

Most of the work described in Sections 2 and 4 has not yet been published, and therefore detailed summaries are given.

2. Studies of Laminates Under Axial and Torsional Deformation

The research effort last year was directed toward selection of rectangular bar specimens, development of experimental procedures, and development of data reduction schemes. The objective in specimen selection was to determine which specimens which would exhibit a significant coupling effect of rotation and axial deformation on loads in order to be able to critically evaluate the work-potential theory. Laminates of various layups and geometries were tested. Test specimens of Hercules AS4/3502 graphite/epoxy were 24 plies thick and either balanced angle-ply or other balanced symmetric laminates. Tests were run under conditions of proportional and non-proportional straining; instrumentation difficulties voided the results for non-proportional straining and, in fact, resulted in a delay of testing for several months. All layups and geometries were found to exhibit only a small effect of rotation on axial load, while the effect of axial displacement on torque was significant. Test data from proportional straining tests (i.e. the twist was proportional to the axial extension) were evaluated for the existence of a work potential as discussed in [2.1]; references for section 2 start on page 22. The results of some of these tests appear in Figures 3 and 4 of [2.1], which is in the Appendix. These results provided at least a limited check of the existence of a work potential for conditions of proportional straining.

Experimental work was continued in the current reporting year to verify the existence of a work potential for fiber-reinforced plastic laminates subjected to combined axial and torsional loadings. Hexcel T2CT145/F155, a material system consisting of a rubber toughened epoxy matrix with graphite fibers, was used to fabricate $[\pm 35^\circ]_{6s}$ flat bar specimens. These were tested under the conditions of proportional straining. Typical test results

expressed in terms of "nominal" stresses and strains appear as the dotted lines in Figures 2.1 and 2.2. The nominal stresses and strains are defined by Equation (39) in [2.1]. The test data was evaluated for the existence of a work potential by the method outlined in [2.1]. The "nominal" axial stress-strain responses for cases of combined axial and torsional loadings, were predicted from the experimentally determined work potential. The predicted responses are shown as the solid lines appearing in Figure 2.2. The predictions shown in this Figure represent tests run at intermediate values of ε/γ, the ratio of nominal axial strain to shear strain. These tests span the levels of ε and γ where sufficient data were available for calculation purposes. Tests were run at ε/γ = .25, 2, and 4 but could not be predicted since they represent limit cases and a lack of data exists at the strain levels reached in these tests. As seen in Figure 2.2 the predicted responses agree well with experiment. It is tentatively concluded that a work potential exists for conditions of proportional straining and increasing material damage.

Data from the proportional straining tests on laminates constructed of the Hexcel material system were analyzed to determine an analytical representation of the work potential. The theory in [2.1] was used to characterize the material and make predictions of material response for conditions of combined axial and torsional loadings. The relationship used to characterize the test data is that corresponding to Equation (28) of [2.1]. The form used in this work is

$$W_T = W + W_D \tag{2.1}$$

where W_T = the total mechanical work, W = the strain energy density function, and W_D = the work of damage. All quantities appearing in Equation (2.1) are

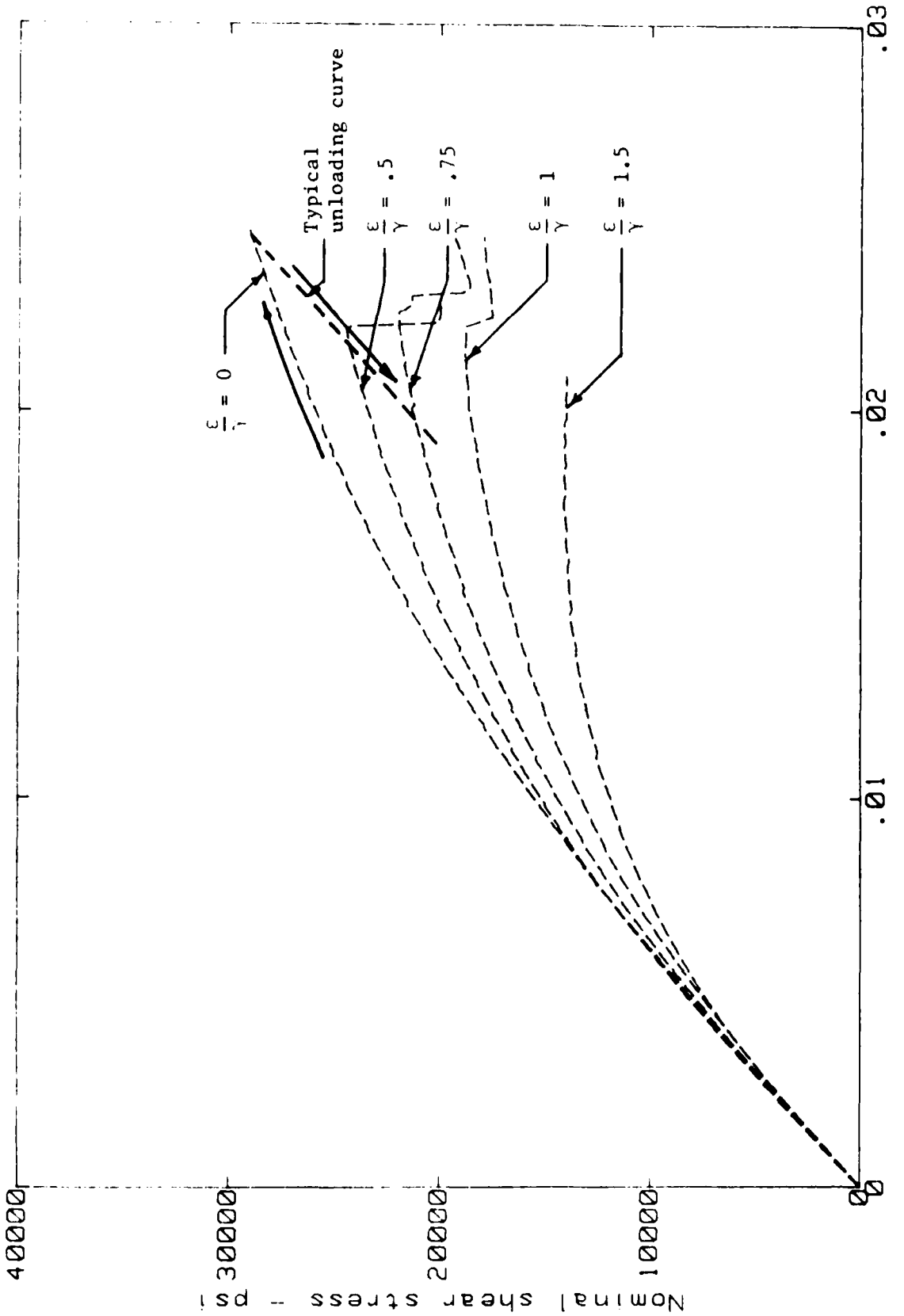

Figure 2.1 Representative experimental stress-strain curves with proportional axial and torsional straining. $[\pm 35]_{6s}$; 8.5 in. long x .5 in. wide x .145 in. thick.

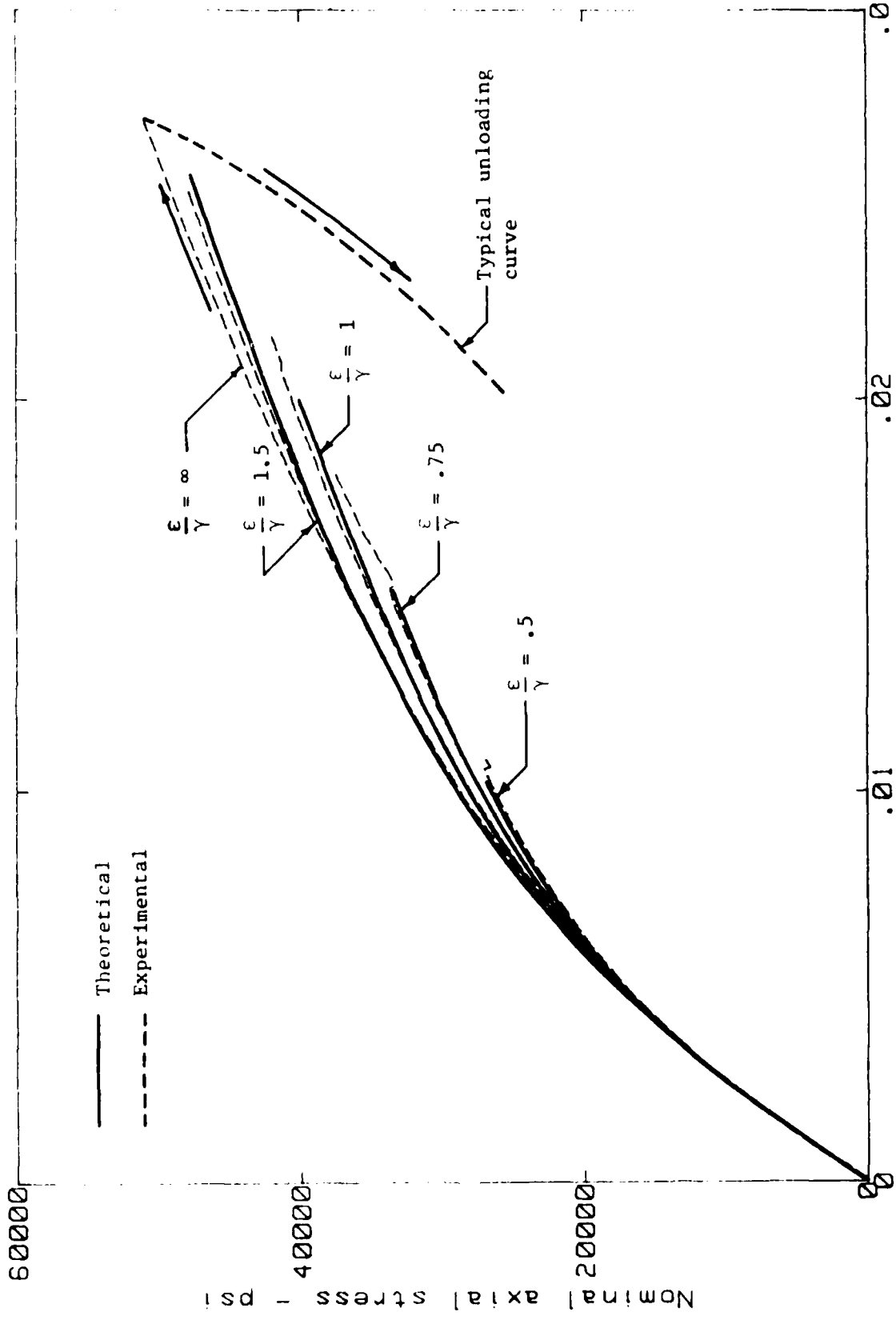

Figure 2.2 Representative axial stress-strain curves with proportional axial and torsional straining for the same tests used for Figure 2.1.

expressed on a per unit initial volume basis.

The total mechanical work input is defined by

$$W_T = \int_1^2 Q_i dq_i \tag{2.2}$$

where q_i = the generalized displacements and Q_i = the generalized forces (i=1,2). The integral is taken from generalized displacement state 1 to generalized displacement state 2. For stable microcracking and some other damaging mechanisms, it has been shown that the integral appearing in Equation (2.2) is independent of path [2.1]. W_T will be referred to as the work potential. From Equation (2.2)

$$Q_j = \partial W_T / \partial q_j \tag{2.3}$$

A basic assumption of this theory is that the strain energy density function $W = W(q_i, D_k)$ exists and is defined by

$$Q_j = \partial W / \partial q_j \tag{2.4}$$

where D_k (k=1,2,....,K) are damage parameters. The set D_k includes all the parameters needed to account for any structural changes occurring in the material during loading. Such structural changes could include microcracking, delamination, and fiber breakage. For the purposes of obtaining an initial analytical representation of the experimental data it is assumed that one damage parameter accounts for all the structural changes. This damage parameter is taken to be W_D. The damage W_D will change with the applied displacements q_i; thus $W_D = W_D(q_i)$. From Equations (2.1), (2.3), and (2.4) the equation for predicting the current value of W_D becomes

$$\partial W / \partial W_D = -1 \tag{2.5}$$

provided this equation predicts $dW_D/dt > 0$. For cases when $dW_D/dt < 0$ it can be shown from thermodynamics that W_D must be constant.

For the test data under examination the generalized forces and displacements are taken as $q_1 = \varepsilon$, $q_2 = \gamma$, $Q_1 = \sigma$, $Q_2 = \tau/3$ where ε, γ, σ, and τ are the nominal strains and stresses defined in Equation (39) of [2.1]. In terms of these variables Equation (2.2) is rewritten as

$$W_T = \int_0^{\varepsilon} \sigma \, d\varepsilon' + \int_0^{\gamma} \frac{\tau}{3} \, d\gamma' \tag{2.6}$$

where the initial values of the generalized displacements are taken as zero (unstrained state). For the purposes of analyzing the experimental data the strain energy density function is taken to be

$$W = \frac{1}{2} C_\sigma \varepsilon^2 + \frac{1}{2} C_\tau \gamma^2 \tag{2.7}$$

where C_σ and C_τ are functions of W_D. The strain energy density function, W, as given by Equation (2.7) is that of a linear elastic material when W_D is constant. Substitution of Equations (2.6) and (2.7) into Equation (2.1) yields

$$W_D = \int_0^{\varepsilon} \sigma \, d\varepsilon' + \int_0^{\gamma} \frac{\tau}{3} \, d\gamma' - \frac{1}{2} C_\sigma \varepsilon^2 - \frac{1}{2} C_\tau \gamma^2 \tag{2.8}$$

from which W_D is seen to be the sum of the shaded areas under the σ versus ε and $\tau/3$ versus γ curves as shown in Figures 2.3 and 2.4. From Equation (2.4)

$$\begin{aligned} \sigma &= C_\sigma \varepsilon \\ \frac{\tau}{3} &= C_\tau \gamma \end{aligned} \tag{2.9}$$

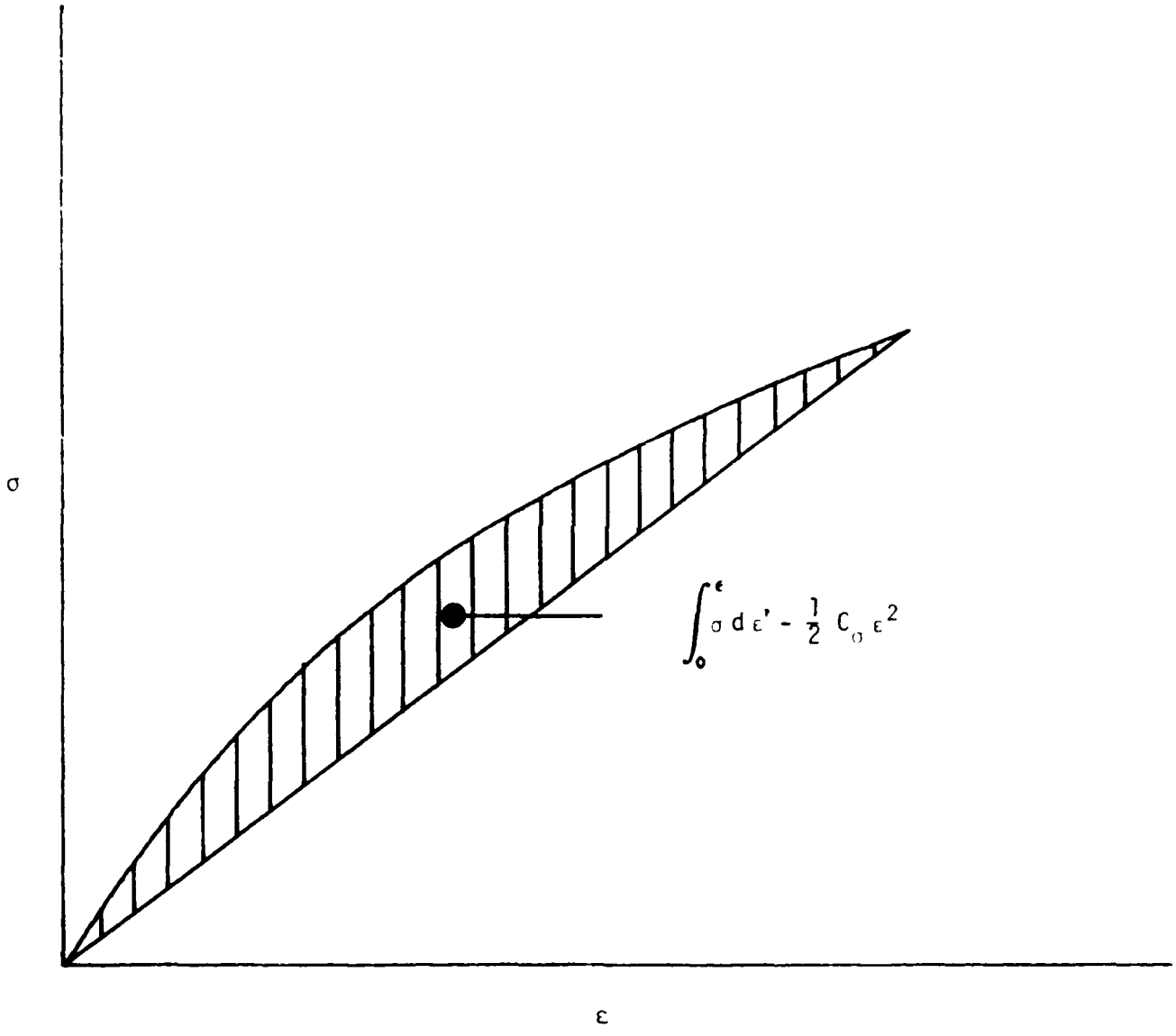

Figure 2.3 Area under the axial stress-strain curve contributing to the work of damage W_D.

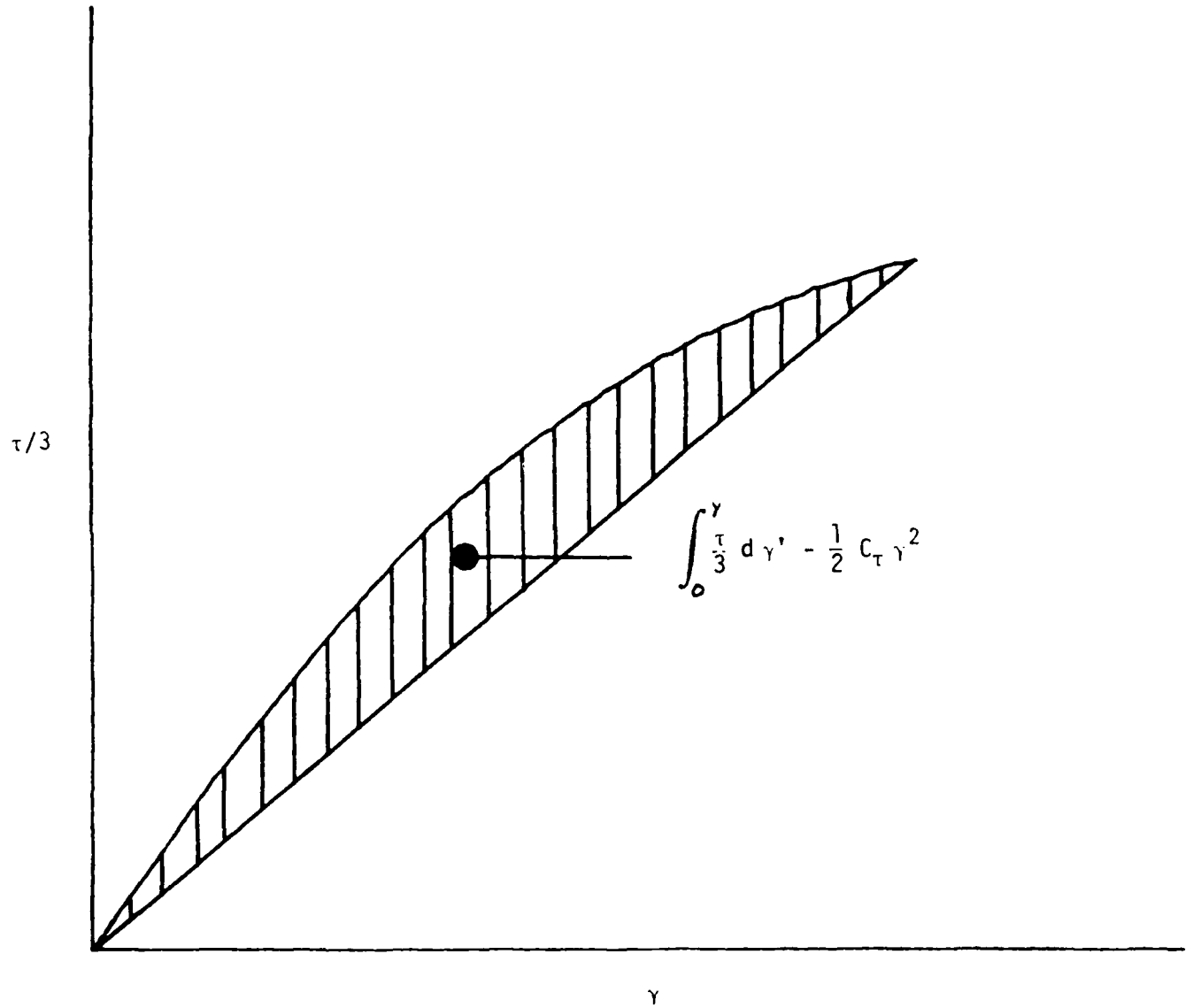

Figure 2.4 Area under the shear stress-strain curve contributing to the work of damage W_D.

Equation (2.8) shows that when W is evaluated on the loading curve, C_σ and C_τ correspond to the secant moduli of the σ versus ε and $\tau/3$ versus γ curves, respectively.

Equations (2.8) and (2.9) were used to obtain values of C_σ and C_τ as functions of W_D for proportional straining tests run at ε/γ = 0, .5, .75, 1, 1.5, 2, 4, and ∞. The results of these calculations appear in Figure 2.5. It was found that the test ran at ε/γ = 1.5 experienced the greatest amount of damage as defined by the maximum value of W_D. Analytical expressions were then obtained for C_σ and C_τ as functions of W_D for this one test. These are shown as the solid lines in Figure 2.5. The analytical expressions for these curves were used with Equations (2.5) and (2.9) to predict the material response for tests run at the same values of ε/γ as those appearing in Figures 2.1 and 2.2. The results of these predictions are shown in Figures 2.6 and 2.7. These figures show that the predicted responses for $\varepsilon/\gamma > 1$ agree reasonably well with experiment while those for $\varepsilon/\gamma < 1$ do not. The reason for this appears to be that a second damage mechanism becomes significant at the larger levels of twist. This would require that a second damage parameter be incorporated into the model. The additional damage mechanism is apparent for the data shown in Figure 2.8. Appearing in Figure 2.8 are the secant moduli plotted against each other for ε/γ = .5, .75, 1, 1.5, 2, and 4. These data show that the curves for the different tests are essentially the same except for ε/γ = .5 and .75; the two tests correspond to the greatest levels of twist reached for conditions of combined axial and torsional loadings. Characterization of the second damage mechanism is presently under study.

Physically, the second damage mechanism may be delamination. For the angle-ply layup, delamination would have a large affect on the torsional stiffness but only a small affect on the axial stiffness.

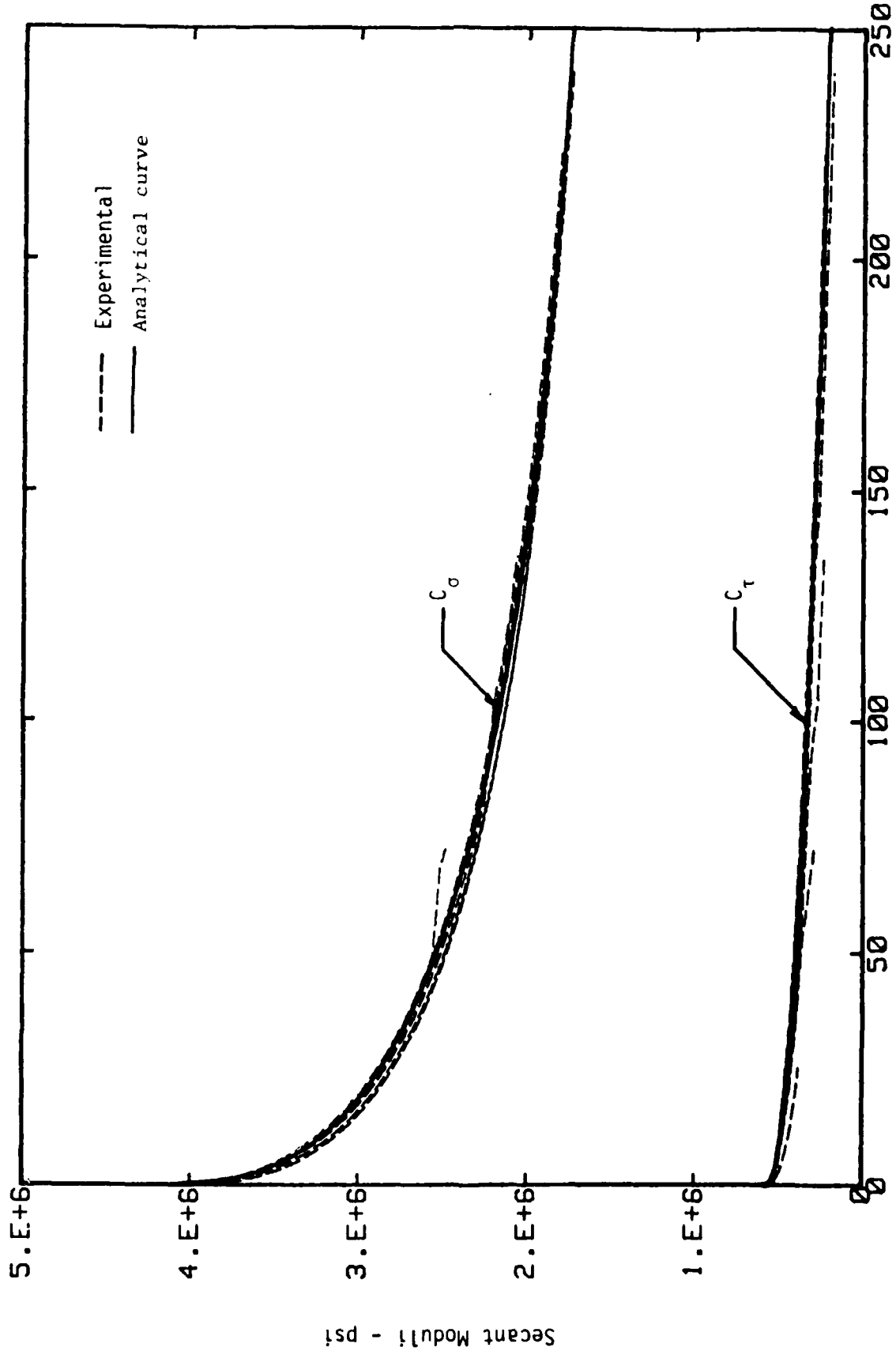

Figure 2.5 Experimental and analytical secant moduli curves.

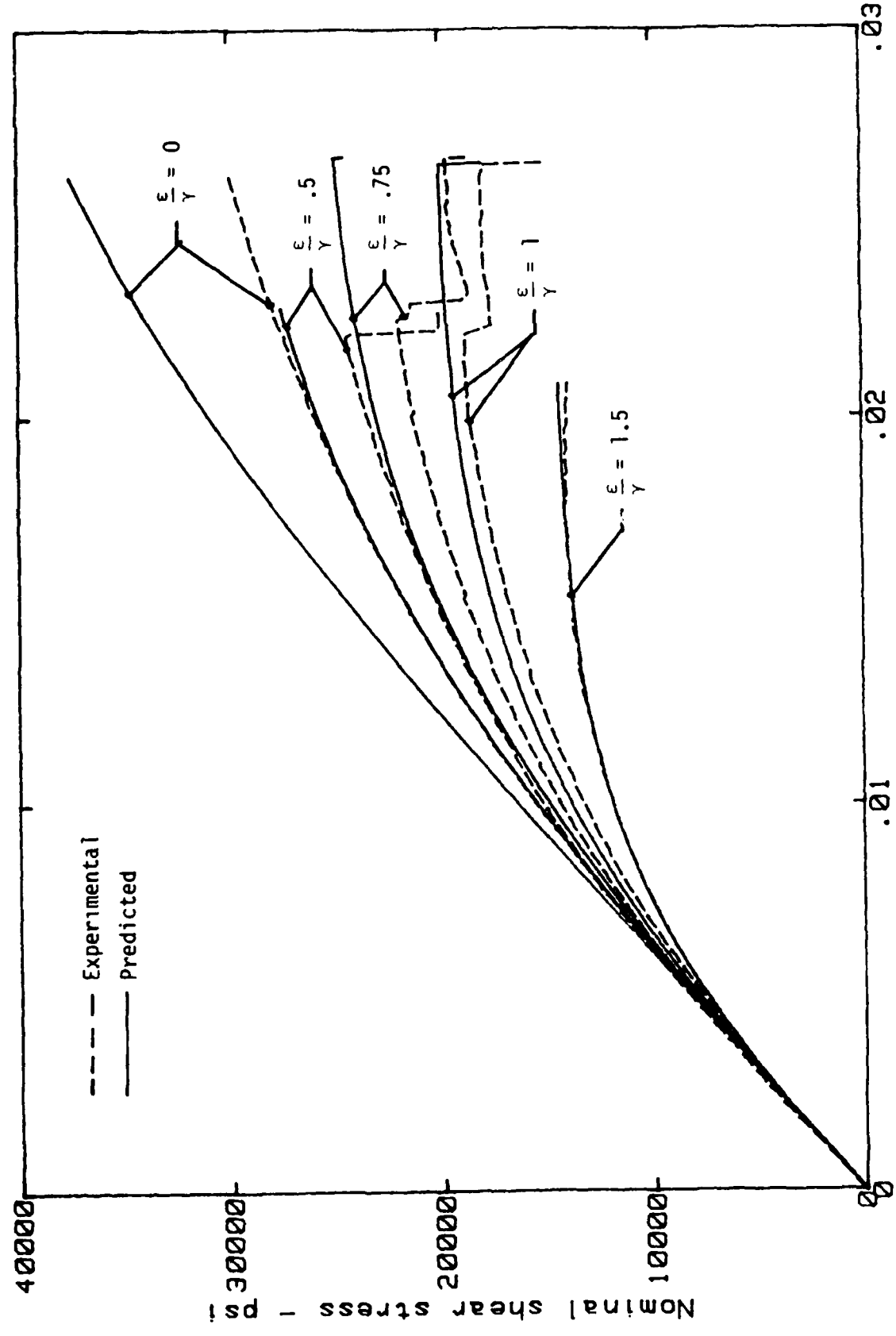

Figure 2.6 Predicted and experimental shear stress-strain curves with proportional axial and torsional straining. Hexcel F155; 24 plies $[\pm 35]_{6S}$; 8/5 in. long x 0.5 in. wide x 0.145 in. thick.

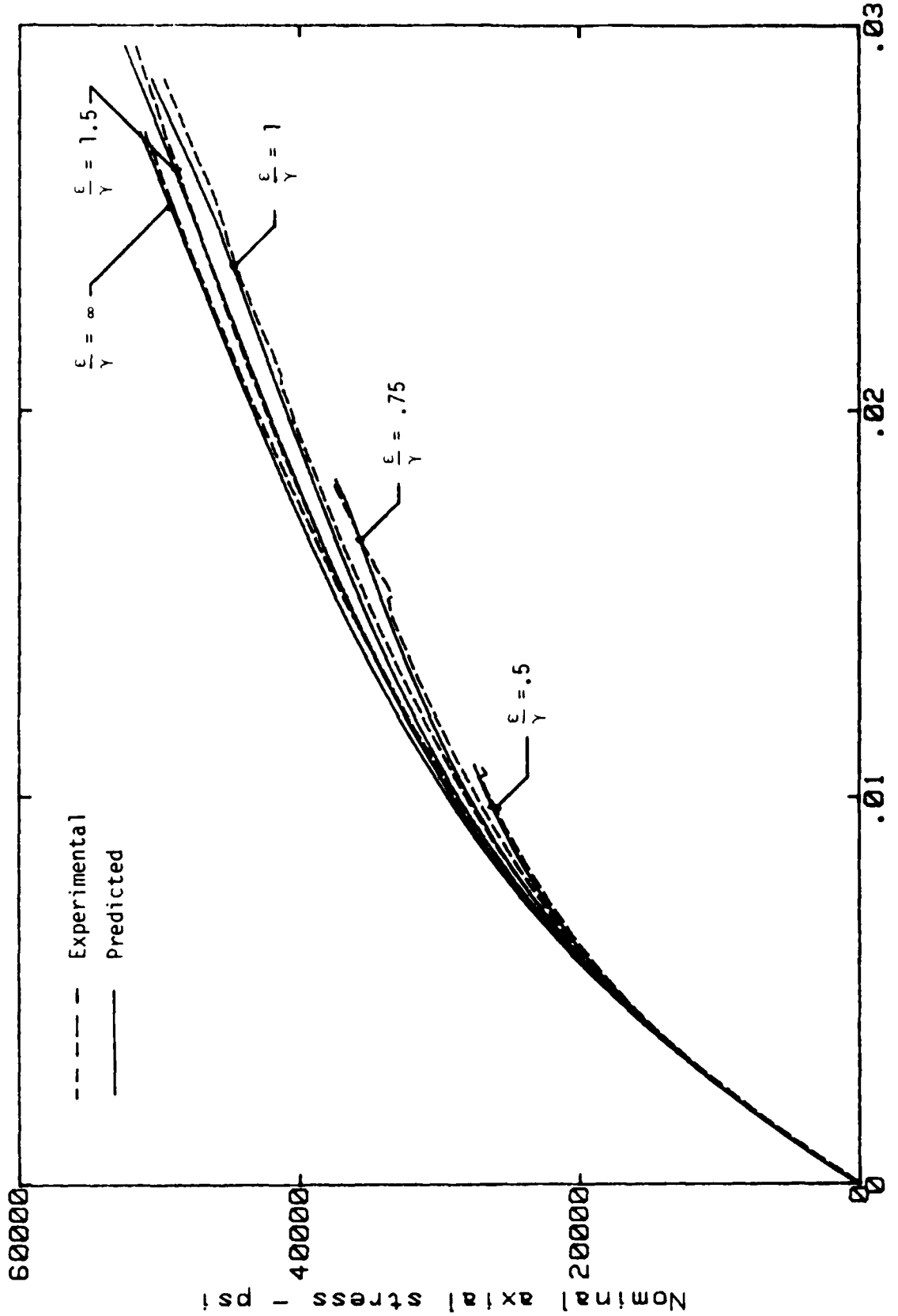

Figure 2.7 Predicted and experimental axial stress-strain curves with proportional axial and torsional straining for the same tests used for Figure 2.5.

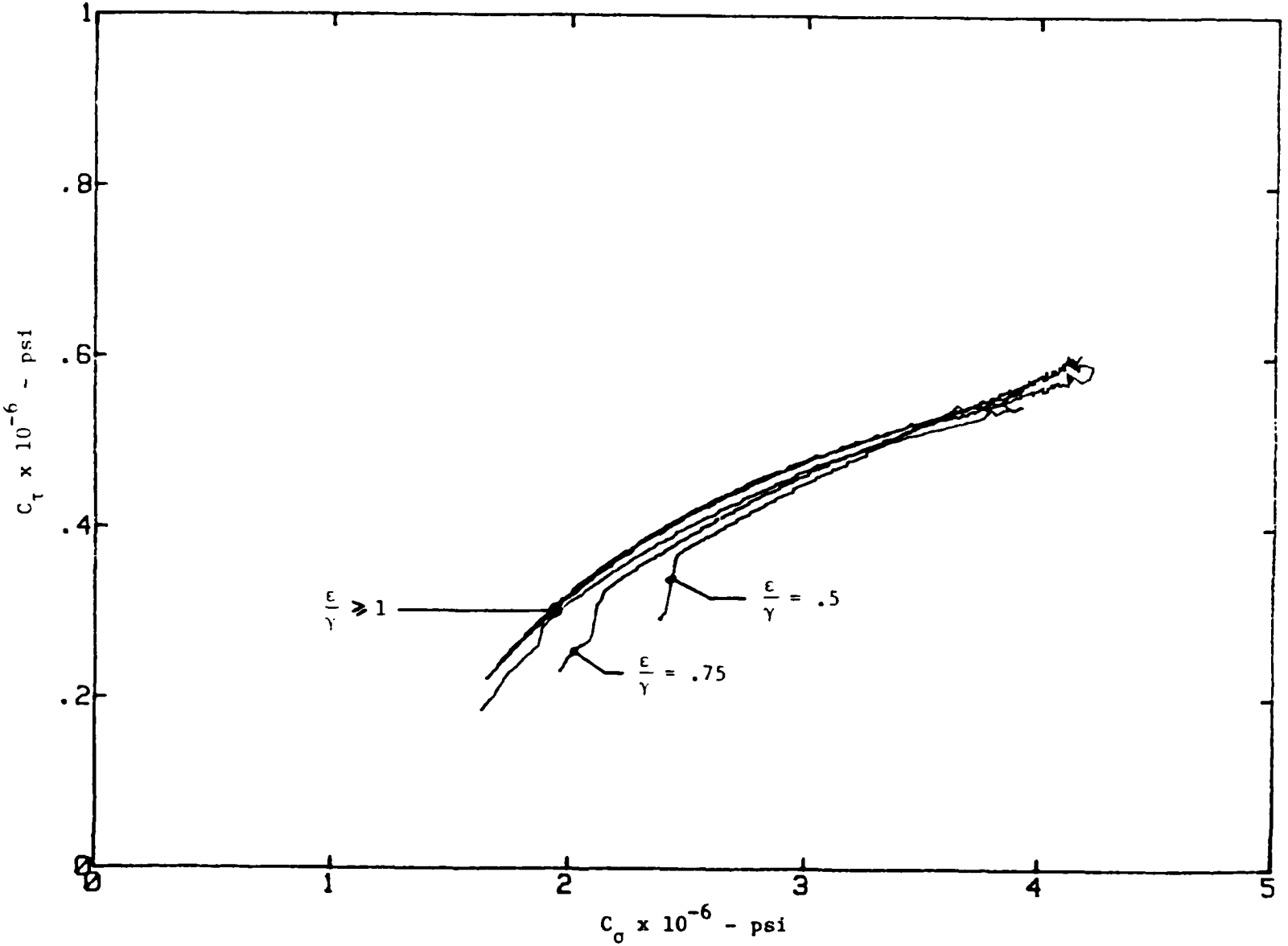

Figure 2.8 Curves of C_τ versus C_σ showing the change in material behavior at large torque levels due to second damage mechanism.

New Test Methods and Equipment: During the course of these tests, experimental procedures were refined. Deficiencies in measurement procedures were recognized and corrected. A computer program was developed to check data from a series of proportional straining tests for the existence of a work potential. The program was tested using data from a series of tests on aluminum under combined axial and torsional loads. The program verified the existence of a work potential for the aluminum well into the yielded state, as expected.

New equipment has been purchased to aid in the experimental work. A load cell which is more sensitive to low torque levels than the one used last year has been acquired and is currently in use. The fiber-reinforced plastic laminates that have been tested in combined axial and torsional loading typically experience maximum torque levels of 350 in-lbs. The new load cell has torque range settings of 400 in-lbs. and 200 in-lbs, while the previous load cell had a minimum torque range setting of 1000 in-lbs. The axial capacity of both old and new load cells is the same.

A new computer system was purchased to aid in data acquisition and reduction. The new system provides increased data acquisition speed as well as increased data handling capabilities. This system is currently being used in the experimental work.

Problems were experienced with the computer controller for the MTS axial-torsion testing machine. The problem involved the unplanned loading of test specimens when control switched from manual to the computer. In some instances this damaged or failed the test specimens. Computer control is beneficial when complicated displacement and rotation histories are used as input. Work is currently underway by MTS to resolve the problem.

Related Studies: A literature survey was performed to review prior work

concerned with mode III fracture of metals and composite materials. It was found that little data were available on mode III fracture characterization of materials. The majority of the available data were from studies on metals. An investigation of the experimental methods used to characterize metals subjected to mode III deformation indicates that these methods would be unsuitable for mode III delamination studies of fiber-reinforced plastic laminates.

Studies concerned with the mode III fracture characterization of fiber-reinforced composite materials are few. Experimentally determined values for the critical energy release rate, G_{IIIc}, have been obtained for a randomly oriented short fiber composite [2.2] and a fiber-reinforced plastic laminate [2.3]. In both cases the measured value of G_{IIIc} was found to be greater than measured values of G_{Ic} and G_{IIc} for the same materials. For the case of the fiber-reinforced plastic laminate the critical energy release rate in mode III was determined for three different layups. The value of G_{IIIc} was found to be greater than G_{Ic} and G_{IIc} for all layups. A recent finite element study determined energy release rates for laminates subjected to pure torsional loading [2.4]. For the three layups studied, the energy release rate in mode III was found to be greater than that in modes I and II, and pure mode III was achieved in a $[0°]_{8s}$ laminate.

Analytical Studies Related to Torsion and Torsion-Induced Delamination: To gain a better understanding of the torsion problem of a laminate, a closed form solution to the linear elastic torsion problem for a cross-ply laminate was obtained. The solution satisfies the field equations on a ply-by-ply basis. Displacement and stress continuity conditions are required at the interfaces between 0° and 90° plies. The result is a Fourier series solution for the stress function of each ply. Convergence of the solution at the

interfaces between plies is not necessarily guaranteed and is currently under investigation. This type of solution may provide reasonable predictions of material response for angle-ply laminates with a large number of plies and may be used in test specimen design.

The torsion problem of cracked isotropic plates was also studied theoretically and experimentally. An isotropic plate with a through-the-thickness crack was analyzed (Figures 2.9 and 2.10). Shown in Figure 2.9 is such a plate subjected to torsional loading. As indicated in Figure 2.9, the separated sides of the plate will bend as beams under torsional loads. It was an important aspect of this study to examine the effect of grip restraint on bending and thereby determine the increase in torsional rigidity of the separated plate. The torsional rigidity in the presence of the crack (Figure 2.10) was predicted using standard torsion theory and a strength of materials approach which accounts for the bending of the separated sides. Figure 2.10 shows the results of a test made on an aluminum plate and the predictions made by the two theories. It is apparent from these results that resistance to bending has a significant affect on the torsional response of separated plates. These results suggest that bending resistance of the grips may also have a significant effect on the torsional response of fiber-reinforced plastic laminates with edge delaminations.

Additional Studies of Rectangular Bars: Research on a new grant will concentrate on two areas needing further investigation. One topic area deals with the question of the existence of a work potential. The experimental work to-date has verified the existence of a work potential under conditions of proportional deformation when the deformations increase in time. The existence of a potential for these conditions does not guarantee its existence for all deformation histories. Future work will investigate the existence of

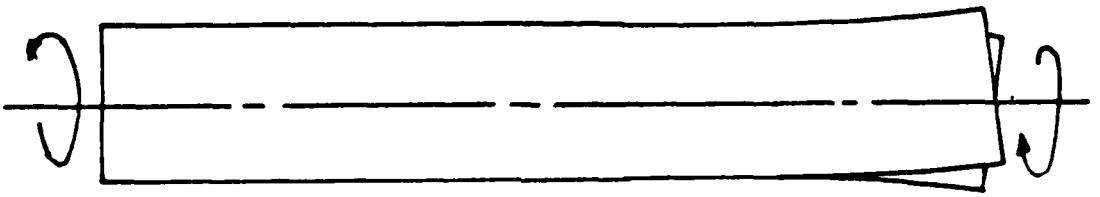

Figure 2.9 Bending due to rotation about a point other than the center of the cross section.

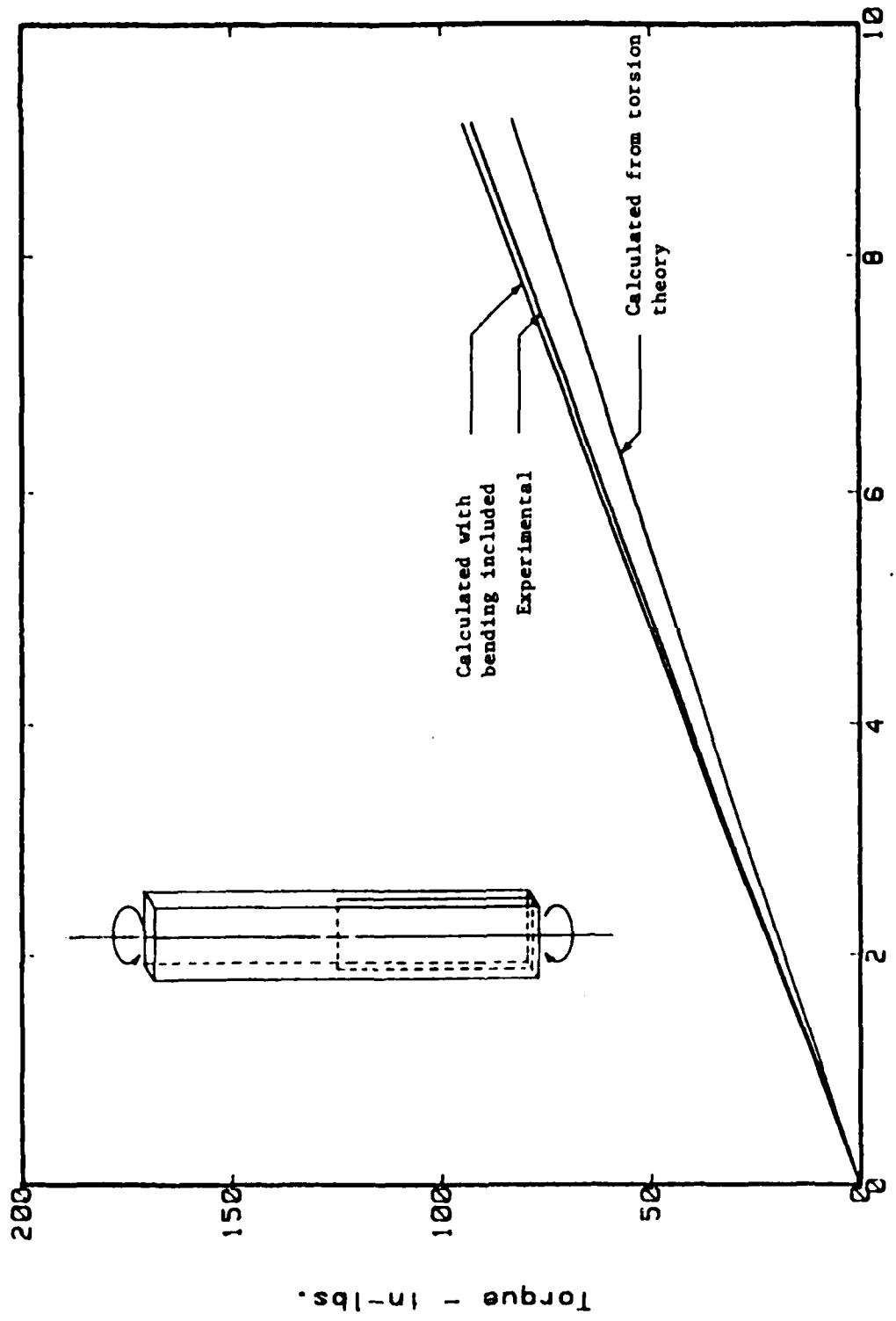

Figure 2.10 Comparison of experimental and predicted torque reponse curves.

a work potential for non-proportional deformation histories, including histories where the deformations decrease in time. These input deformation histories should include processes where some damage mechanisms would remain inactive while others would be active. These would correspond to different branches of the multivalued potential. The existence of a potential along these different branches needs verification. The question of the existence of a work potential when viscoelastic effects are significant also needs investigation. For such cases as these, the theory outlined in [2.1] and [2.5] will be used to check for the existence of a work potential. For processes where it is verified that a work potential exists, the generalized J integral theory given in [2.5] will be used in mode III and mixed mode fracture studies.

Mode III fracture characterization of fiber-reinforced plastic laminate is an area requiring further investigation. As previously mentioned, studies of this type are few. The tentative test specimen which will be used for mode III characterization studies is a rectangular plate laminate with pre-fabricated edge and through-width delaminations. It is the intent of future research to use this test specimen to study mixed-mode and mode III delamination of fiber-reinforced plastics laminates. At present a $[0°]_{24}$ plate of the Hexcel composite has been fabricated with teflon release paper used to form pre-existing edge delaminations.

A X-ray machine is being purchased so that X-ray fractography may be used to monitor delamination and other damage growth. This equipment should also be useful in identifying other damage mechanisms.

Studies of Thin-Walled Tubes: A Ph.D. dissertation involving experimental work on tubular specimens was completed by Richard Tonda during the grant period. A significant part of the study was concerned with development of a

technique for modifying stress-strain data on fibrous composites so that the effects of changing damage may be observed without the complicating effects of matrix viscoelasticity. The method, which is based on micromechanical considerations and is not limited to tubular specimens, reduces the behavior to that of an equivalent elastic composite with damage. The fibers are assumed to be continuous and linearly elastic. The theoretical basis is developed and then the method is illustrated using results from cyclic axial-torsional loading of tubular specimens of graphite/epoxy laminates. This work is reported in [2.6].

References for Section 2

2.1 Schapery, R. A. "Deformation and Fracture Characterization of Inelastic Composite Materials Using Potentials," Polymer Engineering and Science, Vol. 27, No. 1, pp.63-76

2.2 Agarwal, B. D., and Giare, G. S. "Fracture Toughness of Short Fibre Composites in Modes II and III," Engineering Fracture Mechanics, Vol. 15, No. 1-2, 1981, pp.219-230

2.3 Donaldson, S. L. "Interlaminar Fracture Due to Tearing (Mode III)," ICCM Sixth International Conference on Composite Materials," Edited by F. L. Matthews, N. C. R. Buskell, J. M. Hodgkinson, and J. Morton, Vol. 3, 19[illegible]7, pp. 3.274-3.283

2.4 Chan, W. S., and Ochoa, O. O. "An Integrated Finite Element Model of Edge-Delamination Analysis for Laminates Due to Tension, Bending, and Torsion Loads," presented at the AIAA/ASME/ASCE/AHS Twenty Eighth Structures, Structural Dynamics, and Materials Conference, Monterey CA., April 6-8,1987

2.5 Schapery, R. A. "Correspondence Principles and a Generalized J Integral for Large Deformation and Fracture Analysis of Viscoelastic Media," International Journal of Fracture, 25, 1984, pp. 195-223

2.6 Tonda, R. D. and Schapery, R. A., "A Method for Studying Composites with Changing Damage by Correcting for the Effects of Matrix Viscoelasticity," To appear in Damage Mechanics in Anisotropic Composite Materials, Proc. Winter Annual Meeting, Dec. 1987

3. Analysis of Crack Growth in Damaged Media Using a Generalized J Integral

A Ph.D. dissertation on analysis of crack growth was completed by Randall Weatherby during the grant period. The work is summarized here.

In most materials, macrocrack extension is accompanied by inelastic phenomena (such as microcracking or plastic deformation) throughout a region surrounding the crack tip. Immediately ahead of that crack tip, strain localization occurs in a small volume of heavily damaged material referred to as the failure zone or fracture process zone. In this study, the failure zone and the surrounding zone of inelastic material are treated as two distinct regions. The failure zone is assumed to be thin relative to its length and is represented in a two-dimensional finite element model as tractions which act across the crack faces near the tip. An opening mode of crack tip deformation is assumed. The normal traction at any point on the crack surface in the failure zone is specified as a decreasing function of the crack opening displacement which vanishes after a critical value of displacement is reached. Two different rate-independent, inelastic continuum characterizations based on multivalued work-potentials are used; one models metal plasticity and another represents microcracking in brittle materials. Both constitutive models allow for the definition of a generalized J integral developed by Schapery, which has the same value for most paths around the crack tip for realistic distributions of plasticity or damage in the material surrounding a stationary or propagating crack. This path independence and the equivalence between J and the work input to the last ligament of material in the failure zone are verified numerically in a transient crack growth problem; both initiation and propagation are studied under conditions of small-scale inelasticity. In addition, steady-state crack growth is studied in two different specimen geometries. Simplified J integral analyses are used to estimate the work input to the failure zone for these steady-state problems. The J-integral estimations are compared with finite element results to determine the accuracy of the simplifed analyses.

4. Determination of the Mode I Delamination Toughness of Multidirectional Laminates

The objective of this study is to develop a procedure for determining the mode I delamination fracture toughness of multidirectional composite laminates. To date, the focus of the work has been on application of the J integral to double cantilever beam (DCB) tests in order to investigate the importance of geometry, layup, rate effects, and fracture morphology. The general goal is to synthesize principles which can guide the prediction of delamination performance using limited material data. The following discussion highlights the method used and results obtained.

The material used in this study is T2CT145/F155, manufactured by Hexcel. It uses a rubber-toughened epoxy matrix with about 6 % rubber by weight. The nominal fiber volume fraction for all the material tested was 57%. This material system was chosen in order to accentuate possible nonlinear and viscoelastic responses for a commercially available toughened composite. It is also currently being used for other work on this contract and other contracts at Texas A&M, allowing sharing of material data. Three layups were used. Hereafter, they will be referred to using the following designations:

Designation	Layup	No. Plies
unidirectional	$[0_{24}]$	24
fiber-dominated	$[+-45/0_8/-+45]_{antisym.}$	24
angle-ply	$[+-45/(-+45)_2/(+-45)_2/-+45]_{antisym.}$	24

These designations will also be used in the captions of the figures to be discussed below. The unidirectional layup is the one which has been most commonly used in the literature to characterize delamination. In this study it was used not only to examine delamination between zero degree plies where ply interpenetration could occur, but to give a baseline for evaluating data

for multidirectional layups. The fiber-dominated layup was used to study delamination at a +-45 degree interface. Each leg of the DCB specimen was made balanced and symmetric in order to eliminate stretching-shearing and stretching-bending coupling. Antisymmetry about the midplane of the laminate was designated in order to put the delamination plane at a +-45 degree interface. The stacking sequence for the angle-ply was chosen to minimize bending-twisting coupling as well.

All data shown in the following figures were generated using DCB specimens. The fracture toughness was calculated using the J integral method of [4.1], which allows for nonlinear elastic or inelastic behavior. In this formulation the J integral is calculated using the moment at the crack tip during crack extension and the moment-curvature relationship for one leg of the specimen. The J integral is twice the area to the left of the moment-curvature curve divided by the specimen width, as shown in Fig. 4.1. In the following discussion, J will correspond to this integral definition. The energy release rate was also calculated for comparison. The symbol G will signify the energy release rate calculated by the area method [4.2], which allows for nonlinear elastic behavior. The area method comes from the derivative definition of energy release rate, and provides an average value for an increment of crack growth. The symbol G_1 will refer to the energy release rate calculated using the equation for a linear elastic beam,

$$G_1 = \frac{3P_c \delta_c}{2ba} \qquad (1)$$

where P_c is the load at crack extension, δ_c is the load line displacement at crack extension, b is the specimen width, and a is the crack length.

Motivation for using a J integral analysis came from the need for an

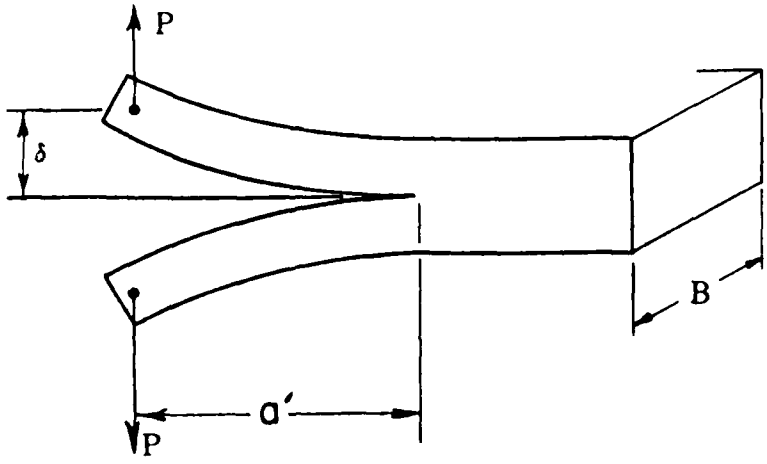

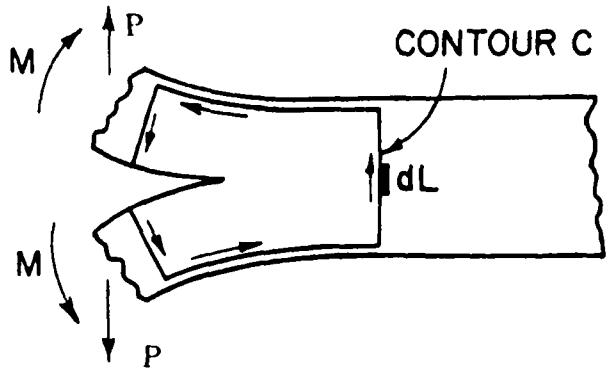

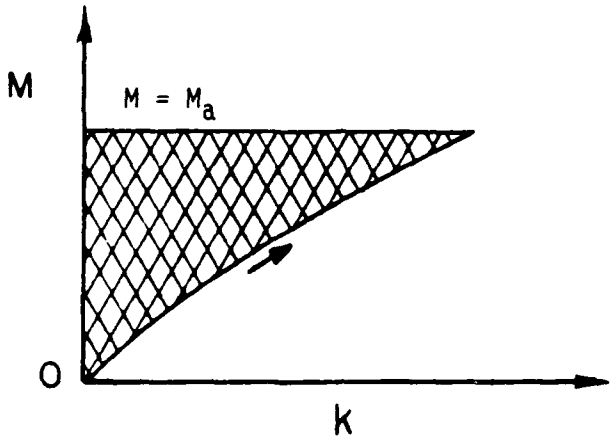

$$J_c = \frac{2}{B}\int_0^{M_a} K(M)\,dM$$

B = width

M_a = crack-tip moment

Figure 4.1 Double cantilever beam specimen, integration path, and moment-curvature diagram for calculation of J [after 1]

analysis which would allow for continuum damage such as might be generated throughout the legs of a DCB specimen during testing; the value of J is only the work input to the crack tip during self-similar crack growth. The area method of calculating the energy release rate allows for geometric and material nonlinearity, as does J, but does not differentiate between energy which goes into driving the delamination and that which causes general damage away from the crack tip, leading to overestimation of toughness. The difference is illustrated in Fig. 4.2, where G and J are plotted versus crack length for three angle-ply DCB specimens. Note that for each specimen G is significantly higher than J. The presence of damage (and a small amount of viscoelastic behavior) is illustrated by the moment-curvature relationship for the angle-ply layup, as shown in Fig. 4.3. Note that the unloading portion of the moment-curvature plot does not retrace the loading portion.

For layups containing a high percentage of 0 degree fibers, one would expect that G and J would give better agreement, since the effect of continuum damage on beam deformations would be small. The moment-curvature relationships for the unidirectional and fiber-dominated layups were linear, and the unloading portions of the curves retraced the loading portions. When this is the case and linear beam theory applies, it can be shown that J is equal to G_1 calculated using equation 1. This formulation is helpful when comparing energy release rate and J because G_1 is calculated for a particular crack length (as J is for the linear and nonlinear cases), avoiding averaging over crack lengths as in the area method. Figure 4.4 is the load-displacement record from a fiber-dominated specimen which displayed the development and breakdown of a tie zone, causing the delamination resistance to increase and then suddenly drop with crack growth. The corresponding G_1 and J are plotted in Fig. 4.5. Both initiation and arrest values are shown. The two methods

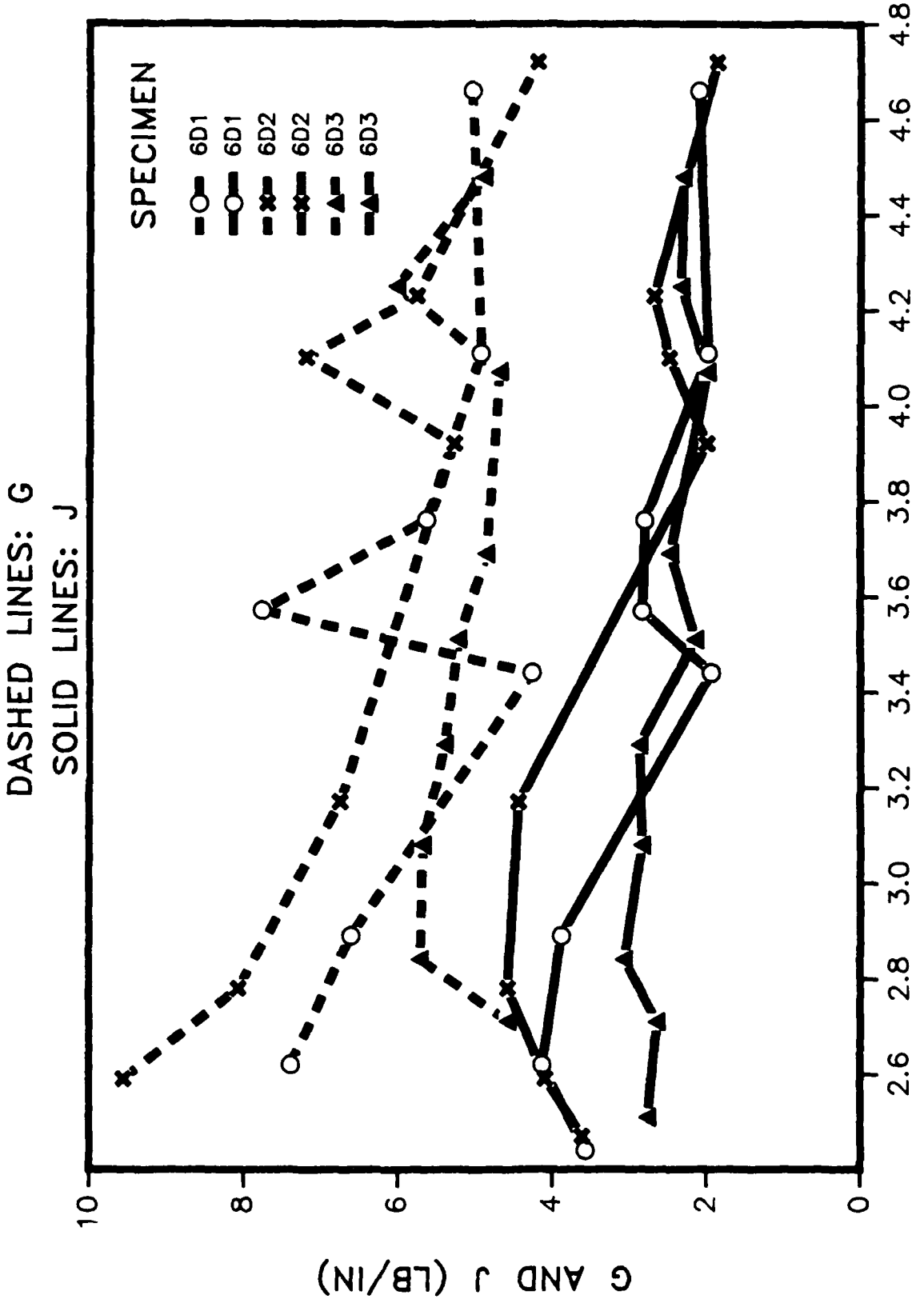

Figure 4.2 G and J vs. crack length for three angle-ply specimens

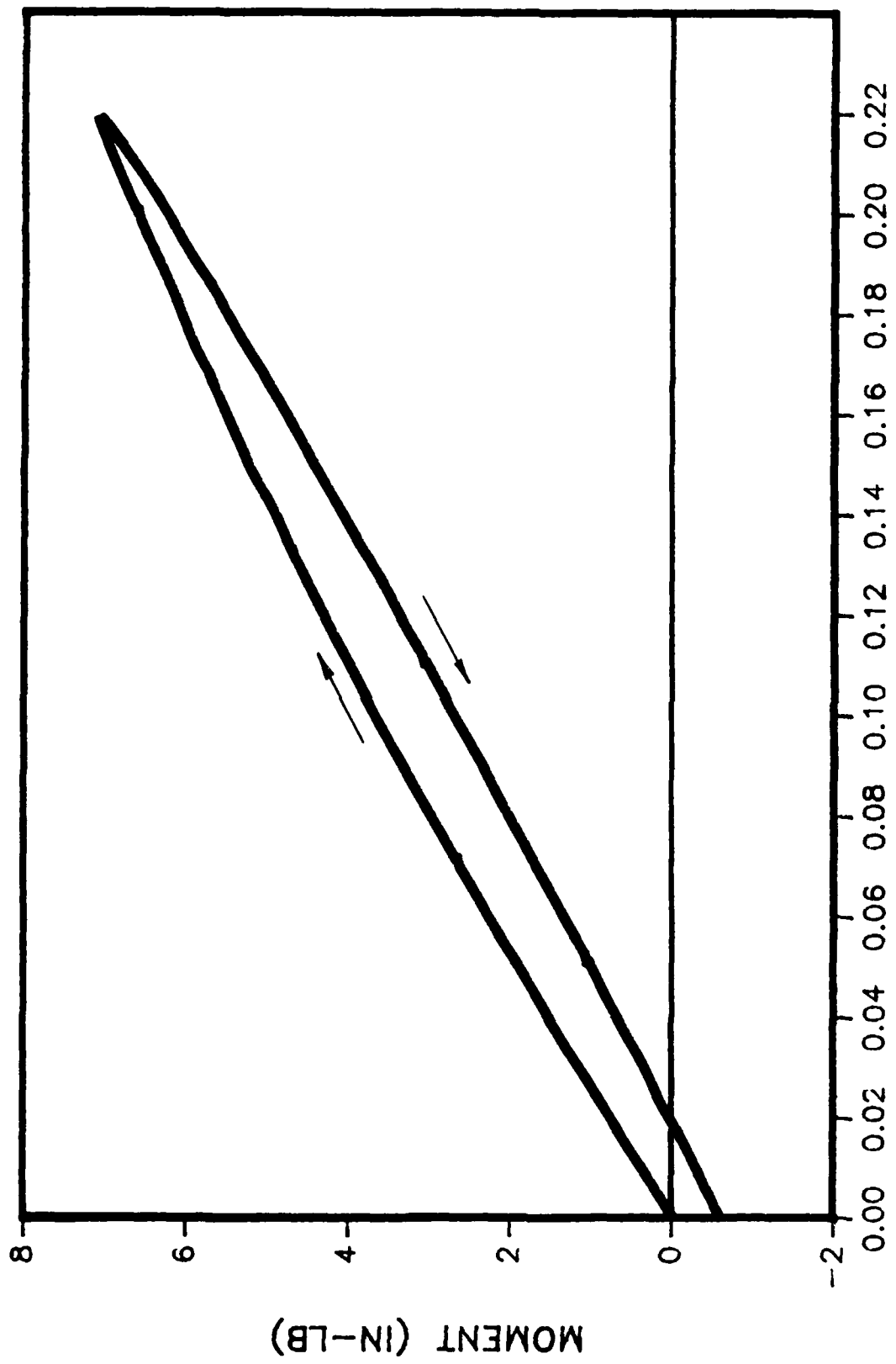

Figure 4.3 Moment vs. curvature diagram for an angle-ply layup

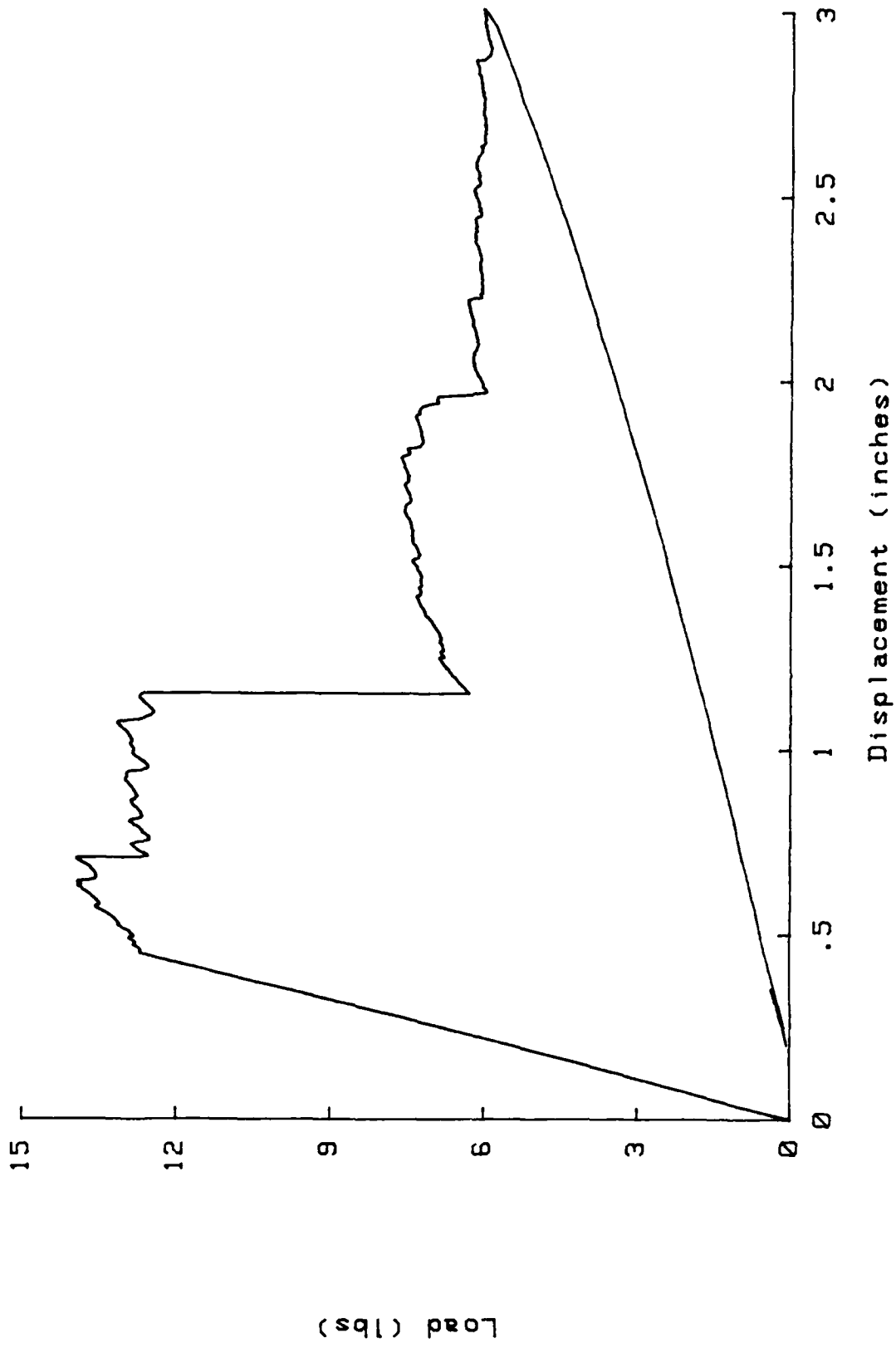

Figure 4.4 Load vs. displacement plot for a fiber-dominated DCB specimen The layup is $[+-45/0_8/(-+45)_2/0_8/-+45]$.

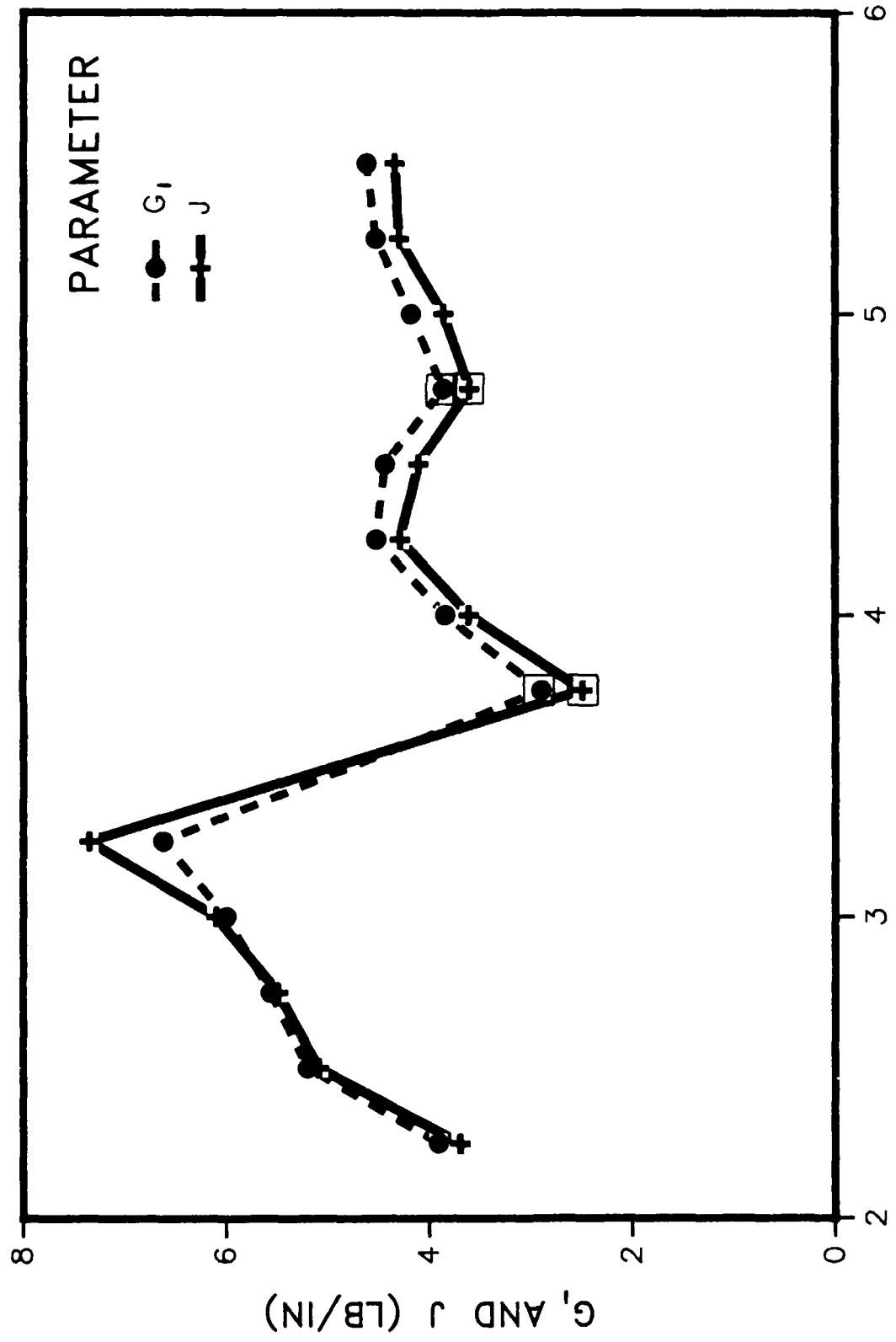

Figure 4.5 G_1 and J vs. crack length for the fiber-dominated specimen of figure 4.4. Arrest values are marked by squares around data points. The layup is $[+-45/0_8/(-+45)_2/0_8/-+45]$.

are in reasonably close agreement, supporting the interpretation of the difference between energy release rate and J for the angle-ply layup as being caused by damage. Even when damage is not present, the simple expression in equation 1 does not always hold; when geometric nonlinearity is present due to large rotations of the legs, the energy release rate must be calculated using either the area method (possibly losing information due to averaging) or using nonlinear beam theory [4.3].

The usefulness of J as a characterizing parameter depends on its independence of geometry, such as specimen width. To investigate the effect of specimen width, angle-ply specimens 1/2, 1, and 2 inches wide were tested. Representative results are given in Fig. 4.6. The high values for the 1 inch wide specimen for shorter crack lengths were found to be associated with the complex fracture morphology which developed near the starter crack. For more nearly self-similar crack advance, it appears that width does not have much effect on the fracture toughness measured over the range of widths and crack lengths studied. Recent work at Texas A&M [4.4] indicates that the state of stress in the legs of the DCB specimen is in the transition range between plane strain and plane stress over the practical range of crack length to width aspect ratios. However, the effects of the transition on J were not seen for the aspect ratios in our tests. There is another type of specimen behavior which does show a marked width effect. Unlike unidirectional composites, multidirectional composites exhibit significantly curved crack fronts in DCB tests. The curvature depends on the width of the specimen. Figure 4.7 compares the normalized crack front profile for 1/2 inch, 1 inch, and 2 inch wide specimens for several crack lengths. The thickness of one leg is 0.062 inch. Apparently the crack front curvature has two sources: the anticlastic curvature of the DCB leg and free edge effects. The general trend

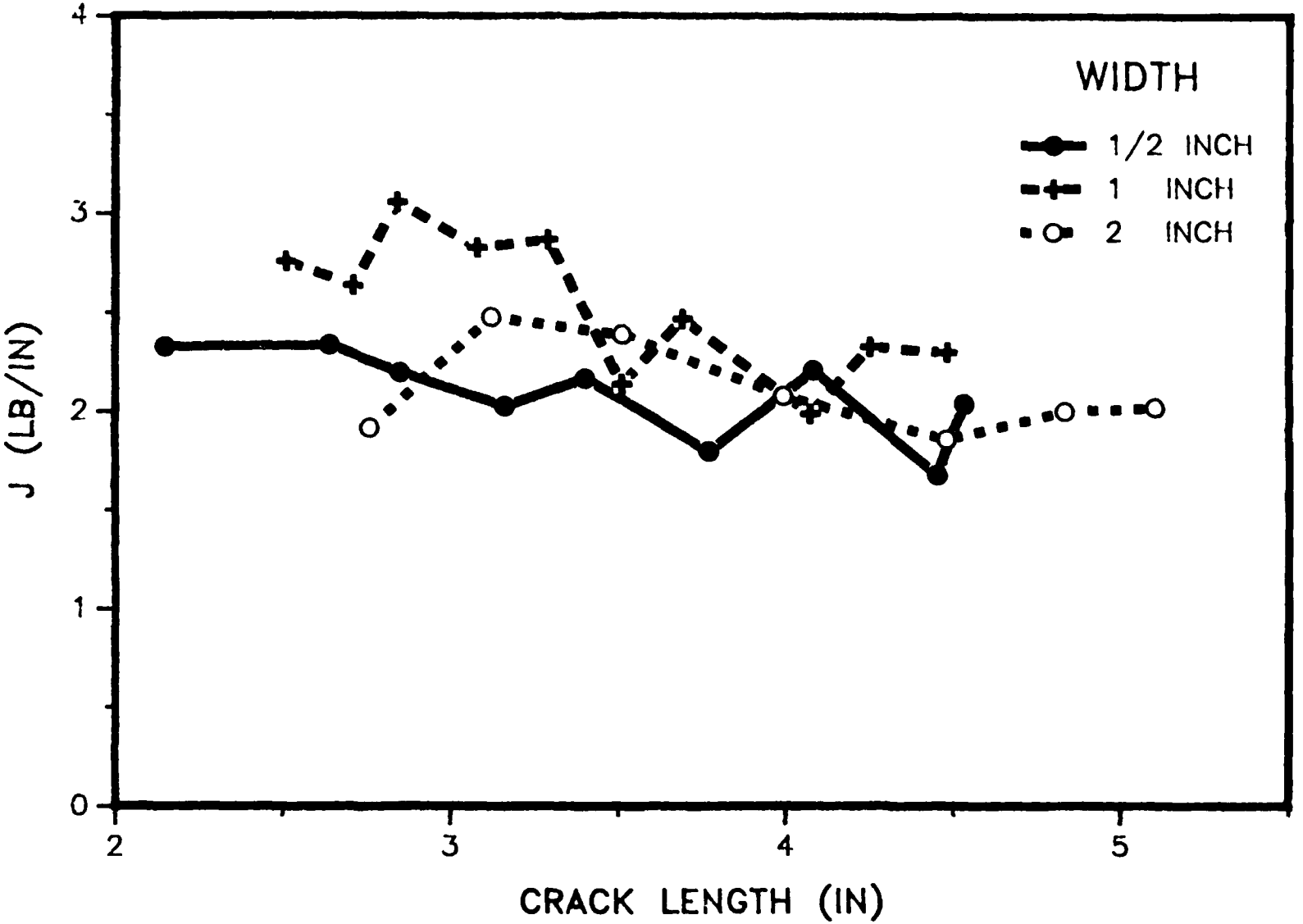

Figure 4.6 J vs. crack length for three angle-ply DCB specimens of different widths

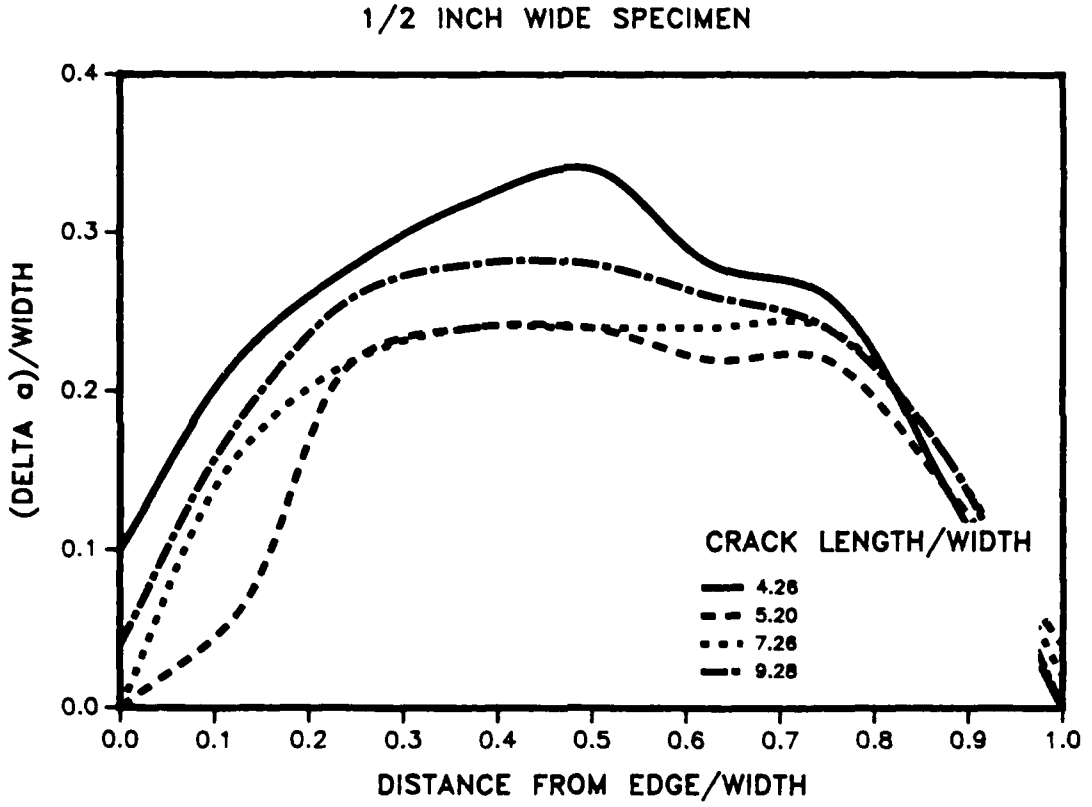

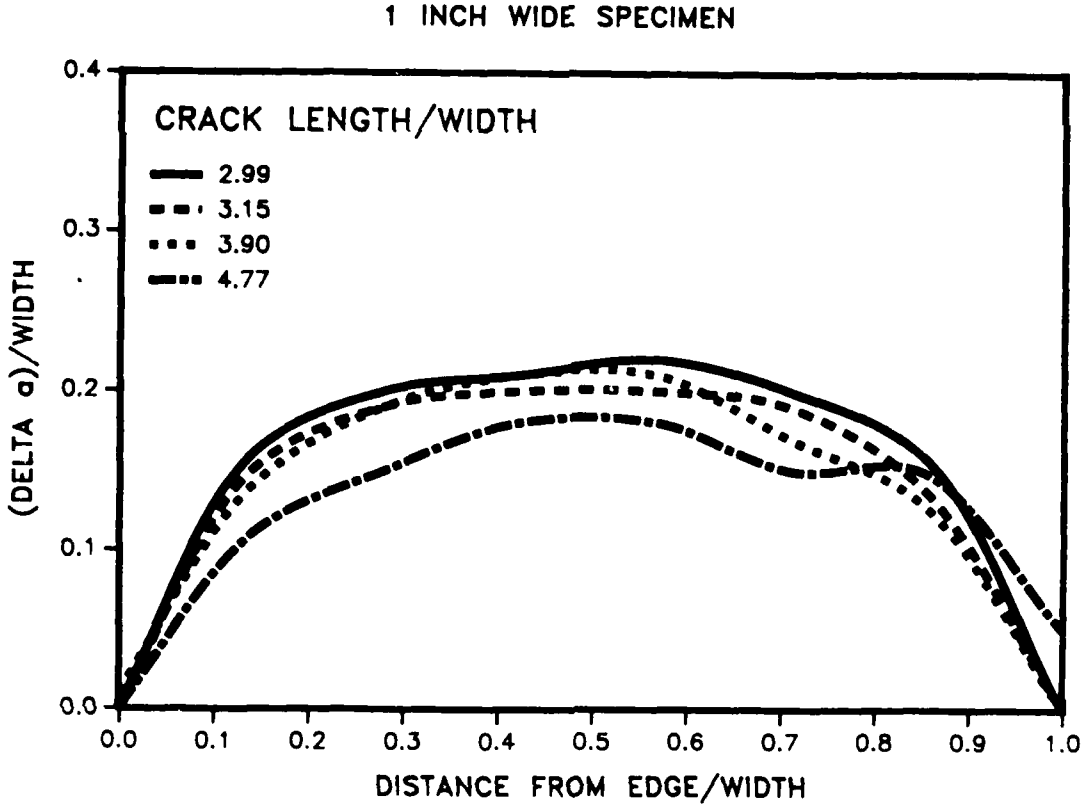

Figure 4.7 Normalized crack front profiles for three angle-ply DCB specimens of different widths. The profiles for various crack lengths have been superimposed.

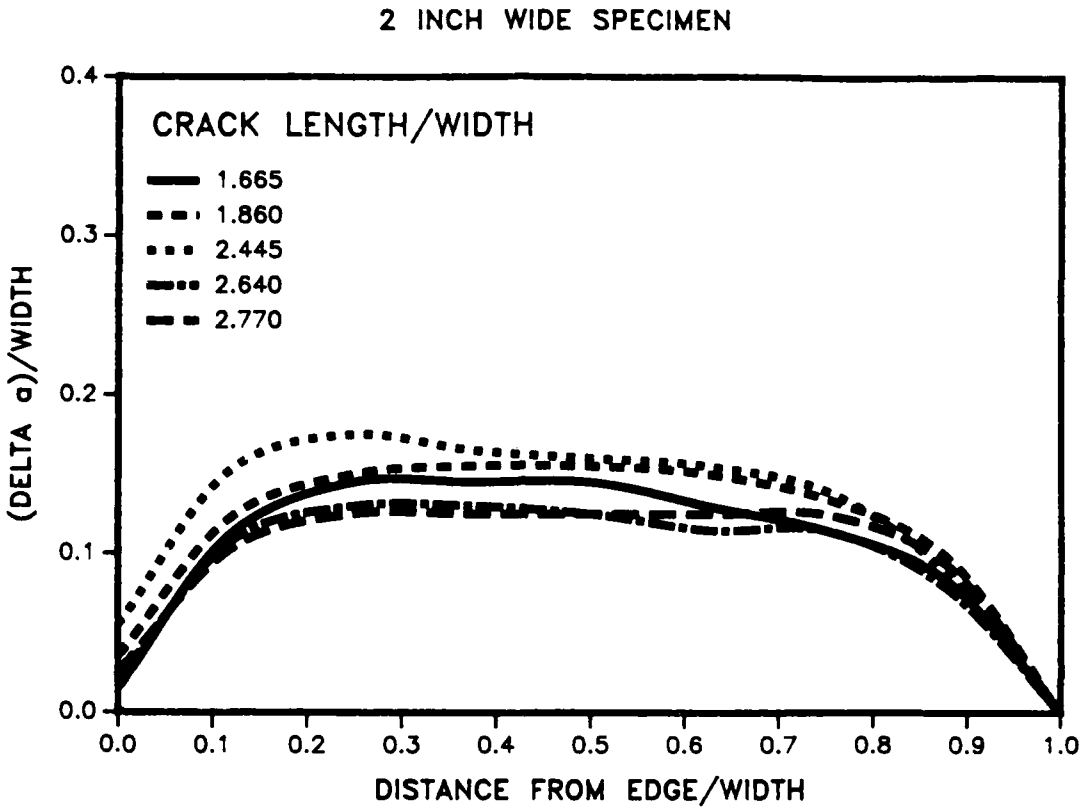

Figure 4.7 (continued)

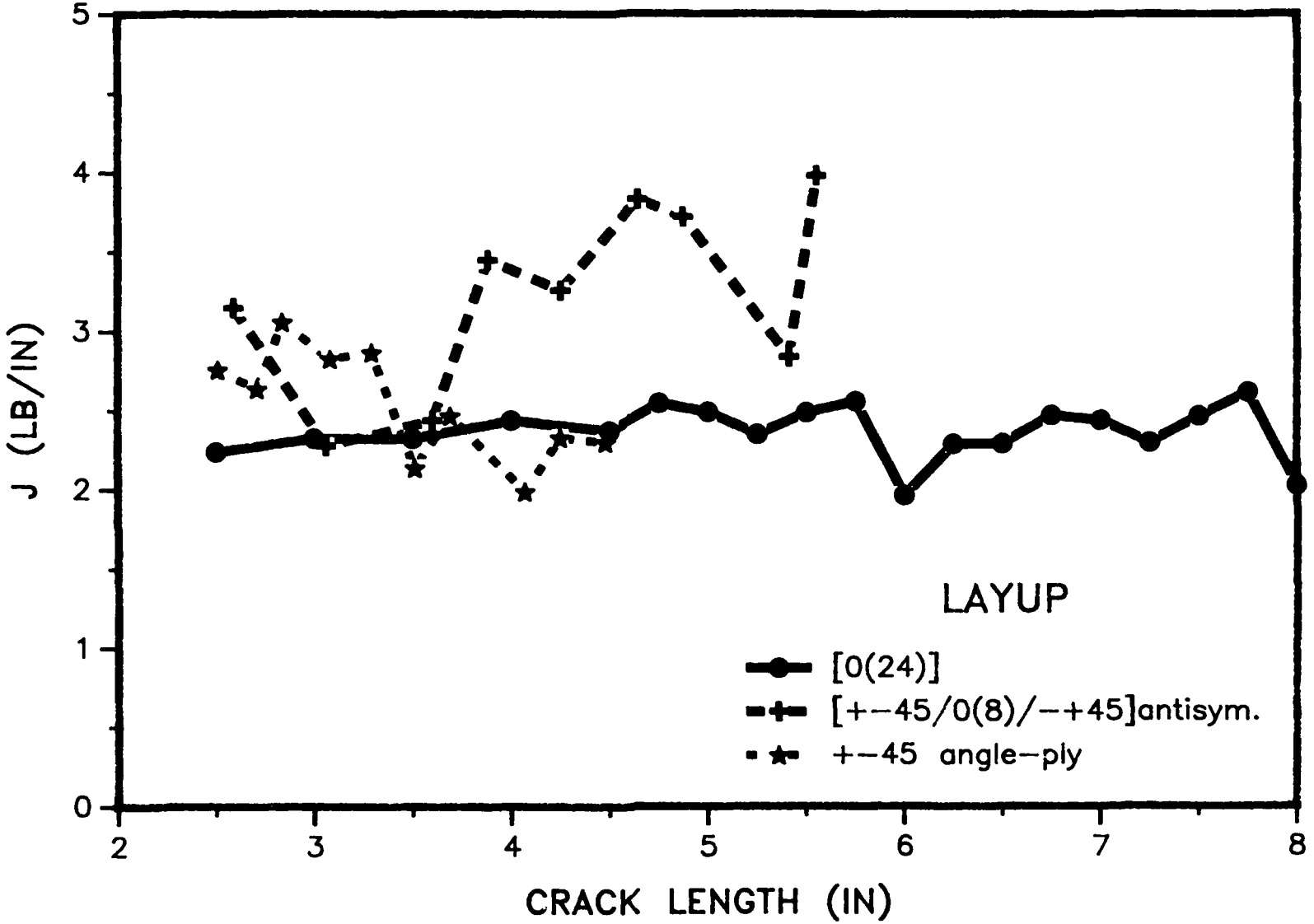

Figure 4.8 J vs. crack length for three different layups

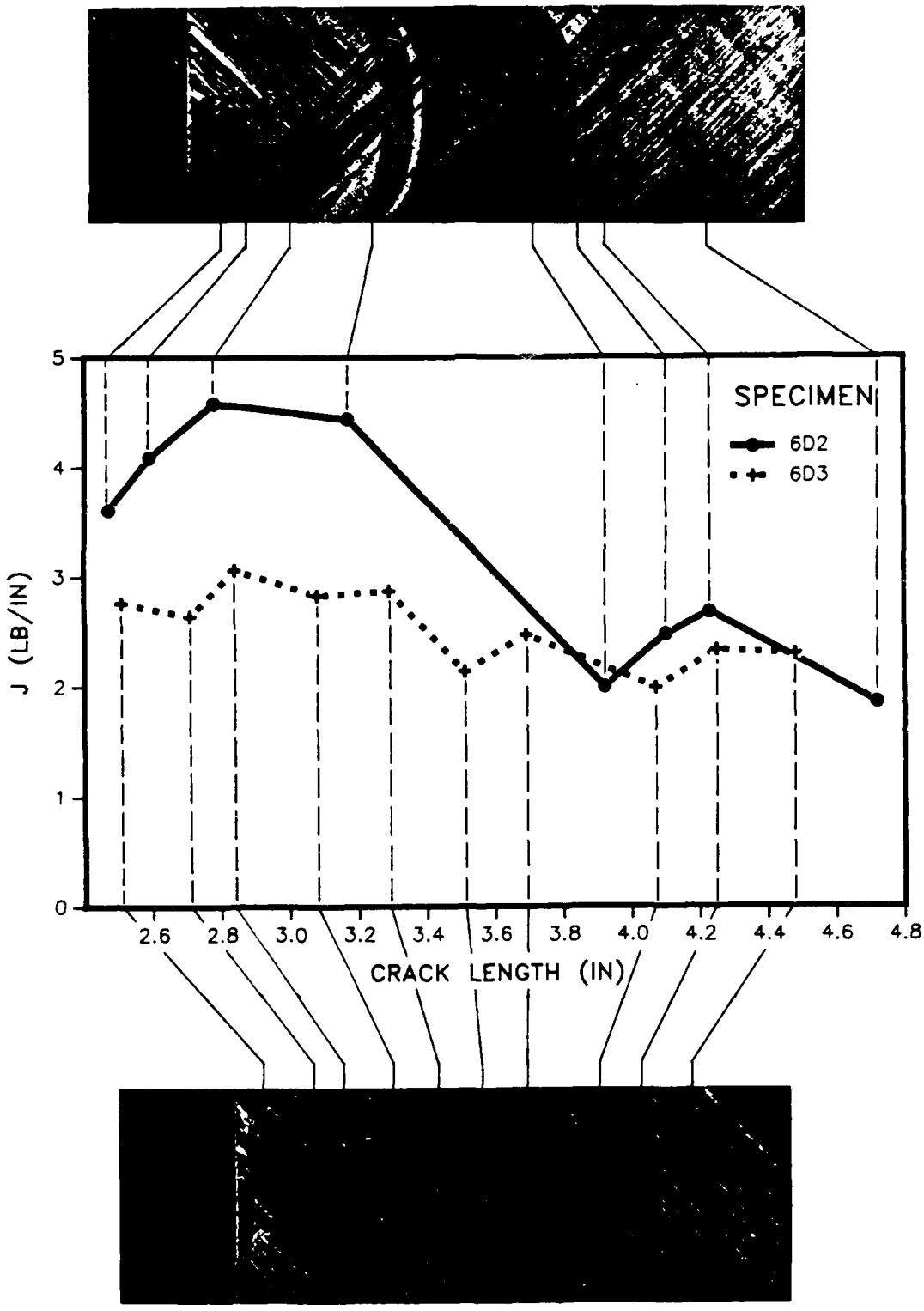

Figure 4.9 Correlation of fracture surface morphology with measured delamination fracture toughness for two angle-ply specimens

measured. Note that once a more or less uniform fracture morphology was established, the toughness values settled into better agreement. The two angle-ply specimens shown were next to each other in the plate of material before cutting. Dark and light bands were formed when the crack tip jumped forward, then arrested. Dark regions were formed during rapid crack advance; light regions correspond to slow crack growth. These studies of the effect of layup illustrate a major difference between unidirectional and multidirectional laminate delamination behavior. The opportunity for more mechanisms of fracture leads to a greater complexity of behavior. It is therefore essential that attention be paid to the fracture morphology when interpreting the data.

Tests were done to investigate the dependence of J on crack speed. The results for a unidirectional layup and a fiber-dominated layup are given in Fig. 4.10. In both cases there is a slight decreasing trend in J with increasing crack speed. This trend agrees with the observation that when sudden crack jumping occurred, a low value of toughness was usually measured. It is significant to note that no strong trend can be established for the range of crack speeds experienced by one specimen. Thus rate effects are not important in interpreting data for individual specimens.

The importance of considering the fracture morphology when interpreting the delamination toughness data has already been mentioned. Macro- and microfractography were done to document the fracture mechanisms which were observed. Two items are of particular interest. First, when off-axis plies were present at the fracture plane, toughness values were sometimes elevated even in the absence of complex fracture mechanisms. Apparently this was due to increased surface roughness caused when bundles of fibers were pulled away from the fracture surface. This feature was only observed for layups with

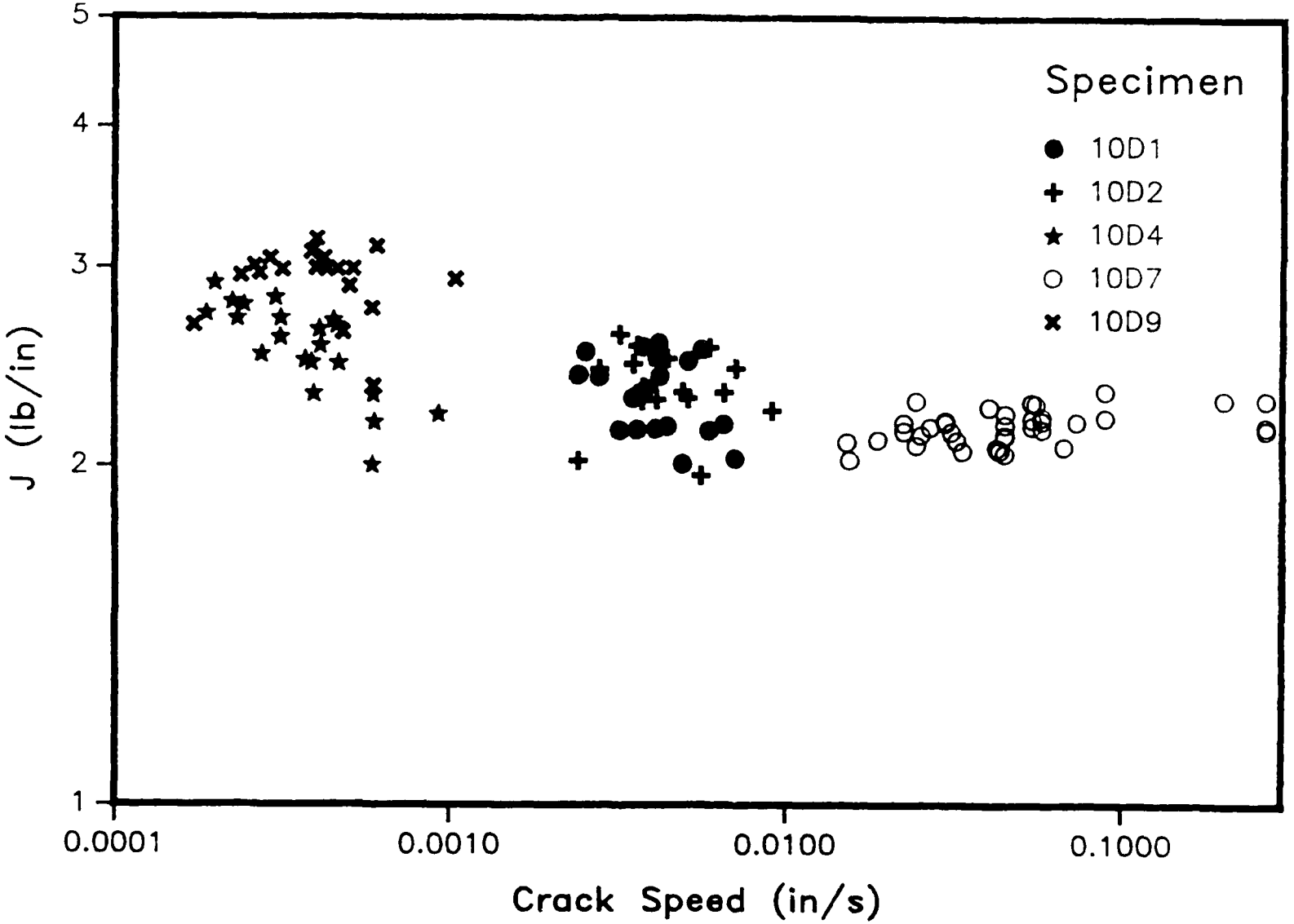

Figure 4.10a J vs. crack speed for unidirectional DCB specimens

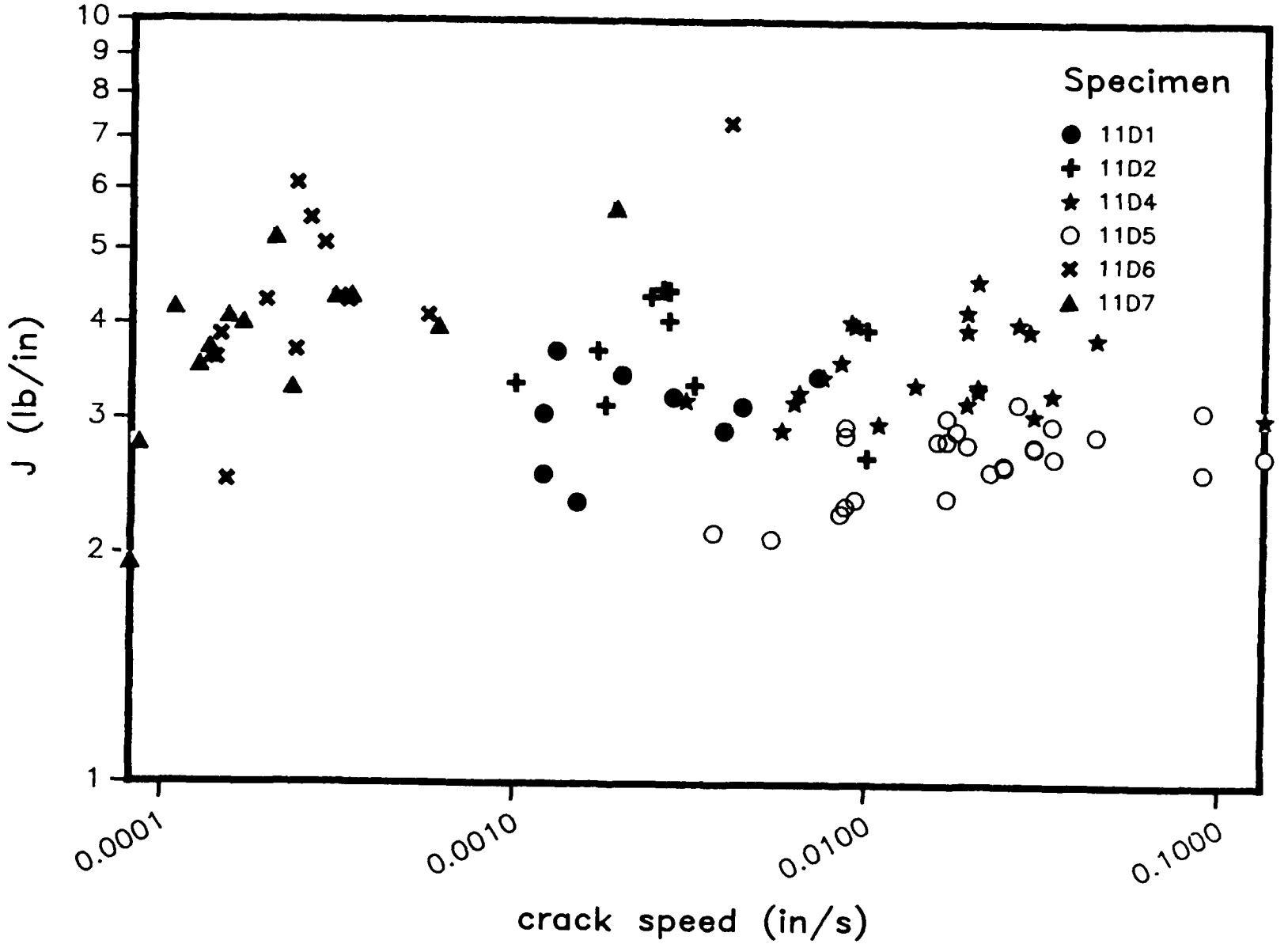

Figure 4.10b J vs. crack speed for fiber-dominated DCB specimens. The layup is $[+-45/0_8/(-+45)_2/0_8/-+45]$

off-axis plies at the delamination plane. For a more brittle system the phenomenon was found to give differences of a factor of two in toughness between unidirectional and off-axis specimens [4.7]. Figure 4.11 is a cross-section of a specimen (normal to the direction of crack propagation) at the fracture surface. A bundle of fibers is separated from the surface at this plane, but is attached to it at another point.

A second phenomenon which is of significance is that in almost all specimens tested delamination was found to occur within a ply rather than between two plies. Figure 4.12 shows a typical situation on a polished cross section at a fracture surface. Note that the fracture plane does not pass through the interply region, but stays a few fiber diameters away from it. Practically, the presence of resin-rich regions and ply interfaces has only an indirect impact on the mode I delamination toughness when such steady-state morphology is present.

Additional Studies: Future work under the follow-on grant will expand on the investigations of the effect of geometry, layup, rate effects, and fracture morphology. Further experiments will be performed to explore the effect of specimen width, especially as it relates to crack front curvature. The effect of the number of plies and the bending stiffness of the legs of the DCB specimen need to be addressed. Also, tests will be conducted with various fiber angles at the delamination plane. The dependence of delamination toughness on crack speed for matrix-dominated layups will be investigated. An attempt will be made to systematize the correlation between fracture morphology and delamination toughness. In addition to these continuing activities, new study will be begun to understand the effect of continuum damage on the apparent toughness. This will probably include delamination tests which simulate mechanical states in real structures, such as tests using

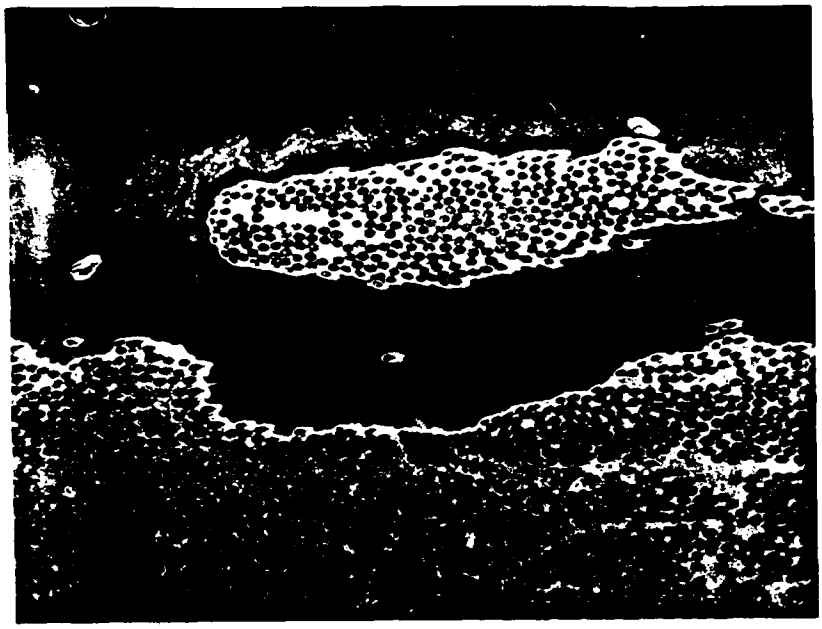

Figure 4.11 Micrograph of a polished section of a failed DCB specimen showing the fracture surface. A bundle of fibers has been pulled away from the surface. (150X)

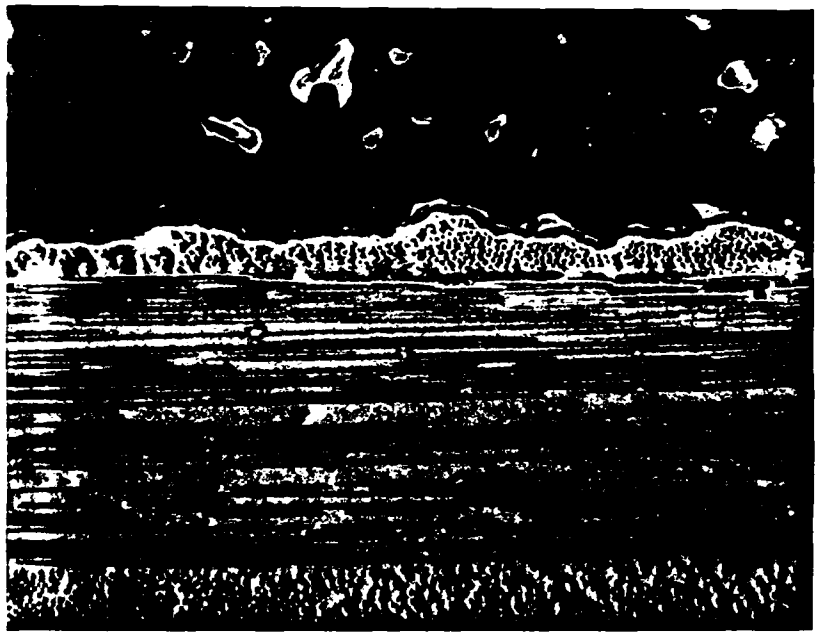

Figure 4.12 Micrograph of a polished section of a failed DCB specimen showing the fracture surface. The large circles at the top are the material used to mount the specimen for polishing. (100X)

a modified DCB specimen with bending and stretching inputs. Some testing of specimens with fatigue predamage is planned. In these studies of damage, emphasis will be on exploring the general applicability of the J integral.

References for Section 4

4.1. Schapery, R.A., "Deformation and Fracture Characterization of Inelastic Composite Materials Using Potentials," Polymer Engineering and Science, v. 27, 1987, pp. 63-76

4.2. Whitney, J.M., Browning, C.E., and Hoogsteden, W., "A Double Cantilever Beam Test for Characterizing Mode I Delamination of Composite Materials," Journal of Reinforced Plastics and Composites, v. 1, Oct. 1982, pp. 297-313

4.3. Devitt, D.F., Schapery, R.A., and Bradley, W.L., "A Method for Determining the Mode I Delamination Toughness of Elastic and Viscoelastic Composite Materials," Journal of Composite Materials, v. 14, Oct., 1980, pp. 270-285

4.4. Davidson, B.D., and Schapery, R.A., "Effect of Finite Width and Crack Tip Constraint on Deflection and Energy Release Rate of a Double-Cantilever Specimen," to appear in Journal of Composite Materials

4.5. Chai, H., "The Characterization of Mode I Delamination Failure in Non-woven, Multidirectional Laminates," Composites, v. 15, Oct. 1984, pp. 277-290

4.6. Nicholls, D.J., and Gallagher, J.P., "Determination of G_{IC} in Angle Ply Composites Using a Cantilever Beam Test Method," Journal of Reinforced Plastics and Composites, v. 2, Jan. 1983, pp. 2-17

4.7. Schapery, R.A., Jordan, W.M., and Goetz, D.P., "Delamination Analysis of Composites with Distributed Damage Using a J Integral," Proc. of the Int. Symp. on Composite Materials and Structures, Beijing, China, June 10-13, 1986

III. PUBLICATIONS AND SPOKEN PAPERS

Publications:

1. Schapery, R.A., "Correspondence Principles and a Generalized J Integral for Large Deformation and Fracture Analysis of Viscoelastic Media," Int. J. Fracture, Vol. 25, 1984, pp. 195-223.

2. Schapery, R.A., "Time-Dependent Fracture: Continuum Aspects of Crack Growth," Encyclopedia of Materials Science and Engineering, Pergamon Press (1986), pp. 5043-5053.

3. Schapery, R.A., Jordan, W.M., and Goetz, D.P., "Delamination Analysis of Composites with Distributed Damage Using a J Integral," Proc. Int. Symp. on Composite Materials and Structures, Beijing, Technomic Pub. Co., 1986, pp. 543-548.

4. Schapery, R.A., "Deformation and Fracture Characterization of Inelastic Composite Materials Using Potentials," Polymer Eng. Sci., Vol. 27, 1987, pp. 63-76.

5. Fang, G.P., Schapery, R.A., Weitsman, Y., "Thermally Induced Fracture in Composites," Proc. ASME Symposium on Composites, Anaheim, CA. (Dec. 1986).

6. Davidson, B.D., and Schapery, R.A., "Effect of Finite Width on Deflection and Energy Release Rate of an Orthotropic Double Cantilever Specimen." To be published in J. Composite Materials.

7. Tonda, R.D. and Schapery, R.A., "A Method for Studying Composites with Changing Damage by Correcting for the Effects of Matrix Viscoelasticity." To appear in Damage Mechanisms in Anisotropic Composite Materials, Proc. ASME Winter Annual Meeting, Dec. 1987.

8. Schapery, R.A., "A Constitutive Theory for Composite Materials with Damage Growth Based on Multivalued Work Potentials. To be submitted to Mechanics of Materials.

Spoken Papers (Principal Investigator's Activities)

1. "A J Integral for Viscoelastic Fracture Analysis." ASME/AMD Conference, San Antonio, June 1984.
2. "Research Directions for the Mechanics of Composites." ASME/AMD Conference, San Antonio, June 1984.
3. "Deformation Properties of Composites." Progress in Paper Physics: A Seminar, Stockholm, June 1984. Also chairman of workshop on deformation properties.
4. "Behavior of Composites with Distributed Damage." Owens-Corning Fiberglas Corp., Granville OH, Oct. 1984.
5. "Matrix Controlled Deformation and Fracture Analysis of Fibrous Composites." Tenth Annual Mechanics of Composites Review, Dayton OH, Oct. 1984.
6. "Mechanics of Deformation and Fracture of Polymeric Materials." Three lectures, National Taiwan Univ., Taipei, Jan. 1985.
7. "Fracture Analysis of Nonlinear Viscoelastic Materials." Mechanics Seminar, Tel-Aviv Univ., Tel-Aviv, Feb. 1985.
8. "Fracture Analysis of Composite Materials." Composites Group at Israel Aircraft Industries, Tel-Aviv, Feb. 1985.
9. "Recent Developments on Damage Growth and Fracture of Composite Materials." Plenary lecture at Israel Aeronautics Conference, Haifa, March 1985.
10. "Deformation and Fracture Characterization of Inelastic Nonlinear Materials Using Potentials." Mechanics Seminar, Univ. of Texas, Austin, April 1985.
11. "A Micromechanical Model for Nonlinear Viscoelastic Behavior of Particle-Reinforced Rubber with Distributed Damage." Int. Union of Theoretical and Applied Mechanics Conf. on Fatigue and Damage, Technion, Haifa, July 1985.

12. "Deformation and Fracture Characterization of Inelastic Composite Materials Using Potentials." International Symposium on Nonliner Deformation, Fracture and Fatigue of Polymeric Materials, National Meeting of the American Chemical Society, Chicago, Sept. 1985.

13. "Delamination Analysis of Composite Materials With Distributed Damage Using a J Integral." Int. Conf. on Composites, Beijing, China, June 1986.

14. "Crack Tip Deformation and Work in Viscoelastic Materials with Growing Cracks." Workshop on Fracture of Polymers and Metals, Cornell Univ., Aug. 1986.

15. "Deformation and Fracture of Composite Materials with Distributed Damage." Seminar, Texas A&M Univ., Sept. 1986.

16. "Some Micromechanical Models for Predicting Deformation and Fracture of Viscoelastic Composite Materials." Alcoa Centennial Seminar, Hilton Head, June 1987.

IV. PROFESSIONAL PERSONNEL INFORMATION

1. List of Professional Personnel

Richard Schapery, Principal Investigator

Douglas Goetz, Graduate Research Assistant

Mark Lamborn, Graduate Research Assistant

Richard Tonda, Graduate Research Assistant

Randall Weatherby, Graduate Research Assistant

Bob Harbert, Assistant Research Engineer, (Laboratory Staff Member)

Carl Fredericksen, Electronics Technician, (Laboratory Staff Member)

2. Degrees Awarded

Randall Weatherby, Ph.D. in Mechanical Engineering, May 1986.

Richard Tonda, Ph.D. In Interdisciplinary Engineering, August, 1987.

V. APPENDIX

1. Reprint of paper "Deformation and Fracture Characterization of Inelastic Composite Materials Using Potentials" by R.A. Schapery.
2. Reprint of paper "Time-Dependent Fracture: Continuum Aspects of Crack Growth" by R.A. Schapery.
3. Abstract of dissertation "Finite Element Analysis of Crack Growth in Inelastic Media" by J.R. Weatherby.
4. Abstract of dissertation "Techniques for Characterizing Damage Zones in Composite Materials" by R.D. Tonda.

Deformation and Fracture Characterization of Inelastic Composite Materials Using Potentials

R. A. SCHAPERY

Mechanics and Materials Center
Department of Civil Engineering
Texas A&M University
College Station, Texas 77843

An approach using strain energy-like potentials to characterize deformation and fracture of inelastic, nonlinear composite materials is described. The inelasticity may be due to various causes, including microcracking, microslipping, and rate processes responsible for fading memory (viscoelasticity). The concept of work potentials is introduced first, and then arguments are given for their existence for inelastic materials. Emphasis in the paper is on elastic composite materials with changing or constant states of distributed damage. Experimental results on polymeric composites are subsequently presented to illustrate this approach to deformation and fracture characterization. Finally, extension to viscoelastic behavior is discussed.

INTRODUCTION

Many important results on the deformation and fracture of linear and nonlinear elastic materials have been obtained by using strain energy functions or potentials to characterize material response. The thermodynamics of reversible processes provides theoretical support for the existence of these potentials and identifies them as free energy and internal energy for isothermal and adiabatic processes, respectively (e.g., Fung (1)). Besides serving as the basis for powerful methods of exact and approximate structural analysis, strain energy functions have been used in the prediction of effective or average constitutive properties (or their upper and lower bounds) of linear multiphase media in terms of properties and geometry of the phases, as reviewed by Hashin (2). Included in the many publications in this area are studies of the influence of small distributed cracks on the effective stress-strain behavior of monolithic and composite materials, like those described by Hashin (2) and Kachanov (3).

Methods of characterization and analysis using local and global strain energy-like potentials for certain inelastic materials, namely viscous, plastic, and elementary types of viscoelastic bodies, have been discussed in an early work by Hill (4). Constitutive equations normally employed for linear and nonlinear viscous bodies are fully analogous to those for elastic media, in which strain rate replaces strain (4). For the *linear* viscous and viscoelastic cases one may use irreversible thermodynamics (5) or special types of material symmetry, i.e., cubic and isotropic (6), to argue for the existence of strain energy-like constitutive potentials in terms of physical or Laplace-transformed variables (7). While experimental data on multiaxial *nonlinear* viscous behavior of metals (corresponding to the secondary creep stage) may be characterized analytically through a potential, a general theoretical basis for this constitutive potential does not appear to exist in either irreversible thermodynamics or in models of micromechanisms. Rice (8) concluded that there is no sufficiently general physical model of slip that is capable of providing a firm basis for the existence of a creep potential. Duva and Hutchinson (9) give a good illustration on the use of potentials to construct approximate effective constitutive equations of nonlinear viscous composites. In this analysis the composite is a homogeneous, isotropic, incompressible, power-law nonlinear material with a given dilute concentration and size of spherical voids or penny-shaped cracks.

In using a potential to characterize constitutive equations, it is often sufficient to account explicitly for only a dependence of the potential on the stress or strain (or strain rate) tensor. If the effect of different temperatures or other parameters, such as microvoid or microcrack fractions and sizes, are of interest, then one

would of course have to consider how these quantities affect the constitutive potential. An example of such a potential for an elastic material with damage is the volume-averaged strain energy density of a material specimen, $W(e_{ij}, D_k)$, where e_{ij} are components of a suitably defined volume-averaged strain tensor, and D_k represents a set of "damage" parameters that define the current damage state (e.g., microcrack sizes). The stresses for this material are then obtained by differentiating W with D_k fixed.

$$s_{ij} = \partial W/\partial e_{ij} \tag{1}$$

In Refs. 2, 3, and 9, the effects due to specified sizes and concentrations, D_k, of microcracks are considered. If it is further desired to characterize the effective constitutive behavior when the D_k change with time as a result of straining, then relationships governing these changes must be determined. For discussion purposes suppose that these relationships are known and that one may solve the equations so as to express the damage parameters D_k in terms of the instantaneous strains e_{ij}. For some cases, it may then be possible to find a strain energy-like potential $\dot{W}(e_{ij})$, say, from which the effective constitutive equations can be derived by differentiation,

$$s_{ij} = \partial \dot{W}/\partial e_{ij} \tag{2}$$

This consitutive potential would depend on only the instantaneous strains but yet account for changing damage. If such a potential could be found, it would be like that used to characterize elasto-plastic behavior of metals by the Hencky deformation theory (10). Similarly, it would be analogous to the potential for metals discussed by Rice (8) for stationary creep. In his case the "damage" is an idealized set of internal slips that contribute to the average strain rate but do not appear explicitly in the effective stress-strain rate equations for the metal.

The present paper deals in large part with the question of whether potentials analogous to $\dot{W}(e_{ij})$ exist for elastic, viscous, and viscoelastic composites with changing damage (or, more generally, changing microstructure); emphasis is on elastic behavior with damage. Theory and related experimental work using data on a particle-filled rubber and fiber-reinforced plastics are discussed.

We should add that there are already many publications on the thermodynamic and micromechanistic bases for constitutive potentials for different types of inelastic materials; e.g., Rice (8, 11), Coleman and Gurtin (12), and Schapery (13 to 15). However, these potentials depend explicitly on "internal" parameters which reflect the microstructure state, and are thus like $W(e_{ij}, D_k)$ in *Eq 1*. They do not necessarily lead to the simplified form $\dot{W}(e_{ij})$ of particular interest here.

Strain energy potentials have been used widely in fracture mechanics (e.g., Broek (16)). For fully elastic materials, the mechanical work available at a crack tip for producing an increment of crack growth is equal to the decrease in potential energy (consisting of global strain energy and the boundary-work potential). Use of this relationship has resulted in remarkably successful investigations of fracture of rubber in its nonlinear range of behavior, which are reviewed by Lake (17), as well as fracture of linear elastic materials (16). Andrews (18) assumed a strain energy-like potential exists for rubber with hysteresis, and suggested how the hysteresis would affect crack growth. When a potential exists it is often possible to use Rice's J integral theory (19) to simplify fracture analysis. Schapery (20) recently extended the potential energy and J integral theories to elastic and viscoelastic materials with damage.

Concepts from fracture mechanics are used in the section on Multidimensional Theory to obtain the equations needed to predict microcrack growth, and thus help provide the basis for potentials, such as $\dot{W}(e_{ij})$ in *Eq 2*. Also, potentials are used in the section on Delamination in Double Cantilevered Beam to account for the effect of inelastic material behavior (which may be due to microcracking) on the growth of a macrocrack in the form of a delamination.

In most of this paper it is assumed the materials are elastic when the damage is constant. In the Viscoelastic Behavior section, a special representation of viscoelastic behavior proposed by Schapery (15, 20) is used to extend the elastic theory with damage to linear and nonlinear viscoelasticity; viscous behavior appears as a special case.

Finally, it should be mentioned that for lack of a better term we are using "damage" when referring to characteristics of the microstructure or fabric of a material which affect constitutive behavior but are not accounted for in elastic or fading-memory viscoelastic characterizations of continua. Furthermore, a damaging process, such as considered here, could be associated with crack growth, crack healing, dislocation creation and motion, breaking or reforming entanglement points along polymer chains in rubber, etc., and therefore may be structurally detrimental or beneficial.

ONE-DIMENSIONAL THEORY

The definition of a potential for elastic materials with damage may be explicitly introduced through the uniaxial stress-strain curve in *Fig. 1*. Let us suppose that a previously unloaded specimen is strained monotonically until the strain is e_m. (By definition, the initial state is "undamaged.") The strain is then reduced, as shown in *Fig. 1*. Assuming that the bar is elastic and has constant damage during the unloading

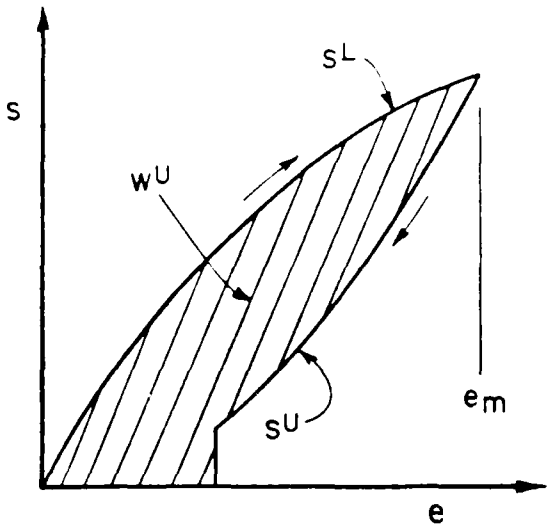

Fig. 1. Uniaxial stress-strain curve for material with increasing damage during loading and constant damage during unloading.

period, with instantaneous stress s^U and using the same idealization as Gurtin and Francis (21) in which the maximum strain e_m serves to define the amount and effect of damage,

$$s^U = f(e, e_m) \tag{3}$$

On the loading curve, the maximum strain is the current strain. Hence, viewing the loading stress as a point at the upper end of an unloading curve, we may write

$$s^L = f(e, e) \tag{4}$$

The mechanical work (per unit initial volume) during loading to an arbitrary strain is

$$W^L = W^L(e) = \int_0^e s^L\, de' = \int_0^e f(e', e')de' \tag{5}$$

where the prime denotes a dummy variable of integration. The net work input to the sample at any time during unloading is the shaded area in *Fig. 1*.

$$W^U = W^U(e, e_m) = W^L(e_m) + \int_{e_m}^e s^U de' = W^L(e_m) + \int_{e_m}^e f(e', e_m)de' \tag{6}$$

Observe that during loading and unloading, respectively,

$$s^L = dW^L/de, \qquad s^U = \partial W^U/\partial e \tag{7}$$

It is convenient to let W denote a continuous quantity which equals W^L during loading ($e_m = e$) and equals W^U during unloading ($e \le e_m$). Then, we may write for both loading and unloading processes,

$$s = \partial W/\partial e \tag{8}$$

The strain energy-like quantity W is actually the net work to the material at any stage of loading or unloading, and thus it will be called a *work potential*. It becomes the usual strain energy density when the loading and unloading curves are identical. Obviously, a work potential W can always be constructed, given the uniaxial stress-strain behavior, *Eqs 3* and *4*.

Derivatives of multidimensional equations are needed in the next section. The one-dimensional model, *Eqs 3* and *4*, is useful for clarifying some of the analysis ahead of time. In particular, observe that the slope of the unloading curve is,

$$\frac{\partial s^U}{\partial e} = \frac{\partial f}{\partial e} = \frac{\partial^2 W^U}{\partial e^2} \tag{9}$$

The loading curve s^L is a function of only e. However, when using the upper end of the unloading curve to define s^L, both arguments in $f(e, e_m)$ must be considered in computing the derivative,

$$\frac{ds^L}{de} = \frac{\partial f}{\partial e} + \frac{\partial f}{\partial e_m}\frac{\partial e_m}{\partial e} = \frac{\partial f}{\partial e} + \frac{\partial f}{\partial e_m} \tag{10}$$

where we have used the fact that $e_m = e$ on the loading curve. (The last term in *Eq 10* is the difference in slopes of the two curves at $e_m = e$). We may rewrite *Eq 10* using *Eq 3* and the second expression in *Eq 7* to obtain

$$\frac{ds^L}{de} = \frac{\partial^2 W^U}{\partial e^2} + \frac{\partial^2 W^L}{\partial e \partial e_m} \tag{11}$$

where the derivatives of W^U are to be evaluated at $e_m = e$ after differentiation.

MULTIDIMENSIONAL THEORY

For characterization of multiaxial stress-strain behavior, or for other responses that depend on more than one independent input, a work potential does not necessarily exist. However, it can be expected to exist for some realistic situations, which will be discussed here. For the sake of generality, let us use as independent inputs the generalized displacements q_j ($j = 1, 2, \ldots J$). The responses are the generalized forces Q_j, which are defined in the usual way by the condition that, for each j,

$$\delta(Wk) = Q_j \delta q_j \tag{12}$$

where $\delta(Wk)$ is the virtual work input associated with the virtual displacement δq_j. Suppose, for example, that we let each q_j represent a gradient, $\partial u_m/\partial x_n$ ($m, n = 1, 2, 3$) of a three-dimensional displacement field, u_m, and let $\delta(Wk)$ be virtual work per unit initial volume. Then $J = 9$, and *Eq 12* implies the Q_j are the components of a stress tensor s_{mn}, say (for large or small strains, Fung (1)). In order to characterize the behavior of laminates using classical plate theory (22), one may want to associate the set q_j with the middle surface curvatures and

strains. In this case, the Q_j would correspond to moments and in-plane forces per unit length, and $\delta(W'k)$ would be virtual work per unit area.

As in the uniaxial example, we assume that when the damage is constant, the body (material element, test specimen, or complete structure) is elastic in the usual sense; namely, a work potential W^e exists with the property that

$$Q_j = \partial W^e / \partial q_j. \tag{13}$$

(Rather than using the terms "loading" and "unloading" we shall instead now refer to "damaging processes" and "constant damage processes," since we do not want to imply that the damage is always constant when the magnitude of one or more loads or displacements decreases with time.) The effect of damage on Q_j is assumed to be fully represented by a set of "damage parameters" F_{cn} $(n = 1, 2, \ldots N)$ in the next subsection.

A Special Case

Following Schapery's (20) arguments, it will be shown that for a suitably chosen W^e a work potential W^D exists during damaging processes such that

$$Q_j = \partial W^D / \partial q_j \tag{14}$$

where W^D is a function of only the current values of q_j. One special W^e discussed in Ref. 20 is,

$$W^e = W_o(q_j) + \sum_{n=1}^{N} W_n(F_n, F_{cn}) \tag{15}$$

where W_o is a work potential without damage effects. It is assumed that all of the functions $F_n = F_n(q_j)$ are such that the N conditions $F_{cn} = F_n$ are satisfied simultaneously during all damaging processes. (The uniaxial case, *Eqs 3* and *4*, is recovered when we set $N = 1$ and take $W_o = 0$, $F_1 = q_1 = e$, $F_{c1} = e_m$.) To prove that W^D exists, it is necessary and sufficient to show that the generalized forces during damaging processes satisfy

$$\partial Q_j / \partial q_i = \partial Q_i / \partial q_j \qquad (i, j = 1, 2, \cdots J) \tag{16}$$

assuming the derivatives in *Eq 16* are continuous (e.g., Greenberg (23)). The forces during a damaging process are taken equal to those in *Eq 13* when $F_{cn} = F_n$ (which is analogous to saying a stress on the loading curve in *Fig. 1* is at the upper end of an unloading curve). Consequently, we may evaluate the derivatives in *Eq 16* by first substituting *Eq 15* into *13*,

$$Q_j = \frac{\partial W_o}{\partial q_j} + \sum_{n=1}^{N} \frac{\partial W_n}{\partial F_n} \frac{\partial F_n}{\partial q_j} \tag{17}$$

and then setting $F_{cn} = F_n$ and differentiating *Eq 17* (cf. *Eq 11*),

$$\frac{\partial Q_j}{\partial q_i} = \frac{\partial^2 W_o}{\partial q_j \partial q_i} + \sum_{n=1}^{N} \left[\frac{\partial W_n}{\partial F_n} \frac{\partial^2 F_n}{\partial q_j \partial q_i} + \left(\frac{\partial^2 W_n}{\partial F_n^2} + \frac{\partial^2 W_n}{\partial F_n \partial F_{cn}} \right) \frac{\partial F_n}{\partial q_j} \frac{\partial F_n}{\partial q_i} \right] \tag{18}$$

Clearly, the right-hand side of *Eq 18* is the same when i and j are interchanged, and therefore *Eq 16* is satisfied.

Generalizations

Extensions of W^e for which W^D exists are discussed in Ref. 20, and W^D itself is given. For example, at any given time some of the terms W_n in *Eq 15* may be for constant damage processes while others are for damaging processes. Also, the potentials may depend explicitly on time, and thus provide for effects of aging or changing physical environments. The theory in Ref. 20, which allows for large deformations, uses displacement gradients and Piola stresses instead of generalized displacements and forces. However, the earlier formulation, including its extension to viscoelastic behavior, carries over fully in terms of the generalized variables used here. Thus, as in *Eq 8*, we may introduce a continuous work potential W for which

$$Q_j = \partial W / \partial q_j \tag{19}$$

even if the damage parameters in some components W_n are constant while others vary in time.

Regardless of the process,

$$\partial Q_j / \partial q_i - \partial Q_i / \partial q_j = 0 \qquad (i, j = 1, 2, \cdots J) \tag{20}$$

except at the points of change from one process to another, considering all W_n. The derivatives in *Eq 20* are, in general, discontinuous at these transition points (cf. *Fig. 1* at $e = e_m$) and thus *Eq 20* does not apply there. Evidence of transition points may appear in experimental data as significant but somewhat random non-zero values of this difference of derivatives (for $i \neq j$) over short-time intervals. This experimental behavior would indicate that a process has changed from one type to another, damaging to constant damage or vice versa.

It is not the goal here to develop specific physical models that give rise to the form for W^e in *Eq 15*. We only mention that one based on a simple microcracking model is given by Schapery (20). Also, for characterizing laminates using classical plate theory, each F_{cn} might be proportional to a ply or ply-pair failure surface (such as represented by the Tsai-Wu theory (2), expressed in terms of the local ply strains) or other local invariant. Since the local strains are (linear) functions of the mid-plane strains and curvatures, one obtains $F_n = F_n(q_i)$ if the latter strains and curvatures are included in the set

q_i; the summation in *Eq 15* would extend over all plies.

It is not necessary for the constant-damage potential to have the form in *Eq 15* for the work potential in *Eq 19* to exist. For example, a different form for W^* was given in Ref. 20 which contains the Henky deformation theory of plasticity (with elastic unloading). Another example is given in the next subsection.

Micro- and Macrocracking

The work potential W in *Eq 19* may be a constitutive potential in the sense that this equation could be a stress-strain equation for a composite or monolithic material. Alternatively, W may be the total work input to a structure under a general set of boundary displacements q_i whose constitutive response is defined by a work potential density. In either case, the constitutive potential may account for some effects of microcracking, microvoiding, slipping, etc., through the damage parameters F_{cn}. However, the form of the underlying potential W^* for constant damage, which has been discussed so far, is not completely general. Also, effects of macrocracking (such as large-scale delamination) have not yet been explicitly introduced. Thus, it is of interest to know if a work potential exists when there is macrocracking and a relatively general distribution of growing microcracks. This question will now be examined by embedding additional cracks in the body characterized by W; the index k will be used to indentify each of these cracks, assumed to be K in number. The cracks may have a wide range of sizes, but it is assumed that the scale of the crack tip failure process zone, which determines the work required for increments of growth, is such that the local material surrounding the failure zone can be approximated as a continuum, and that the effect of the failure zone on the continuum can be represented by tractions acting along the local crack plane. Then, the virtual work equation with crack growth (see *Eq 13* in Ref. 20), which applies with or without changing damage in the continuum and regardless of whether or not growth is self-similar, gives the *available* crack tip work per unit of new surface area as $-\delta W/\delta A_k$; δW is the change in the work potential for the total body due to the increase in area δA_k of the k^{th} crack with all q_i fixed. Denoting the *available* work as G_k, we may thus write

$$G_k = -\partial W/\partial A_k \tag{21}$$

where $k = 1, 2, \cdots K$; also, W is considered to be a function of generalized displacements q_i and oriented crack areas A_k. The quantity G_k is commonly called the *energy release rate*. The work potential may also depend on damage parameters F_{cn} in that it is the W in *Eq 19* except for the fact that the body now has K additional cracks; the virtual work (*Eq 13* in Ref. 20) from which *Eqs 19* and *21* follow, is shown in Ref. 20, to be valid with crack growth in bodies with other distributed damage.

In order to predict this growth we also need to specify the work *required* G_{ck}, say, for a unit of new area of the k^{th} crack area; this quantity is the so-called *critical energy release rate*. It is not necessary to assume G_{ck} is constant or is the same for all cracks. However, we do assume it can be derived from a fracture work potential $W_f(A_k)$, where

$$G_{ck} = \partial W_f/\partial A_k \tag{22}$$

For example if the critical energy release rate for all cracks is constant, but not necessarily the same,

$$W_f = \sum_{k=1}^{K} G_{ck} A_k \tag{23}$$

Stable (quasi-static) growth of any one of the K cracks is specified by the condition that required work equals available work, $G_{ck} = G_k$; thus,

$$\partial W_f/\partial A_k = -\partial W/\partial A_k \tag{24}$$

if

$$\partial W_f/\partial A_k < -\partial W/\partial A_k \tag{25}$$

unstable growth occurs, whereas if

$$\partial W_f/\partial A_k > -\partial W/\partial A_k \tag{26}$$

there is not growth.

Returning now to the question of whether a work potential exists with crack growth, we shall see that it does for the model defined above if the growth is stable. The potential is denoted as W_T, and it will be shown that it is simply the work of fracture plus the work of deformation of the elastic or inelastic continuum W; namely,

$$Q_j = \partial W_T/\partial q_j \tag{27}$$

where

$$W_T = W_f + W \tag{28}$$

The proof is made by first evaluating the derivatives of W_T while allowing for the stable growth of an arbitrary number of the cracks; hence

$$\frac{\partial W_T}{\partial q_j} = \sum_k \left(\frac{\partial W_f}{\partial A_k} + \frac{\partial W}{\partial A_k}\right)\frac{\partial A_k}{\partial q_j} + \frac{\partial W}{\partial q_j} \tag{29}$$

For those cracks that do not grow, $\partial A_k/\partial q_j = 0$. In view of *Eq 19* as well as *Eq 24* for the growing cracks, *Eq 29* reduces to *Eq 27*, which was to be shown.

Equation 24 is a set of $K'(0 \le K' \le K)$ equations whose solution gives the areas $A_k(q_i)$ of K' growing cracks in terms of the generalized displacements. If we assume a unique solution exists (at least for small changes in q_i), then the areas (or their changes) could be substituted into W_f and W in *Eq 28*. In this form W_T would be a function of q_j and only those A_k that are constant.

Pursuing this representation further, let us

suppose for simplicity that all areas A_k simultaneously either constant or vary; denote the constant values by A_{ck}. Then for a constant damage process (apart from possible effects of F_m and F_n),

$$W_T^c = W_T(q_j, A_{ck}) \tag{30}$$

and for a damaging process, $A_{ck} \rightarrow A_k(q_j)$,

$$W_T^D = W_T(q_j, A_k(q_j)) \tag{31}$$

Equation 30 does not necessarily have the special form of *Eq 15*, but yet a work potential exists for constant and changing damage; the limitation is instead in the form of the relationship governing $A_k(q_i)$, viz. *Eq 24*.

Unstable Crack Growth

Unstable crack growth occurs when $G_k > G_{ck}$. The excess work predicted from quasi-static analysis is then modified by dynamic effects, and the quantity W_T in *Eq 28* is not equal to the work input to the body. This does not necessarily mean a work potential does nto exist. In fact, the assumption of quasi-static crack growth was not used to arrive at *Eq 19*. The functions $F_n(q_j)$ may reflect, at least in part, an average effect of unstable rapid steps of microcrack growth.

Significance of the Areas A_k

Through principles of fracture mechanics we obtained a work potential W_T, and furthermore related it to physically identifiable parameters A_k and material-related functions W_j and W. Conceptually, all cracks are considered to preexist with given initial sizes and orientations; but many or all may be so small initially that they have no real effect on the work potential. In principle, as many A_k are to be used as are needed to fully define the instantaneous location and orientation of all crack surfaces and their growth. For example, a crack edge that advances nonuniformly along its length may require the use of many small areas or parameters A_k to define the changing geometry. With complex arrays of cracks, this formulation is not practical unless idealizations, such as periodicity and regular shapes, or statistical representations are introduced. Non-unique solutions $A_k(q_j)$ would further complicate the problem, giving rise to effects of the history $q_i(t)$. In such a case, one may have to solve for changes in A_k using small changes in q_i. Of course, our purpose was simply to argue that a work potential exists; nevertheless, it should be recognized that even with a work potential, there could be effects of the displacement history. Additional complications could arise with friction between adjacent crack faces, in that a work potential does not always exist if there is appreciable energy dissipation through sliding processes; however, it should be recalled that significant plastic deformation (slip) processes may occur in metals and yet a potential exists for some histories, as modeled by the deformation theory of plasticity.

One could think of the parameters A_k as "internal variables," such as used in irreversible thermodynamic formulations; they need not be areas as long as they fit the above mathematical model. Although it is not necessary here, we may write the equations that govern their growth, *Eq 24* or equivalently $G_{ck} = G_k$, in a rate form similar to that used in thermodynamic models. First differentiate $G_{ck} = G_k$ with respect to time,

$$\sum_m \frac{\partial G_{ck}}{\partial A_m}\frac{dA_m}{dt} = \sum_m \frac{\partial G_k}{\partial A_m}\frac{dA_m}{dt} + \sum_j \frac{\partial G_k}{\partial q_j}\frac{dq_j}{dt} \tag{32}$$

where, for simplicity, explicit time-dependence (e.g., aging) in G_{ck} and G_k is omitted.
Solve for dA_m/dt,

$$\frac{dA_m}{dt} = \sum_{kj} H_{mk}\frac{\partial G_k}{\partial q_j}\frac{dq_j}{dt} \tag{33}$$

where H_{mk} is the inverse of the matrix G_{km},

$$G_{km} = \partial G_{ck}/\partial A_m - \partial G_k/\partial A_m \tag{34}$$

Complimentary Work Potential

In many problems it is desirable to use the Q_j instead of q_j as the independent variables. All of the preceding theory could have been formulated in this way, in which a complementary work potential W_c, say, would be used, where

$$q_j = \partial W_c/\partial Q_j \tag{35}$$

For the one-dimensional case in *Fig. 1*, W_c is the area to the left of the curves,

$$W_c = \int_0^s e\,ds' \tag{36}$$

where $e = f(s', s_m)$ or $e = f(s', s')$, depending on the curve to be used, and s_m is the maximum stress. The relationship between W_T and W_c is

$$W_T + W_c = \sum_{j=1}^{J} Q_j q_j \tag{37}$$

Observe that we may start with *Eq 27* and then define W_c by *Eq 37*; differentiation of the latter equation yields *Eq 35*. Alternatively, we could reverse the process. Thus, if W_T exists so does W_c, and vice-versa. It should be noted that these potentials are multivalued, and therefore one has to interpret their interrelationships on a process-by-process basis. For instance, in identifying a particular (s, e) pair for the example in *Fig. 1*, it is obviously necessary to specify whether the loading or unloading curve is to be used.

ANGLE-PLY COMPOSITE BARS UNDER AXIAL AND TORSIONAL LOADING

The multidimensional theory provides support for using work potentials to characterize

the behavior of materials and structures with damage. In this and in the next two Sections we describe studies of polymeric composite materials that give preliminary experimental confirmation of this characterization for damaging processes.

Work using laminates of graphite fiber-reinforced epoxy under axial and torsional loading is described in this Section. The tests specimens are flat bars, as illustrated in *Fig. 2*, which consist of several plies or layers, each being a relatively brittle, elastic composite with continuous, unidirectional fibers having an angle θ with respect to the bar's axis; $\theta = \pm 30°$ are used in the specimens discussed here. The unidirectional material was supplied in pre-preg form by Hercules, Inc., and is designated as AS4/3502. It should be emphasized that even though there are strain gradients and consequent nonuniform damage (primarily in the form of distributed microcracks and, at high loads, edge delaminations) the multidimensional theory may be used. (Basic stress-strain behavior using thin-walled tubes will be studied in the near future after acquiring additional laboratory equipment.)

The generalized variables of the Section on Multidimensional Theory will be identified with the specific mechanical variables for the bar as follows: axial elongation, $u = q_1$; rotation angle between ends, $\Omega = q_2$; axial load, $F = Q_1$; and torque, $T = Q_2$. The total work potential W_T, *Eq 28*, is the work input to the entire bar through the relatively rigid grips.

The necessary and sufficient conditions for existence of a potential, *Eq 16*, for the present problem reduce to the single equation,

$$\partial F/\partial \Omega = \partial T/\partial u \qquad (38)$$

Before using *Eq 38* with experimental data, it is helpful to replace the variables by measures of stress and strain. This normalization process eliminates first-order effects of specimen-to-specimen dimension differences. Specifically, we shall use "nominal" stresses and strains defined as

$$s = F/bc \qquad \tau = 3T/bc^2 \qquad e = u/L \qquad \gamma = c\Omega/L \qquad (39)$$

where b = width, c = thickness, and L = length (between grips). For the special case of long, thin homogeneous specimens ($L \gg b \gg c$) s and e are the uniform axial stress and strain respectively, and τ and γ are the in-plane shear stress and strain respectively at the surface. This is shown by Timoshenko and Goodier (24) for linear isotropic materials. For orthotropic materials whose planes of symmetry are parallel to the specimen surfaces, it can be shown that the same formulas apply except the width is modified by a ratio of moduli. The shear strain magnitude is zero at the mid-plane and increases linearly to the specimen faces ($L \times b$) in *Fig. 2*. Whether the stated conditions apply, the variables in *Eq 39* are useful for normalizing data. *Equation 38* becomes

$$\partial s/\partial \gamma = \partial(\tau/3)/\partial e \qquad (40)$$

This equation has been used to analyze the data in *Figs. 3* and *4* by first writing

$$\tau/3 = \tau_o/3 + g \qquad (41)$$

where $\tau_o = \tau_o(\gamma)$ is the shear stress for $e = 0$; also $g = g(e, \gamma)$ in which $g(o, \gamma) = 0$. Next, integration of *Eq 40* with respect to γ yields

$$s = \frac{\partial}{\partial e}\int_o^\gamma g(e, \gamma')d\gamma' + s_o \qquad (42)$$

where $s_o = s_o(e)$ is the axial stress when $\gamma = 0$. Thus, the quantity

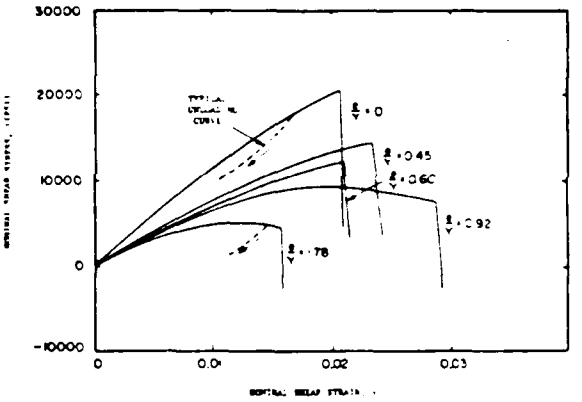

Fig. 3. Representative shear stress-strain curves with proportional axial and torsional straining. Hercules AS4/3502 graphite/epoxy: 24 plies [30]$_{6S}$, 2.5 in. long x 0.25 in. wide x 0.13 in. thick.

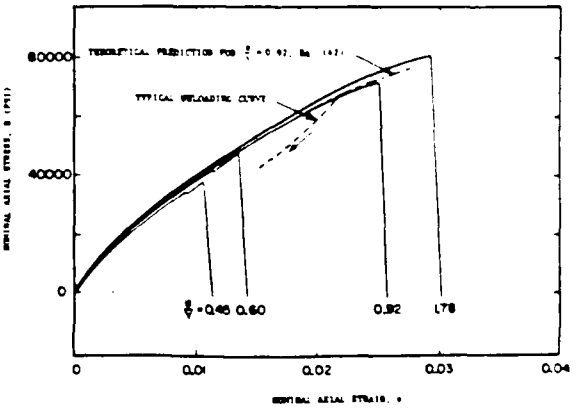

Fig. 4. Representative axial stress-strain curves with proportional axial and torsional straining from the same tests used for Fig. 3.

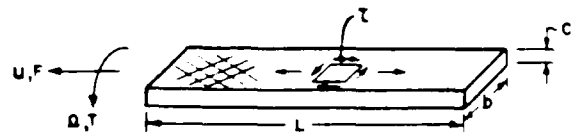

Fig. 2. Laminate specimen used in axial-torsional tests.

$$\Delta s = \frac{\partial}{\partial e}\int_0^\gamma g(e, \gamma')d\gamma' \qquad (43)$$

is the change in axial stress due to the twist induced shear strain. This integrated form is to be preferred over the original *Eq 40* because of the inaccuracy resulting from differentiation of experimental data, especially considering the small amount of data available.

The procedure used to check for the existence of a work potential was to cross-plot the data in *Fig. 3* so as to obtain g (which is proportional to the change in shear stress due to axial strain) as a function of γ, for fixed values of e, and then predict the modification to axial stress, *Eq 43*. Considering the limited amount of data available, it is desirable to curve fit analytical expressions to the data to aid the needed interpolations and extrapolations. It was found for a wide range of strains that

$$\int_0^\gamma g(e, \gamma')d\gamma' = A\gamma^{2.55}e^{(B+C\gamma)} \qquad (44)$$

where A, B, and C are constants. Using this expression in *Eq 43* yields the change in axial stress due to twist. Only for $e/\gamma = 0.92$ is there a significant effect of twist prior to fracture; the prediction is drawn in *Fig. 4*. The agreement between theory and experiment is relatively good.

In the series of tests shown in *Figs. 3* and *4* there is only one specimen for each deformation history, and thus the small differences between most curves in *Fig. 4* could be as large as specimen-to-specimen differences. Nevertheless, it is encouraging that all of the predictions from *Eq 43* turned out to be of the same order as the observed differences in axial stress. Axial stress for $\gamma = 0$ is not shown, but it was essentially the same as for $e/\gamma = 1.78$ in *Fig. 4* until premature failure occurred; the latter results were used in the theoretical predictions. Although not needed to check for the existence of a potential, it is of interest to observe that when there is little or no coupling effect of twist and axial deformation, the stress-strain curves obey power laws over a wide range of strains; this is shown in *Fig. 5* where

$$s \sim e^m \quad \text{and} \quad \tau \sim \gamma^n \qquad (45)$$

We have conducted additional exploratory tests using proportional straining of laminates with various widths, thicknesses, and fiber angles, all of the angle-ply design ($\pm\theta$) with balanced, symmetric layups. The behavior is similar to that already discussed, with comparable verification of *Eq 43*. Close to the end point of the curves, where large scale delamination or failure at the grips occurs, theoretical and experimental curves tend to separate, as seen in *Fig. 4*. This difference may be due to inaccuracy in the extrapolations needed for *Eq 43* (considering the small number of specimens used), a change from damaging to constant damage processes and vice versa (cf. discussion of *Eq 20*), or an inability to use a potential in a highly damaged state. Future studies using proportional and nonproportional straining should help to explain this behavior.

For some layups with sufficient twist, mode III edge delamination occurs prior to significant material fracture near the grips. As a result, properly designed bar specimens with and without initial delaminations may be useful for studies of this type of delamination. When a work potential exists, one often can use the J integral theory or energy release rates to account for the effect of distributed damage on the delamination growth.

A HIGHLY-FILLED ELASTOMER UNDER AXIAL LOADING AND PRESSURE

Several years ago Farris (25) described large deformation studies of crosslinked rubber containing 65 volume percent of relatively hard particles. Specimens in the shape of slender rectangular bars were subjected to confining pressure and uniaxial loading. He used *reversible* thermodynamics as a basis for predicting the effect of pressure on the axial stress-strain behavior. These predictions were in quite good agreement with the measurements, in spite of strong effects from the *irreversible* processes of microcracking and void growth. Here we reexamine the behavior and use the present work potential theory as a basis for making similar predictions.

The specimen and relatively rigid grips are shown schematically in *Fig. 6*. This assembly was placed in a chamber, where it was first pressurized to a constant value p and then stretched axially at a constant crosshead rate; the axial force acting on the grips is F. Representative stress-strain and dilatation-strain data are in *Fig. 7*.

In order to select the generalized variables in *Eq 12*, we use for $\delta(Wk)$ a virtual work per unit initial specimen volume,

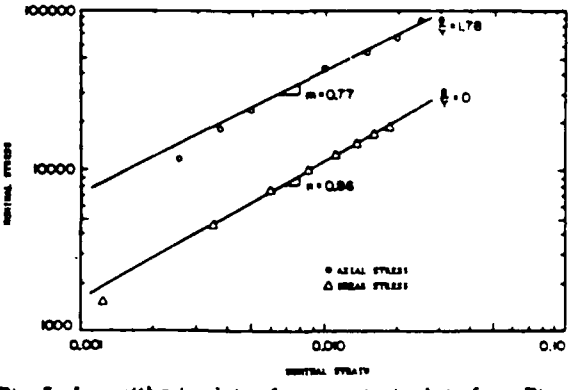

Fig. 5. Logarithmic plots of stress-strain data from Figs. 3 and 4 showing power law behavior.

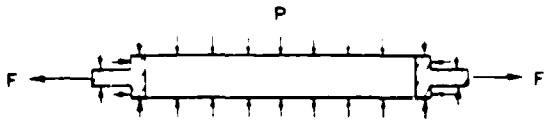

Fig. 6. Particle-filled elastomer under pressure and axial loading.

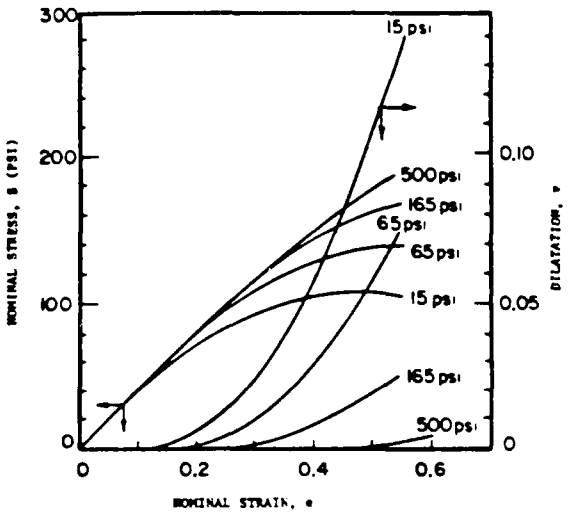

Fig. 7. Stress-strain and dilatation-strain behavior of a highly filled elastomer (65 volume percent) at a series of hydrostatic pressures c.f. Farris (25).

$$\delta(Wk) = \frac{1}{V_0}\int_A \mathbf{T}\cdot\delta\mathbf{u}\,dA \qquad (46)$$

where $\mathbf{T}$ and $\delta\mathbf{u}$ are the surface traction and virtual surface displacement vectors, respectively, and V_0 is the initial specimen volume; the integration is over the instantaneous area A of the specimen and rigid grips. On all surfaces except on the grip ends where F is applied,

$$\mathbf{T} = -p\mathbf{n} \qquad (47)$$

where $\mathbf{n}$ is the outer unit normal to the surface. It is helpful to write the normal traction on the grip ends in the form

$$T_n = T_1 - p \qquad (48)$$

where T_1 is defined by this equation. Integrating $T_n dA$ over the grip ends with area A_g, regardless of whether or not T_n is uniformly distributed, gives the axial force as

$$F = F_1 - pA_g \qquad (49)$$

where

$$F_1 = \int_{A_g} T_1 dA \qquad (50)$$

is the axial force above that due to the pressure. *Equations 47, 48, and 50*, along with the assumption of purely axial movement of the grips, reduce *Eq 46* to

$$\delta(WK) = \frac{F_1}{V_0}\delta u_1 - p\frac{\delta V}{V_0} \qquad (51)$$

where δu_1 and δV are the virtual axial elongation and volume change of the specimen respectively. Let us now choose for generalized displacements the nominal axial strain, e and dilatation, v, defined in the usual way,

$$q_1 = e = u_1/L_0, \qquad q_2 = v = V/V_0 \qquad (52)$$

where u_1 and V are the increases in specimen length and volume from the initial unstrained state (in which the length is L_0 and volume is V_0). Comparing *Eqs 12* and *51* we see that the generalized forces are

$$Q_1 = s, \qquad Q_2 = -p \qquad (53)$$

where $s = F_1/A_0$, the "nominal stress."

As in the previous Section, we shall use *Eq 16* (with $i = 2$, $j = 1$) in integrated form to determine if a potential exists. Namely, substitute the variables from *Eqs 52* and *53* and integrate with respect to v,

$$s(e, v) = -\frac{\partial}{\partial e}\left(\int_{v_0}^{v} p\,dv\right) + s(e, v_0) \qquad (54)$$

where v_0 is a constant reference value of dilatation. This result is equivalent to that used by Farris except for an additional term arising from surface or fracture energy, which he attributed to the formation of vacuoles. However, he subsequently neglected this term and then used the theory and crossplots constructed from data in *Fig. 7* to make the predictions in *Fig. 8*. For $s(e, v_0)$ the curve for $p = 500$ psi was used; although the dilatation is not constant in this case, it is very nearly so (cf. *Fig. 7*).

It should be noted that *Eq 54* is correct as it stands, in that surface or fracture energy changes are taken into account implicitly when one uses data for damaging processes. The underlying potential is W_T, *Eq 28*, which consists of the work of fracture W_f plus the deformation work W. Furthermore, no restriction has been imposed on the magnitude of the strain or its uniformity; the strains are in fact quite large, and are nonuniform at least close to the grips.

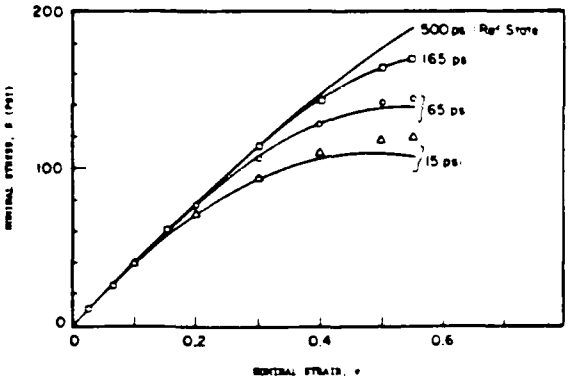

Fig. 8. Comparison of calculated (points, Eq 54) and measured (lines) stress-strain behavior from data in Fig 7 c.f. Farris (25).

The agreement between results from experiment and potential theory is seen in *Fig. 8* to be quite good. The discrepancy is relatively small compared to the differences between the various stress-strain curves and that at 500 psi; the error that does exist may be largely due to the moderate amount of viscoelasticity exhibited by this material. Note that the extent of damage is large at the low pressures, in the sense that without microcracking and the subsequent development of microcavities, the dilatation would be negligible compared to the values in *Fig. 7*. Also, the uniaxial stress-strain curves would be pressure-insensitive since, with increasing pressures, the curves approach that for essentially zero dilatation.

The results in *Figs. 7* and *8* are from tests conducted at constant pressure. Farris also gave the results in *Fig. 9*, which include a test in which the pressure was initially at 500 psi; while the sample was being strained, the pressure was suddenly lowered to 40 psi; following additional straining, it was increased to 500 psi. It is seen that after a short period of time following each pressure change, the stress-strain curve tends to approach the one for which the pressure was constant during the entire straining period. In other words, there is not a strong effect of pressure history in this case.

DELAMINATION IN DOUBLE CANTILEVERED BEAMS

The symmetric split beam test depicted in *Fig. 10* is now commonly used to determine the critical energy release G_c for the opening mode of delamination of fiber-reinforced plastics. When there is a significant volume fraction of fibers that are not parallel to the beam axis, the two legs may be highly inelastic, thus invalidating the standard elastic methods used to obtain G_c from experimental data on load, deflection, and crack length. As an illustration of the use of the

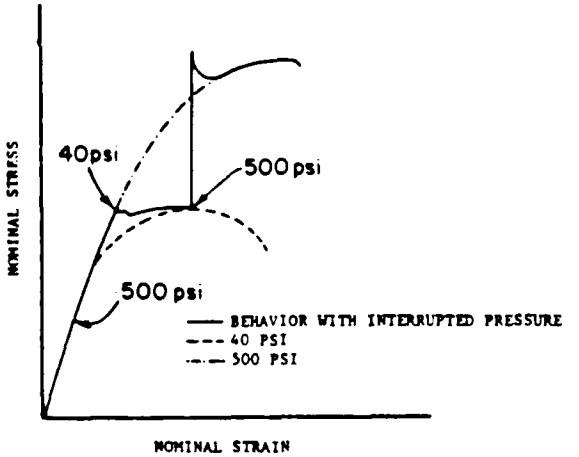

Fig. 9. Stress-strain curve for highly-filled elastomer subjected to changes in the pressure levels. After Farris (25).

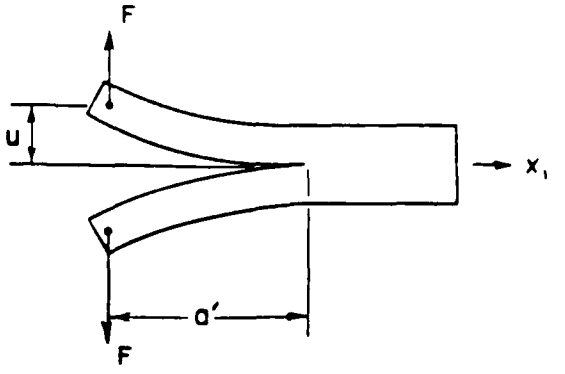

Fig. 10. Double cantilevered beam (DCB) for delamination fracture studies.

potential theory in the section on Multidimensional Theory for fracture analysis, we shall derive an equation for determining G_c in inelastic beams.

It turns out that the complementary work potential W_c, *Eq 35*, is used more conveniently for this problem than the work potential. In the formulation we shall employ, the potential W_T in *Eq 37* will include the fracture work of all microcracks but not that of the delamination. For this case the work that becomes available at the delamination crack tip for a unit of new area of surface A (projected onto the delamination plane), is given by

$$G = \partial W_c/\partial A \tag{55}$$

where the derivative is taken with generalized forces held constant. This formula can be derived by first observing that the total variation of *Eq 37* may be written in the form

$$\left(\frac{\partial W_T}{\partial A} + \frac{\partial W_c}{\partial A}\right)\delta A = \sum_{j=1}^{J}\left[\left(Q_j - \frac{\partial W_T}{\partial q_j}\right)\delta q_j + \left(q_j - \frac{\partial W_c}{\partial Q_j}\right)\delta Q_j\right] \tag{56}$$

The right side vanishes by virtue of *Eqs 27* and *35*, and therefore $\partial W_c/\partial A = -\partial W_T/\partial A$. *Equation 21* then yields *Eq 55* since we may use *Eq 21* for the delamination crack in which the work potential is W_T instead of W, allowing for the work of microcrack extension introduced in *Eq 28*.

For the DCB specimen in *Fig. 10*, let $F = Q_1$ and $2u = q_1$. Use a and b to define the instantaneous crack length and specimen width referred to the unstrained (flat beam) geometry and then take $A = ab$. The complementary work for the total test specimen is

$$W_c = W_c(F, a) = 2\int_0^a w_c dx_1 + W_c' \tag{57}$$

where x_1 is a coordinate along the specimen centerline (which defines the location of material points in the unstrained geometry) and $x =$

0 is at the initial line of load application. The quantity w_c is defined as the complementary work density (based on unit length) for each leg from classical beam theory; namely, the theory based on the assumption that material planes that are initially normal to the beam axis remain plane and normal when the beam is deformed. The correction to beam theory is denoted by W_c'. The energy release rate becomes

$$G = \frac{1}{b}\frac{\partial W_c}{\partial a} = \frac{2}{b}w_c(a) + \frac{2}{b}\int_0^a \frac{\partial w_c}{\partial a}\,dx_1 \quad (58)$$

after neglecting $\partial W_c'/\partial a$. For long beams W_c' is primarily from distortion of the beam immediately to the right of the delamination crack tip, and $\partial W_c'/\partial a$ can be shown to vanish if the beam is long enough that the crack tip is essentially isolated from the ends.

Equation 58 is not restricted to small strains and rotations. As such, the horizontal distance a' in *Fig. 10* may be significantly less than the actual length of the crack surface a. However, we shall simplify the analysis by assuming small strains and rotations and further assume both legs are symmetric and balanced laminates in the undamaged and damaged states. With these conditions there is no mid-plane stretching or twisting, and beam theory gives the simple result

$$w_c = \int_0^M k\,dM' \quad (59)$$

where $k = k(M')$ is the curvature as a function of the moment. A moment-curvature diagram for inelastic material would be similar to the stress-strain diagram in *Fig. 1*; the complementary work, *Eq 59*, is thus to be evaluated taking into account the multivalued relationship, as discussed in the One-Dimensional Theory Section. The local beam moment is

$$M = Fx_1 \quad (60)$$

and therefore the integral in *Eq 58* vanishes as w_c is independent of a. Thus, we obtain

$$G = \frac{2}{b}w_c(a) = \frac{2}{b}\int_0^{M_a} k(M)dM \quad (61)$$

where $M_a = Fa$ is the crack tip moment.

This result has been used by Jordan (26) to analyze delamination of two different graphite/epoxy material systems with plies having various fiber orientations; one system had a rubber-toughened resin and the other a brittle resin system. *Figure 11* gives a typical load-displacement diagram for the latter one. The short inclined lines represent periods of no crack growth following sudden jumping at loads along the dashed line. Measurement of crack length and corresponding loads indicated that the crack tip moment at the beginning of each jump in crack length was approximately constant for all tests in the series. Four-point bend tests were used to develop the moment-curvature diagram of beams with the layup of one-half of the DCB specimen, i.e., for one leg. Knowing the moment for crack growth from the DCB tests and the moment-curvature diagram from the four-point bend tests made it possible to derive the critical energy release rate from *Eq 61*, the average moment at which crack jumping occurred for each DCB specimen was used for M_a. This calculation, which is illustrated in *Fig. 12*, gave values for G_c that were practically the same for all layups of each of the two graphite/epoxy systems. Indeed, the G_c for unidirectional ($\theta = 0°$) laminates was close to that for the layup with multiple fiber orientations. In contrast, standard data analysis based on beam deflection and load gave G_c values that differed considerably for the several layups; some multiple-fiber angle layups had apparent G_c values over twice that for $\theta = 0$.

These findings not only help to support the underlying potential theory, but also reveal sur-

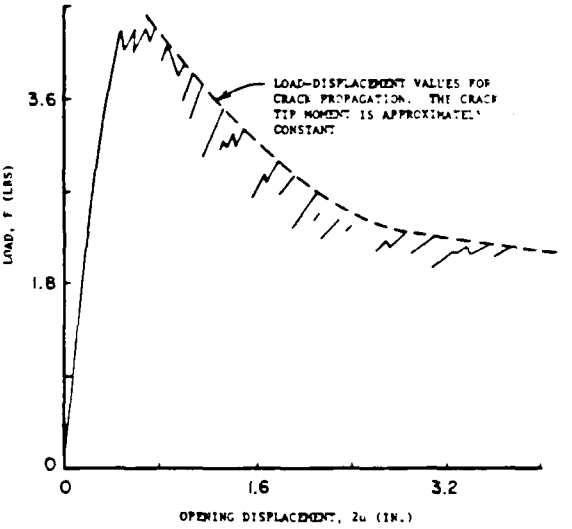

Fig. 11. A typical load-displacement record for opening mode loading of a double cantilevered beam with off-axis plies at the center interface. Hercules AS4/3502 graphite/epoxy. After Jordan (26).

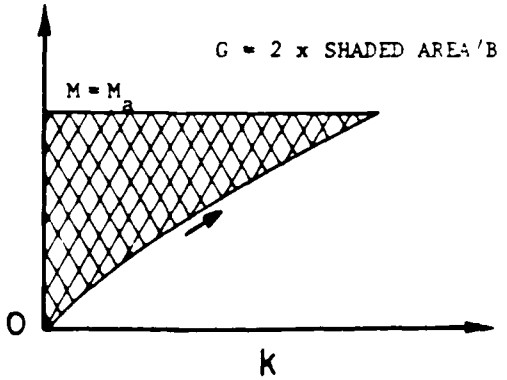

Fig. 12. Moment-curvature diagram for loading, showing energy release rate, G.

prisingly simple behavior, considering especially how much microcracking develops in the specimens whose bending is not fiber-dominated. The layup insensitivity of G_c seems to indicate that the local normal interface stress, rather than local layup-induced shear stress, is the primary factor in delamination. Of course, the findings are from a limited set of tests on only two composite systems, and therefore one should be cautious about extrapolating the findings to other laminates.

Finally, it is of interest to consider the relationship of the above results to Rice's J integral (19), as extended to crack growth in inelastic media with large deformations by Schapery (20). The quantity J is defined by a contour integral, which becomes for the beam problem in *Fig. 13*,

$$J = \int_C \left[w_0 dx_2 - \left(T_1 \frac{\partial u_1}{\partial x_1} + T_2 \frac{\partial u_2}{\partial x_1} \right) dL \right] \quad (62)$$

where w_0 is the work potential density, T_1 and T_2 are tractions along C, and u_1 and u_2 are displacements; the indices indicate components in the x_1 and x_2 directions. This equation is valid for large strains and rotations as long as we interpret x_1 and x_2 to be coordinates of the undeformed geometry. The integration is counterclockwise along the curve C in *Fig. 13*, which includes top and bottom beam surfaces and vertical segments. The right vertical segment is taken far enough from the crack tip that the material is unstressed, and thus gives no contribution. For the top and bottom segments, $dx_2 = T_1 = T_2 = 0$, and thus the only contribution comes from the left segment. Assuming small strains and that the left segment is close enough to the crack tip that we can use small rotation beam theory, yields,

$$J = \frac{2}{b} \int_0^M k(M')dM' - 2 \frac{F}{b} \frac{du_2}{dx_1} \quad (63)$$

where M and du_2/dx_1 are the moment and slope, respectively, at the left vertical segment. Integrate $k = d^2u_2/dx_1^2$ to obtain the slope, and *Eq 63* reduces to

$$J = \frac{2}{b} \int_0^{M_a} k(M)dM \quad (64)$$

where M_a is the crack tip moment. This is the same result derived by Rice (19) for a split beam under end moments M_a. It is seen that the result is independent of the location of the left integration segment and, in fact, is that in *Eq 63* when the segment is located at the crack tip (where $du_2/dx_1 = 0$). It should be mentioned, however, to obtain this path independence (i.e., derive *Eq 64* from *63*) it was necessary to assume if $k(M)$ is multivalued (cf. *Fig. 1*) that the unloading curve is the same for all left vertical segments used. This latter condition will be met for all material (to the left of the current tip) that had experienced the same maximum moment when the crack tip passed by. Inasmuch as the experimental results discussed above indicate the maximum moment is constant (and recognizing that the moment decays with distance from the tip), this condition is met all of the way to the location of the initial crack tip. To the left of the initial tip, the maximum moment is less than M_a and one finds J depends on the location of the left segment. This path dependence in beam theory is fully consistent with that predicted from the exact J integral for a continuum with variable damage in the regions of unloading (20). Some unloading may occur in the continuum very close to the crack tip, possibly causing path dependence and thus affecting *Eq 64*. Weatherby (27) used a finite element analysis to study this dependence for a strongly nonlinear isotropic beam and found that the effect on J is negligible; his analysis predicted a J value very close to that in *Eq 64*.

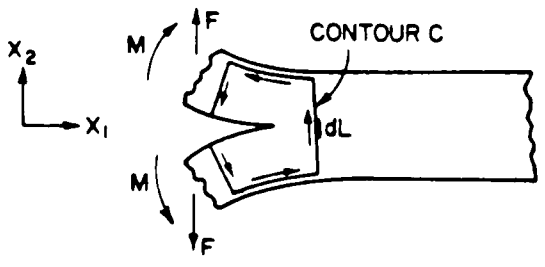

Fig. 13. Contour used to evaluate J integral.

For a crack propagating at a constant moment in a long laminate that is initially homogeneous in the x_1 direction, the state of stress and strain in the neighborhood of the tip is constant in time. This is a type of "self-similar" growth and therefore (19, 20)

$$G = J \quad (65)$$

Equations 61 and *64* agree with this general result. Equally important, *Eq 64* was derived without assuming small rotations (except for the neighborhood of the tip). Therefore, in view of *Eq 65*, we may conclude that the formula for work available at the crack tip, *Eq 61*, is valid even when the DCB legs undergo large rotations and possibly high axial tensile strains from the axial component of F. When this geometric nonlinearity exists one should use a' (cf. *Fig. 10*) instead of a to determine the crack tip moment.

VISCOELASTIC BEHAVIOR

For some types of linear and nonlinear viscoelastic materials the Multidimensional Theory may be used by simply replacing the generalized displacements with "pseudo generalized displacements," q_j^R, where

$$q_j^R = E_R^{-1} \int_0^t E(t - \tau, t) \frac{\partial q_j}{\partial \tau} d\tau \quad (66)$$

Here q_j is the physical generalized displacement

in terms of the dummy time variable of integration τ and other relevant quantities such as coordinates x. The quantity $E = E(t - \tau, t)$ is a relaxation modulus, which imparts hereditary characteristics to the deformation behavior. The second t argument in E allows for aging and other kinds of time-dependence, such as may be due to transient temperature. The coefficient E_R is a "reference modulus," which is an arbitrarily selected constant that is introduced so that q_j^R and q_j have the same units. The basis for using *Eq 66* to extend deformation and crack growth theory to viscoelastic behavior has been given by Schapery (15, 20). Here we mention only that it is an exact approach for linear isotropic viscoelastic materials with a Poisson's ratio that is constant in the undamaged state and for nonlinear viscous materials. The latter case is easily deduced by noting that if the relaxation modulus is proportional to a Dirac delta function, i.e., $E = E_R t_R \delta(t - \tau)$, where t_r is a time constant, then *Eq 66* reduces to

$$q_j^R = t_R dq_j/dt \tag{67}$$

The pseudo displacement is proportional to velocity with this modulus choice. Replacement of q_j by this q_j^R in *Eqs 19, 27,* and *35* converts them to equations for viscous media.

Elastic-viscoelastic correspondence principles were developed (15, 20), which then lead to the development of the theories for effective properties of composites (15) and crack and damage growth (20). To date only limited, but encouraging, experimental work on nonlinear viscoelastic materials has been done to verify this approach based on pseudo displacements (28, 29). In a study (29), a highly-filled elastomer was subjected to complex uniaxial loading histories. The experimentally measured axial displacement u of tensile coupons was converted to nominal strain e and then to pseudo strain e^R using *Eq 66*, and the axial stress was plotted against e^R for constant damage states. It was found that this method of plotting data essentially eliminated viscoelastic effects, thus confirming the approach. For damaging processes, the material behaved as a nonlinear elastic material with history-dependent damage when represented in terms of e^R. Guided by simple models for damage and some test data, the nonlinear viscoelastic stress-strain equation was developed and then verified experimentally using loading histories not included in the characterization process.

Besides employing the maximum value e_m^R to account for damage, as e_m is used in *Eq 3*, a so-called Lebesque norm was used in (29),

$$L_q = \left[\int_0^t |e^R|^q dt\right]^{1/q} \tag{68}$$

where $|\cdot|$ denotes absolute value and q is a positive constant; the damage parameter L_q arises from viscoelastic crack growth theory. If q is sufficiently large L_q (and its generalization to multidimensional problems) may often lead to constitutive equations that are analogous to those discussed in Sections on One-Dimensional Theory and Multidimensional Theory, but there may be explicit dependence of the potentials W, W_f, and W_c on time, and thus they would be like those for aging elastic materials with damage. For example, $e^R \geq 0$ and $q = 6.5$ in Ref. 29, and in this case,

$$L_q \simeq e^R t^{1/q} \quad \text{when} \quad de^R/dt > 0 \tag{69}$$

and

$$L_q \simeq e_m^R t^{1/q} \quad \text{when} \quad de^R/dt = 0 \tag{70}$$

If e^R reaches a maximum at $t = t_m$ and then decreases,

$$L_q \simeq e_m^R t_m^{1/q} \tag{71}$$

Behavior like that in *Eqs 69* and *70* reflects the growth of microcracks until the "driving force" e^R falls below its maximum value.

CONCLUSIONS

An approach using work potentials to characterize deformation and fracture behavior of inelastic materials has been described. Some experimental results on polymeric composites were presented to illustrate it and give a preliminary verification of the theory. If the use of work potentials to account for the effect of damage and other types of inelasticity is further substantiated in future studies, one may take advantage of the simplifications that come from this approach in the mathematical modelling of both deformation and fracture behavior. When pseudo displacements, *Eq 66*, can be used to extend the time-independent characterization to nonlinear viscoelastic behavior, additional experimental requirements and mathematical model complexity are not much more than what is needed for linear viscoelastic behavior.

ACKNOWLEDGMENT

This author is grateful to the U.S. Air Force of Scientific Research, Office of Aerospace Research, for sponsoring this work, and to Mr. Mark Lamborn, graduate research assistant, for doing the axial-torsional testing of laminates and data analysis.

NOMENCLATURE

a	= crack length.
A, A_k	= crack areas.
b	= beam width.
e	= nominal strain (axial extension/initial length).
e_{ij}	= strain tensor.
$E(t - \tau, t)$	= relaxation modulus.
F	= force.
F_n	= damage function.
F_{cn}	= damage parameter.
G, G_k	= energy release rates.

G_c, G_{ck} = critical energy release rates.
J = J integral.
k = curvature.
L = beam length.
L_q = Lebesque norm.
M = moment.
p = pressure.
q_j = generalized displacement.
Q_j = generalized force.
s = nominal stress (axial stress/initial cross sectional area).
s_{ij} = stress tensor.
t = time.
T = torque.
u = displacement.
v = dilatation.
V = increase in volume.
V_0 = initial volume.
w_c = complementary work density.
W_c = complementary work potential.
W, W_T = work potentials.
W_f = fracture work potential.
x_i = Cartesian coordinates.
γ = nominal shear strain.
τ = nominal shear stress.
Ω = angle of twist.

REFERENCES

1. Y. C. Fung, "Foundations of Solid Mechanics," Prentice-Hall, Inc., Englewood Cliffs, New Jersey (1965).
2. Z. Hashin, *J. Appl. Mech.*, **50**, 481 (1983).
3. M. Kachanov, *J. Eng. Mech. Div. ASCE*, **106**, 1039 (1980).
4. R. Hill, *J. Mech. Phys. Solids*, **5**, 66 (1956).
5. M. A. Biot, *Phys. Rev.*, **97**, 1463 (1955).
6. T. G. Rogers and A. C. Pipkin, *ZAMP*, **14**, 334 (1963).
7. R. A. Schapery, *J. Compos. Mater.*, **1**, 228 (1967).
8. J. R. Rice, *J. Appl. Mech.*, **37**, 728 (1970).
9. J. M. Duva and J. W. Hutchinson, *Mechanics of Materials*, **3**, 41 (1984).
10. L. E. Malvern, "Introduction to the Mechanics of a Continuous Medium," Prentice-Hall, Inc., Englewood Cliffs, New Jersey (1969).
11. J. R. Rice, *J. Mech. Phys. Solids*, **19**, 433 (1971).
12. B. D. Coleman and M. E. Gurtin, *J. Chem. Phys.*, **47**, 597 (1967).
13. R. A. Schapery, "Further Development of a Thermodynamic Constitutive Theory: Stress Formulation," AA & ES Report No. 69-2, Purdue Univ. (1969).
14. R. A. Schapery, in B. A. Boley, ed. "Thermoinelasticity," Springer-Verlag, New York, 259 (1970).
15. R. A. Schapery, in S. S. Wang and W. J. Renton, eds. "1981 Advances in Aerospace Structures and Materials," The American Society of Mechanical Engineers, New York, 5 (1981).
16. D. Broek, "Elementary Engineering Fracture Mechanics," 3rd ed., Martinus Nijhoff Publishers, Boston (1982).
17. G. J. Lake, in "Progress of Rubber Technology," Applied Science Publishers Ltd., London, 89 (1983).
18. E. H. Andrews, *J. Mater. Sci.*, **9**, 887 (1974).
19. J. R. Rice, *J. Appl. Mech.*, **35**, 379 (1968).
20. R. A. Schapery, *Int. J. Fracture*, **25**, 195 (1984).
21. M. E. Gurtin and E. C. Francis, *J. Spacecraft and Rockets*, **18**, 285 (1981).
22. R. M. Jones, "Mechanics of Composite Materials," Scripta Book Co., Washington, D.C. (1975).
23. M. D. Greenberg, "Foundations of Applied Mathematics," Prentice-Hall, Inc., Englewood Cliffs, New Jersey, 170 (1978).
24. S. P. Timoshenko and J. N. Goodier, "Theory of Elasticity," 3rd ed., McGraw-Hill, New York (1970).
25. R. J. Farris, *Trans. Soc. Rheol.*, **122**, 303 (1968).
26. W. M. Jordan, "The Effect of Resin Toughness on the Delamination Fracture Behavior of Graphite/Epoxy Composites," PhD Dissertation, Interdisciplinary Engineering, Texas A&M Univ. (Dec. 1985).
27. J. R. Weatherby, "Finite Element Analysis of Crack Growth in Inelastic Media," PhD Dissertation, Mechanical Engineering, Texas A&M Univ. (May 1986).
28. R. A. Schapery and M. Riggins, in R. Dungar, G. N. Pande, and J. A. Studer, eds: "Numerical Models in Geomechanics," A. A. Balkema, Rotterdam, 172 (1982).
29. R. A. Schapery, "Proc. Ninth U.S. Nat. Cong. Appl. Mech.," Book No. H00228, ASME, New York, 237 (1982).

Reprinted from

ENCYCLOPEDIA OF MATERIALS SCIENCE AND ENGINEERING

Editor-in-Chief

Michael B Bever

Massachusetts Institute of Technology

PERGAMON PRESS

Oxford · New York · Toronto · Sydney · Frankfurt

diameter of 1 m or more. The sapwood is pale reddish yellow and clearly demarcated from the heartwood, which varies from dull reddish brown to deep red. Growth rings are distinct and relatively wide, but the summerwood bands are narrow. The grain is straight and the texture coarse and even. The wood is very light and soft and fairly easy to work with hand and machine tools. It dries well without degradation but is easy to cleave. The heartwood weathers well. The wood has a pleasant scent because it contains about 2% of hydroxysugiresinol, and is permeable to preservatives. The timber is used in building construction, panelling, ceiling boards, joinery, furniture, poles, piles, vats and boxes. Species with similar properties and uses are taiwania (*Taiwania cryptomerioides*), Chinese fir or shā mù (*Cuninghamia sinensis* or *C. lanceolata*) and Formosa fir (*C. konishii*). These species are important plantation trees in China and Taiwan.

YEZO SPRUCE (*Picea jezoensis*), also known as yeddo spruce, yezomatsu (Japan), gamunbi namu or ka-munpi (Korea) and yülin-sŏng (China), grows in northeast Asia, northern Japan, Korea and Sakhalin. It is one of the most important plantation trees in Japan, and is a conifer that reaches a height of 30 m and a diameter of 1 m. The sapwood and heartwood are not demarcated, both being pale beige or pale yellow. Fine pitch streaks are found frequently. The grain is straight and the texture fine and even. Planed surfaces are lustrous. The wood is very light, soft and resilient. It machines, seasons and finishes well. The wood splits easily but has excellent weathering properties. Uses are in house construction, interior trim, siding, joinery, musical instruments, poles, ship- and boatbuilding, vehicle bodies and airplanes and for pulp and fiberboard. Species with similar properties and uses are Hokkaido spruce or akayezomatsu (*P. glehnii*), Siberian spruce (*P. obovata*), Japanese fir or todomatsu (*Abies schalinensis*), Taiwan fir (*A. kawakamii*), Taiwan spruce (*P. morrisonicola*), euan sun (*P. asperata*) and others in China (*P. manshurica*, *P. pungsanensis*, *P. tonaiensis*, *P. aurantiaca* and *P. retroflex*).

See also: Timbers of Southeast Asia, Timber Resources of the World, Wood: An Overview.

Bibliography

Brown W H 1978 *Timbers of the World*, Vols. 3–5: *Timbers of Southern Asia, Timbers of South East Asia, Timbers of the Philippines and Japan*. Timber Research and Development Association, High Wycombe.

Hirai S (ed.) 1980 *Encyclopedia of Woods*, Vols. 1–17. Kanae Shobō, Tokyo [in Japanese].

Rendle B J (ed.) 1970 *World Timbers*, Vol. 3: *Asia and Australia and New Zealand*. Benn, London.

A. Takahashi

Time-Dependent Fracture: Continuum Aspects of Crack Growth

The growth of microcracks and macrocracks is affected by time-dependent material behavior, regardless of whether it is limited to the crack tip neighborhood or exists throughout the body. This article is concerned with specific ways in which rheological properties of continua affect both initiation and continuation of crack growth under quasi-static conditions (i.e., when inertial effects due to straining can be neglected). The highly damaged and failing material at the tip of growing cracks is not explicitly modelled; rather, emphasis is on the use of mechanics and properties of the surrounding continuum to predict local crack tip deformation, stresses and the mechanical work available for extending cracks. Deformation fields based on bounded rather than infinite strains at crack tips are used in order to retain important local strain rate effects. The analysis is simplified by using small strain theory for the continuum, while allowing for large strains in the failing material at crack tips.

1. Constitutive Equations

Outside of the highly damaged and failing material at crack tips, the deformation behavior is assumed to be characterized by a nonlinear viscoelastic constitutive equation in the form of a single hereditary integral for the strain tensor:

$$\boldsymbol{\varepsilon}_{ij} = E_R \int_{0^-}^{t} D(t-\tau, t) \frac{\partial \boldsymbol{\varepsilon}^f_{ij}}{\partial \tau} d\tau \qquad (1)$$

The quantity $\boldsymbol{\varepsilon}^f_{ij}$ is a second-order tensor which depends on material properties and, in general, is a function of the stress tensor $\boldsymbol{\sigma}_{ij}$, material point $\boldsymbol{x}_m$, and time t:

$$\boldsymbol{\varepsilon}^f_{ij} = \boldsymbol{\varepsilon}^f_{ij}(\boldsymbol{\sigma}_{kl}, \boldsymbol{x}_m, t) \qquad (2)$$

in which $\boldsymbol{\sigma}_{kl} = \boldsymbol{\sigma}_{kl}(\boldsymbol{x}_i, t)$, with all indices taking the values 1, 2, 3. The coefficient E_R is a free constant which will be termed the reference modulus; it is a useful parameter in discussing special material behavior and introducing dimensionless variables.

When $\boldsymbol{\varepsilon}^f_{ij}$ is used in Eqn. (1), the time argument is specified as the variable of integration; that is, t should be replaced by τ where explicitly shown in Eqn. (2) and in the argument of the stress. To simplify notation, the arguments of stress and strain will not be written out unless required for clarity. For all cases it will be assumed that $\boldsymbol{\varepsilon}_{ij} = \boldsymbol{\varepsilon}^f_{ij} = \boldsymbol{\sigma}_{ij} = 0$ when $t < 0$ and $D(t-\tau, t) = 0$ when $t < \tau$. To allow for the possibility of a discontinuous change in $\boldsymbol{\varepsilon}^f_{ij}$ with time at $t = 0$, the lower integration limit in Eqn. (1) and succeeding hereditary integrals should be interpreted as 0^- unless indicated otherwise.

The quantity $\boldsymbol{\varepsilon}^f_{ij}$ will be called pseudo strain. Its

explicit dependence on x_m in Eqn. (2) accounts when necessary for material nonhomogeneity. t is introduced to allow for aging and time-dependent residual strains (such as those due to thermal expansion (Schapery 1981)). The function $D(t - \tau, t)$ is a creep compliance; it provides creep under constant stress as well as other hereditary effects under time-varying stress in both aging and nonaging materials. The significance of ε_{ij}^{e} and D will be shown by considering some special cases.

First, however, it will be useful to rewrite Eqns. (1) and (2) by expressing stress in terms of strain history. Supposing that the inverses exist, Eqn. (2) becomes

$$\sigma_{ij} = \sigma_{ij}(\varepsilon_{kl}^{e}, x_m, t) \tag{3}$$

where ε^{e} is related to the physical strain through the inverse of Eqn. (1)

$$\varepsilon_{ij}^{e} = E_R^{-1} \int_{-\infty}^{t} E(t - \tau, t) \frac{\partial \varepsilon_{ij}}{\partial \tau} d\tau \tag{4}$$

in which E is a relaxation modulus, its relationship to D is given by

$$\int_{\tau_0}^{t} D(t - \tau, t) \frac{\partial}{\partial \tau} E(\tau - \tau_0, \tau) d\tau = H(t - \tau_0) \tag{5}$$

where $\tau_0 \geq 0$ and $H(t - \tau_0)$ is the Heaviside step function (i.e., $H(t - \tau_0) = 0$ and 1 for $t < \tau_0$ and for $t > \tau_0$, respectively).

A linear viscoelastic material without residual stresses which is isotropic, homogeneous and has a constant Poisson's ratio ν is characterized by Eqn. (1) if we use

$$\varepsilon_{ij}^{e} = E_R^{-1}[(1 + \nu)\sigma_{ij} - \nu\sigma_{kk}\delta_{ij}] \tag{6}$$

where δ_{ij} is the Kronecker delta, and the standard summation convention is followed in which repeated indices imply summation over their range. For a uniaxial stress state, $\sigma_{11} \neq 0$ and all other $\sigma_{ij} = 0$, Eqn. (1) for ε_{11} becomes

$$\varepsilon_{11} = \int_{-\infty}^{t} D(t - \tau, t) \frac{\partial \sigma_{11}}{\partial \tau} d\tau \tag{7}$$

If $\sigma_{11} = \sigma_0 H(\tau - t_0)$, where $t_0 \geq 0$ and σ_0 is constant, Eqn. (7) reduces to $\varepsilon_{11} = D(t - t_0, t)\sigma_0$. Since $\varepsilon_{11}/\sigma_0$ is customarily termed the creep compliance, this name shall be used for D throughout this article. Similarly, if $\varepsilon_{11} = \varepsilon_0 H(\tau - t_0)$ for a uniaxial stress state, where ε_0 is constant, one finds from Eqn. (4) that the relaxation modulus, $\sigma_{11}/\varepsilon_0$, is equal to $E(t - t_0, t)$. When the second argument in D and E in Eqns. (1) and (4) is dropped, so that $D(t - \tau)$ and $E(t - \tau)$ appear in Eqns. (1) and (4), respectively, linear viscoelastic behavior for a nonaging material is described.

The mechanisms which may require the aging form to be used for D and E (e.g., $D = D(t - \tau, t)$) are not limited to chemical processes. For example, this form accounts for the effect of transient temperatures on the creep compliance and relaxation modulus, and includes the familiar thermorheologically simple behavior of polymers as a special case. It should be noted that the expression $D(t, \tau)$ is sometimes used instead of $D(t - \tau, t)$ in characterizing viscoelastic behavior of an aging material. Although both forms are equally general, the latter is used here as it is a more convenient notation in equations which govern crack growth.

Allowing now for nonlinear, anisotropic and nonhomogeneous media, it can be seen that for the special case of a constant relaxation modulus, $E = E_R$, Eqn. (4) reduces to $\varepsilon_{ij}^{e} = \varepsilon_{ij}$. Thus, Eqn. (3) becomes the constitutive equation for an elastic material (in that the current stress depends on the current strain, not past values of strain). An equivalent result is found by using $D = E_R^{-1}$ in Eqn. (1). Viscous behavior results by using $E = t_c E_R \delta(t - \tau)$ in Eqn. (4) (where $\delta(t - \tau)$ is the Dirac delta function and t_c is a time constant), or by setting $D = (t_c E_R)^{-1}(t - \tau)$ in Eqn. (1). In this case the pseudo strain is found to be proportional to the strain rate, that is, $\varepsilon_{ij}^{e} = t_c \partial \varepsilon_{ij}/\partial t$, and thus the current stress becomes a function of the current strain rate; Eqn. (1) takes this form after integrating it by parts, then differentiating and inverting the result.

Hereditary integrals will be used throughout this article, and consequently it is desirable to introduce abbreviated notation for them. Specifically, for any function f of time,

$$\{D\, df\} \equiv E_R \int_{-\infty}^{t} D(t - \tau, t) \frac{\partial f}{\partial \tau} d\tau$$

$$\{E\, df\} \equiv E_R^{-1} \int_{-\infty}^{t} E(t - \tau, t) \frac{\partial f}{\partial \tau} d\tau \tag{8}$$

Thus, Eqns. (1) and (4) become

$$\varepsilon_{ij} = \{D\, d\varepsilon_{ij}^{e}\}, \qquad \varepsilon_{ij}^{e} = \{E\, d\varepsilon_{ij}\} \tag{9}$$

2. Correspondence Principle

The close relationship between mechanical states of nonlinear elastic and viscoelastic media with stationary or growing cracks is given in this section. It is stated in the form of a so-called correspondence principle, and serves as the basis for the development of crack growth theory. First, let us introduce a reference elastic solution σ_{ij}^{R}, ε_{ij}^{R}, u^{R} corresponding to the case in which $D^{-1} = E = E_R$. This solution is defined to satisfy the field equations,

$$\frac{\partial \sigma_{ij}^{R}}{\partial x_j} = 0 \tag{10}$$

$$\boldsymbol{\varepsilon}^{R} = \tfrac{1}{2}\left(\frac{\partial \boldsymbol{u}^{R}}{\partial \boldsymbol{x}} + \frac{\partial \boldsymbol{u}^{R}}{\partial \boldsymbol{x}}\right) \tag{11}$$

$$\boldsymbol{\varepsilon}^{R} = \boldsymbol{\varepsilon}^{e}(\boldsymbol{\sigma}^{R}_{\infty}, \boldsymbol{x}_{\infty}, t) \tag{12}$$

The following correspondence principle will be proved in which the instantaneous geometry (including cracks) is the same for both elastic and viscoelastic problems. Let surface traction $\boldsymbol{T}_i = \boldsymbol{\sigma}_{ij} n_j$ (where $\boldsymbol{n}$ is the normal vector) be a specified function of time and position (which vanishes when $t < 0$) on all surfaces S. Then the nonlinear viscoelastic solution based on Eqn. (11) is

$$\boldsymbol{\sigma}_{ij} = \boldsymbol{\sigma}^{R}_{ij}, \qquad \boldsymbol{\varepsilon}_{ij} = \{D\, d\boldsymbol{\varepsilon}^{R}_{ij}\}, \qquad \boldsymbol{u}_i = \{D\, d\boldsymbol{u}^{R}_{i}\} \tag{13}$$

where the variables with superscript R are defined to satisfy Eqns. (10)–(12) and the traction boundary condition $\boldsymbol{T}_i = \boldsymbol{\sigma}^{R}_{ij} n_j$ on all surfaces.

As proof, first observe that the viscoelastic stress in Eqn. (13) meets the condition $\boldsymbol{T}_i = \boldsymbol{\sigma}_{ij} n_j$ on S (which includes the instantaneous crack faces) and satisfies equilibrium Eqn. (10). The pseudo strain $\boldsymbol{\varepsilon}^{R}$ obeys Eqn. (11) (compatibility condition), and clearly the viscoelastic strain in Eqn. (13) satisfies the same equation without the superscript R (since D is independent of $\boldsymbol{x}$ and the hereditary integral is a linear operator). Thus, except for consideration of displacements due to crack growth, the proposed viscoelastic solution meets the compatibility requirements. With or without crack growth, relative displacement between crack faces, $\Delta \boldsymbol{u}$, is the difference of the displacements in Eqn. (13) evaluated on adjacent faces:

$$\Delta \boldsymbol{u} = \{D\, d\Delta \boldsymbol{u}^{R}\} \tag{14}$$

where $\Delta \boldsymbol{u}^{R}$ is the displacement difference in the reference elastic problem. Since the instantaneous geometry of all cracks in the reference problem is specified to be the same as in the actual viscoelastic body, $\Delta \boldsymbol{u}$ is correctly predicted to vanish until the time t when a crack tip reaches any given physical location. This follows from the fact that $\Delta \boldsymbol{u}^{R} = 0$ at that location when $t < t_c$ (assuming prior cracking and rejoining of crack faces has not occurred), which in turn implies the hereditary integral in Eqn. (14) vanishes when $t < t_c$.

The correspondence principle may be generalized to allow for specification of displacement $\boldsymbol{U}_i$ on some or all surfaces (Schapery 1984). In this case, the specified surface displacement in the elastic problem is $\boldsymbol{U}^{e} = \{I\, d\boldsymbol{U}_i\}$ and, as in Eqn. (13), elastic and viscoelastic stresses throughout the continuum are equal with stationary and growing cracks.

3 *Generalized J Integral and the Crack Tip Model*

The J integral, widely used for fracture analysis of time-independent materials, will be generalized in this section for subsequent use with the nonlinear viscoelastic materials described by Eqn. (3). In the elastic problem the important path independence of the J integral follows in part from the thermodynamically based result that a potential W exists with the property that $\boldsymbol{\sigma}_{ij} = \partial W / \partial \boldsymbol{\varepsilon}_{ij}$. The classical deformation theory of plasticity for the loading of metals may be expressed in terms of a potential analogous to the strain energy density W, and therefore the J integral is often useful even if large-scale plastic deformation exists, as long as there is no significant unloading from the plastic state. Without excluding unloading, equations for crack growth in nonlinear viscoelastic media may be developed and expressed in terms of a J integral in many cases if $\boldsymbol{\sigma}$ in Eqn. (3) can be written as

$$\boldsymbol{\sigma}_{ij} = \partial \Phi / \partial \boldsymbol{\varepsilon}_{ij} \tag{15}$$

It has been shown that the potential Φ exists for materials under general strain histories if they are at least elastic under sudden straining (Schapery 1984). For linear viscous media one may invoke Onsager's principle to establish Eqn. (15). Although thermodynamic arguments alone apparently cannot be used to justify Eqn. (15) for nonlinear viscous behavior, the standard equations used for secondary creep of metals may be written in this form (Leckie and Hayhurst 1974). In analogy with elasticity theory, Φ is called the pseudo strain energy density.

Before developing a fracture theory which uses Eqn. (15), certain simplifications concerning the crack tip must be made. The idealized crack tip geometry and a local orthogonal set of Cartesian axes ($\boldsymbol{x}_i$) are shown in Fig. 1. In the unstrained state the crack surfaces in the neighborhood of the tip are assumed to be planar and to coincide with the local x_1x_3 plane, where x_3 is perpendicular to the plane of the page, and the x_2 axis is embedded in the continuum at any convenient horizontal location. The crack tip or edge is a straight or curved line in space whose intersection with the plane of the page is

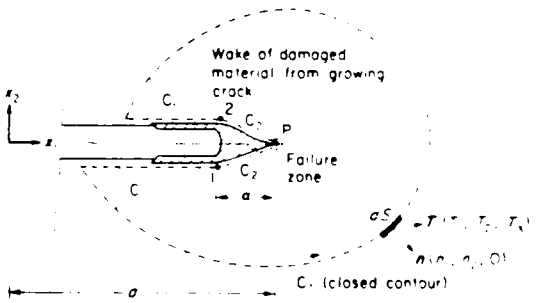

Figure 1
Cross section of crack in nonlinear viscoelastic material showing contours (– – –) used in line integrals. Only the opening mode of displacement is drawn, although the basic formulation allows for shearing deformation.

indicated by the point P. It is assumed the tip is essentially straight and parallel to x_1 in the neighborhood of P. (By definition, the neighborhood of P refers here to the material contained in a sphere which is centered at P and has a radius of about ten times the failure zone length a.)

The region designated as the failure zone in Fig. 1 is where intense damage and material separation occurs. Outside this zone it is assumed that Eqn. (15) applies. This term is preferred over other common names, such as process zone and damage zone, because the material outside may be damaged or otherwise changed and the effects taken into account in a more general theory (Schapery 1984). Also, for analysis purposes it is more convenient to define P as the crack tip location, instead of the left end of the failure zone. The latter position is called the apparent crack tip.

Consider now the line integral

$$\mathcal{L} \equiv \oint \left(\Phi \, dx_2 - \boldsymbol{T}_i \frac{\partial \boldsymbol{u}_i^R}{\partial x_1} ds \right) \tag{16}$$

where the path integration is in the x_1x_2 plane and is any closed contour on and inside of which Φ exists and which does not enclose cracks; one such path is that designated as C_T in Fig. 1. This integral vanishes if (a) a state of plane strain, plane stress, or antiplane strain exists and (b) $\partial\Phi/\partial x_1 = \partial\Phi/\partial x_3 = 0$ on and inside C_T. According to the second condition, the most general admissible form of Φ is $\Phi = \Phi(\boldsymbol{\epsilon}_{ij}^e, x_2, t)$; dependence of $\boldsymbol{\epsilon}_{ij}^e$ on x_1 is permitted, but any material nonhomogeneity is restricted to variations normal to the local crack plane. Note that $\mathcal{L} = 0$ follows directly from elasticity theory for the continuum within the contour C_T (Rice 1968) since $\mathcal{L}$ is expressed in terms of mechanical state variables for the reference elastic problem and the potential Φ is defined by Eqn. (15); recall that $\boldsymbol{\sigma}_{ij}^R = \boldsymbol{\sigma}_{ij}$ and $\boldsymbol{\epsilon}_{ij}^R = \boldsymbol{\epsilon}_{ij}^e$ according to the correspondence principle.

A generalized J integral, denoted by J_v, is now introduced:

$$J_v = \int_{C_1} \left(\Phi \, dx_2 - \boldsymbol{T}_i \frac{\partial \boldsymbol{u}_i^R}{\partial x_1} ds \right) \tag{17}$$

where C_1 is the portion of C_T indicated in Fig. 1; integration starts at point 1 and is taken counterclockwise to point 2. In contrast to the early elasticity theory (Rice 1968), it is not assumed that the crack faces are traction free, and thus that part of C_1 which is adjacent to the surfaces is retained. (A later study by Palmer and Rice (1973) included body forces and crack surface tractions in analyzing slip surfaces in clay without time dependence.) The condition $\mathcal{L} = 0$ may be written as

$$J_v = J_t \tag{18}$$

where

$$J_t = \int_{C_2} \left(\Phi \, dx_2 - \boldsymbol{T}_i \frac{\partial \boldsymbol{u}_i^R}{\partial x_1} ds \right) \tag{19}$$

and integration starts at point 1 and proceeds counterclockwise along the edge of the failure zone to point 2. The path C_1 for J_v is arbitrary except that it starts and ends at the apparent crack tip (points 1 and 2). It is not necessary to use a contour having segments parallel to the crack faces; but if the tractions $\boldsymbol{T}_i$ vanish on such segments to the left of the failure zone, there is no contribution to J_v (since $dx_2 = \boldsymbol{T}_i = 0$) and therefore C_1 could start and end anywhere along the lower and upper crack faces.

Equation (18) provides a basic relationship between the mechanical state of the continuum through J_v and the characteristics of the failing material at the crack tip through J_t. Given that real stresses and strains (including those at P) are not infinite, in many cases one can neglect the contribution to J_t from the tip segment encircling P and assume the tractions $\boldsymbol{T}_i$ are equal (with opposite signs) across the upper and lower parts of C_2; such simplicity obviously exists if the failure zone is thin (in the x_2 direction) relative to a. Then, Eqn. (19) becomes

$$J_t = \int_0^a \left(\tau_{13} \frac{\partial \Delta u_1^R}{\partial \xi} + \sigma_t \frac{\partial \Delta u_2^R}{\partial \xi} + \tau_{12} \frac{\partial \Delta u_3^R}{\partial \xi} \right) d\xi \tag{20}$$

where σ_t is the normal stress and τ_{12} and τ_{13} are the shearing stresses in the x_1 and x_3 directions, respectively, along the interface between the failure zone and continuum; $\Delta \boldsymbol{u}_i^R$ is the relative displacement vector between initially adjacent material points on the crack plane. The normal stress and displacement and the local coordinate $\xi = a - x_1$ are indicated in Fig. 2.

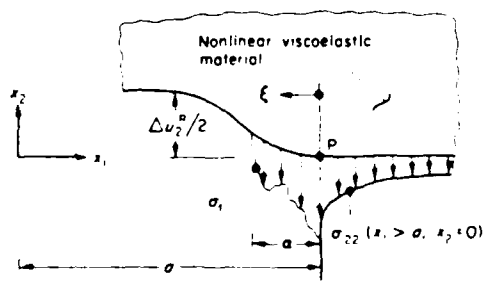

Figure 2
Normal stress and displacement along crack plane

4 Crack Growth

Essential features of equations for predicting the time t_i at which crack growth initiates and subsequent crack propagation speed $\dot{a}$ will be illustrated by assuming a slender failure zone (compare with Eqn. (20)) and the opening mode of crack tip displacement. In this case, sliding displacements along the crack plane are zero in the neighborhood of the tip.

4.1 Initiation of Growth

In order to avoid excessive mathematical complexity in illustrating the prediction of t_i, the failure stress distribution σ_f will be assumed independent of ξ, and denoted by σ_m. Equation (20) becomes $J_f = \sigma_m \Delta u^R_{\xi a}$, where $\Delta u^R_{\xi a}$ is the elastic opening displacement at the fixed location $\xi = a$; the tip P, rather than the apparent tip, may move when $t \leq t_i$ in our crack tip model. Using $J_v = J_f$, the displacement is $\Delta u^R_{\xi a} = J_v/\sigma_m$, and the correspondence principle, Eqn. (13), yields the time-dependent displacement,

$$\Delta u_{2a} = \{D\, d(J_v/\sigma_m)\} \tag{21}$$

where σ_m is not necessarily constant in time. If the criterion for initiation is based on a critical value of opening displacement, Δu_c, it is possible to determine the time at which Δu_{2a} in Eqn. (21) is equal to Δu_c.

An alternative, commonly used criterion is based on mechanical work. In this case, work input from the continuum is equated to work required for failure:

$$\int_0^{t_i} \sigma_{fa} \frac{\partial \Delta u_{2a}}{\partial t}\, dt = 2\Gamma_i \tag{22}$$

where Γ_i is the mechanical work per unit surface area required to break a material column, with cross-sectional area dA, at the left end of the failure zone, designated by the subscript a on the stress and displacement; a factor of 2 is used to account for the two units of surface formed for each unit of cross-sectional area of the column. The so-called fracture initiation energy Γ_i may be affected by the history of Δu_{2a}, depending on the characteristics of the failure zone. For the case in which $\sigma_f = \sigma_m$, Eqn. (22) becomes

$$\int_0^{t_i} \sigma_m [\partial \{D\, d(J_v/\sigma_m)\}/\partial t]\, dt = 2\Gamma_i \tag{23}$$

If σ_m is independent of time and the explicit representation for the hereditary integral is used (compare with Eqn. (8)) then

$$E_R \int_0^{t_i} D(t_i - \tau, t_i) \frac{dJ_v}{d\tau}\, d\tau = 2\Gamma_i \tag{24}$$

For an elastic continuum, where $D = E_R^{-1}$, this equation reduces to $J_v = 2\Gamma_i$; the failure zone may be viscoelastic, and therefore $2\Gamma_i$ is not necessarily constant. If the continuum is a linear or nonlinear viscous material, $D = (t_i E_R)^{-1}(t - \tau)$ where t_i is a time constant, as noted previously. After integrating Eqn. (24) by parts, it becomes

$$(1/t_i) \int_0^{t_i} J_v\, dt = 2\Gamma_i \tag{25}$$

It may be observed that the failure zone length a has not been assumed small in Eqns. (21–25). Also, a generalization of Eqn. (21) is easily obtained if $\sigma_f = \sigma_f(\Delta u^R_\xi, t)$; one finds that a function of J_v and t replaces J_v/σ_m.

4.2 Crack Propagation Speed

The failure criterion based on mechanical work may be written in the form

$$\int_0^a \sigma_f \frac{\partial \Delta u_2}{\partial \xi}\, d\xi = 2\Gamma \tag{26}$$

where the fracture energy Γ, just as Γ_i, is the work required per unit area to rupture a column of material with cross-sectional area dA in the failure zone. In contrast to the initiation problem, this column is not initially at the apparent (free surface) crack tip; instead, the column is initially within or ahead of the current failure zone, and its rupture is coincident with the arrival of the apparent tip. The left side of Eqn. (26) times dA is the total work input to the column, starting with the time the tip P (see Fig. 1) first arrives. For convenience in analyzing continuous growth, the variable of integration has been changed from t (see Eqn. (22)) to ξ, where $\xi = a - x_1$, and the differentiation and integration in Eqn. (26) are made with x_1 held constant. The time-dependent opening displacement at any point in the failure zone is $\Delta u_2 = \{D\, d\Delta u^R_\xi\}$, which is to be substituted into Eqn. (26). The result for predicting $\dot{a}$ is rather complex, even if Δu_2 is used in a critical displacement criterion, because σ_f may depend on ξ or directly on Δu_2 or Δu^R_ξ, and σ_f affects the displacement.

The problem can be greatly simplified if (a) σ_f and Δu^R_ξ for fixed ξ, $\dot{a}$ and a are essentially constant during the time interval $a/\dot{a}$ when the crack propagates a distance a and (b) aging changes in the creep compliance during this same interval are negligible. With these conditions and the observation that the relation between Δu_2 and Δu^R_ξ is the same as for a linear viscoelastic material, an approximate evaluation of the hereditary integral may be used (Schapery 1975 pp. 369–88) to find

$$\Delta u_2 = E_R D(\tilde{t}, t) \Delta u^R_\xi \tag{27}$$

where $\tilde{t} = k\xi/\dot{a}$ and k is a factor which is a very weak function of the slope $n = \partial \log D / \partial \log t$; this factor is practically 1/3 for the entire range of slopes ($0 \leq n \leq 1$) encountered in practice. For a linear viscous body ($n = 1$), $k = 1/3$ exactly if $\xi = a$ and $\sigma_f = \sigma_m$. Equation (27) stems from the smooth cusp-

shaped opening displacement predicted for linear materials and the typically weak dependence of n on $\log t$. Assuming the strains are continuous at the tip P, the behavior of the local displacement in nonlinear media is expected to be close to that for linear prestressed media (Brockway and Schapery 1978) and therefore cusp-shaped. Thus, although more careful study of this behavior is needed for highly nonlinear materials, the cusp shape is expected to exist in many cases, permitting the use of Eqn. (27) and a constant value for k. Substituting Eqn. (27) into Eqn. (26) and using the same type of approximation as in the linear theory (Schapery 1975 pp. 369–88), which does not require σ_t to be spacewise uniform, there results

$$E_R D(k\alpha/\dot{a}, t)\int_0^{\alpha} \sigma_t \frac{\partial \Delta u_\xi^R}{\partial \xi}\, d\xi = 2\Gamma \qquad (28)$$

In view of Eqns. (18) and (20), the integral in Eqn. (28) may be replaced by J_v to derive a very simple result for predicting $\dot{a}$:

$$E_R D(k\alpha/\dot{a}, t)J_v = 2\Gamma \qquad (29)$$

The integration and differentiation in Eqn. (28) are for fixed x_1, while those in Eqn. (20) are for fixed t (i.e., fixed crack tip location); however, for the steady-state propagation assumed during the time $\alpha/\dot{a}$, these integrals are equal. Also, t in the second argument of D accounts for aging in the creep compliance, and the aging is assumed small during the time interval $\alpha/\dot{a}$. In spite of the assumed constancy of $\dot{a}$ and aging during $\alpha/\dot{a}$, they may vary appreciably during the total time of crack propagation. Likewise, the size α is not necessarily constant, as it is related to other variables such as J_v; its prediction is illustrated in Sect. 5 for a nonlinear power law material. Also, it has not been necessary to assume α is small in deriving Eqns. (27) and (29); it is sufficient to assume the change in σ_t and Δu_ξ^R is small due to the change in distance between the crack tip and nearby geometric features (such as another crack tip) during the generic period $\alpha/\dot{a}$.

The similarity of the formulas for initiation, Eqn. (24), and continuous growth, Eqn. (29), is noteworthy. As a special case, suppose J_v is constant for $t > 0$. Then Eqn. (24) reduces to

$$E_R D(t_i, t_i)J_v = 2\Gamma_i \qquad (30)$$

This result and Eqn. (29) yield $t_i = k\alpha/\dot{a}$ if $\Gamma = \Gamma_i$ and aging is negligible. Thus, with $k = 1/3$, the time required for initiation is only one-third of that required for subsequent growth of an amount α. On this basis, it can be expected in some problems that t_i will be negligible compared with the total time required for failure of a structure.

Whether or not Γ equals Γ_i depends on the hereditary and multiaxial stress characteristics of the failure zone, the physical environment (since the left edge, $\xi = \alpha$, is at the surface during $0 < t < t_i$) and on the state of the initial crack tip. In any event, it should not be assumed that these energies are equal without adequate support from experimental data.

4.3 Energy Release Rate

The J_v integral is equal to the energy release rate for self-similar crack growth ($\Delta u_\xi^R = \Delta u_\xi^R(\xi)$ over $0 \le \xi \le \alpha$) in the reference elastic problem, which is a well-known and useful relationship for experimental and theoretical determination of J_v. Namely,

$$J_v = -\partial P_v/\partial A \qquad (31)$$

where dP_v is the change in potential energy of the reference elastic continuum and applied forces, dA is the increase in crack-plane area. This relationship is easily derived by considering the work done by a general three-dimensional elastic continuum on a failure zone which is advanced an amount da along a segment of the crack edge (Schapery 1984).

5. Power Law Nonlinearity

Here, the specific effects of nonlinearity on the opening mode of crack growth are illustrated using a power law nonlinear material. By definition, the pseudo strain energy density in this case for isotropic or anisotropic materials is a homogeneous function of degree $N + 1$,

$$\Phi(c\boldsymbol{\varepsilon}_{ij}^e) = |c|^{N+1}\Phi(\boldsymbol{\varepsilon}_{ij}^e) \qquad (32)$$

where N and c are constants and $|\ |$ denotes absolute value. For notational simplicity, the superscripts e and R will be omitted in succeeding equations until specific results are applied to viscoelastic crack growth analysis. With the definitions

$$\boldsymbol{\varepsilon}_{ij}' \equiv c\boldsymbol{\varepsilon}_{ij}, \quad \Phi' \equiv \Phi(\boldsymbol{\varepsilon}_{ij}'), \quad \operatorname{sgn}(c) \equiv \text{sign of } c \qquad (33)$$

it follows from Eqns. (15) and (32) and application of the chain rule to $\partial\Phi'/\partial\boldsymbol{\varepsilon}_{ij}$ that

$$\frac{\partial \Phi'}{\partial \boldsymbol{\varepsilon}_{ij}'} = \operatorname{sgn}(c)|c|^N \frac{\partial \Phi}{\partial \boldsymbol{\varepsilon}_{ij}}, \qquad \boldsymbol{\sigma}_{ij}' = \operatorname{sgn}(c)|c|^N \boldsymbol{\sigma}_{ij} \qquad (34)$$

For a uniaxial strain state the second relation implies $\sigma_{11} \sim \operatorname{sgn}(\varepsilon_{11})|\varepsilon_{11}|^N$; the same form is predicted for uniaxial stress (Schapery 1981). Equation (32) contains as a special case the power law strain energy function commonly used for isotropic materials (Rice and Rosengren 1968).

Let us introduce a set of dimensionless coordinates and mechanical state variables,

$$\hat{\boldsymbol{x}}_i \equiv \boldsymbol{x}_i/\alpha, \qquad \hat{\boldsymbol{\sigma}}_{ij} \equiv \boldsymbol{\sigma}_{ij}/\sigma_m$$
$$\hat{\boldsymbol{\varepsilon}}_{ij} \equiv \operatorname{sgn}(\sigma_m)\,\sigma_0\,\sigma_m^{1/N}\boldsymbol{\varepsilon}_{ij}$$
$$\hat{\boldsymbol{u}}_i \equiv \operatorname{sgn}(\sigma_m)\,\sigma_0\,\sigma_m^{1/N}\boldsymbol{u}_i/\alpha \qquad (35)$$

The quantities σ_m and σ_0 are parameters with dimensions of stress. They are independent of $\boldsymbol{x}_i$, and are introduced for the purpose of defining a dimen-

sionless failure stress distribution f and strain energy density Φ_N,

$$f \equiv \sigma_i / \sigma_m, \qquad \Phi_N \equiv \Phi / \sigma_0 \tag{36}$$

The parameter σ_0 is assumed to depend at most on aging time. When these definitions are substituted into Eqns. (10), (11) and (15), and Eqn. (34) is used, the field equations become

$$\frac{\partial \dot{\sigma}_{ij}}{\partial \hat{x}_j} = 0, \qquad \dot{\epsilon}_{ij} = \frac{1}{2}\left(\frac{\partial \dot{u}_i}{\partial \hat{x}_j} + \frac{\partial \dot{u}_j}{\partial \hat{x}_i}\right), \qquad \dot{\sigma}_{ij} = \frac{\partial \dot{\Phi}_N}{\partial \dot{\epsilon}_{ij}} \tag{37}$$

where $\dot{\Phi}_N \equiv \Phi_N(\dot{\epsilon}_{ij})$. Allowance is made for negative values of σ_i through the factor σ_m; for unloading of a viscoelastic material this stress could be negative in limited periods of time without crack face contact.

Locating the origin of the coordinates at the crack tip P ($a = 0$ in Fig. 2), and assuming the crack faces are traction free outside of the failure zone, then, with the additional definition $\eta \equiv (\xi - a) \equiv -\hat{x}_1$, the solutions to Eqn. (37) must satisfy the traction boundary condition $\dot{\sigma}_{22} = f(\eta)H(1-\eta)$ for $\eta > 0$ as well as meet the symmetry conditions associated with the opening mode. These solutions will depend at most on the dimensionless coordinates $\hat{x}_i$, apart from parameters in Φ_N and f and those arising from conditions imposed on the continuum surrounding the failure zone. For example, the solution for dimensionless crack-opening displacement is simply $\Delta \dot{u}_2 = g(\eta)$. From Eqn. (35),

$$\Delta u_2 = \mathrm{sgn}(\sigma_m)(a\,\sigma_m\,\sigma_0^{N-1})^{1/N} g(\eta) \tag{38}$$

Equations (18), (20), (35) and (38) yield

$$a = \left|\frac{\sigma_0}{\sigma_m}\right|^{1/N} \frac{J_N}{|\sigma_m| I_f} \tag{39a}$$

where

$$I_f = \int_0^1 f(\eta)\frac{dg}{d\eta}\,d\eta \tag{39b}$$

From Eqns. (38) and (39),

$$\Delta u_2 = (J_N/\sigma_m I_f) g(\eta) \tag{40}$$

The results in Eqns. (38–40) are not limited to a small-scale failure zone and are valid for materials which age and are physically nonhomogeneous with respect to x_2; the dependence of Φ on x_2 and t and related material parameters has been suppressed to simplify the notation. The dimensionless displacement g, stress f and integral I_f could in general depend on all dimensionless parameters that influence continuum deformation in the neighborhood of the crack tip. Considerable simplification in this dependency results if the continuum is physically homogeneous (at least locally) and if a is small relative to the distance to other geometrical features. The immediate continuum surrounding the crack tip neighborhood can then be analyzed by using a method similar to that in Rice and Rosengren (1968) for an isotropic power law material. With a polar coordinate system (r, θ) centered at P (compare with Fig. 2) it is found that for $r \gg a$,

$$\begin{aligned} \dot{u}_i &= \dot{r}(I_f/\dot{r})^{1/(N+1)} h_i(\theta) \\ \dot{\epsilon}_{ij} &= (I_f/\dot{r})^{1/(N+1)} f(\theta) \\ \dot{\sigma}_{ij} &= (I_f/\dot{r})^{N/(N+1)} g_{ij}(\theta) \end{aligned} \tag{41}$$

where $\dot{r} = r/a$. The integral I_f is related to J_N through Eqn. (39a), and the functions of θ are determined from the solution of Eqn. (37) and the condition of traction-free crack surfaces for $\dot{r} > 0$. The failure zone traction on the crack plane is neglected in solving this boundary value problem; its effect enters the solution in the form of I_f after path independence of J_N is taken into account through Eqn. (39a) (which is based on Eqns. (18) and (20)). The dependence of Eqn. (41) solutions on r is the same as found by Rice and Rosengren (1968), but the θ dependence is not necessarily the same because the strain energy density used here is more general. Such detailed information is not needed in this study; rather, it is sufficient to know that the entire influence of external loads and other far-field parameters and geometry (such as other cracks) on the dimensionless mechanical state variables in Eqn. (35) in the neighborhood of the crack tip is accounted for by I_f.

With the small-scale failure zone, given the shape function $f(\eta)$ for the failure stress distribution and not using Eqn. (39b), it may be concluded that the predicted shape function $g(\eta)$ for the crack-opening displacement can depend at most on I_f, N and aging time t. Equation (39b) is thus an implicit relationship for predicting I_f. The significance of Eqn. (39b) may be clarified by imagining an analysis in which external loading is increased from zero by using increasing values of I_f in Eqn. (41), but not using Eqn. (39b), until infinite stresses and strains at P are removed. For the linear problem, $N = 1$, it can be verified that the removal occurs when I_f is equal to the integral in Eqn. (39b); with this value for I_f, Eqn. (39a) becomes identical to a dimensionless form of the Barenblatt (1962) condition for finite crack tip stress after the familiar relationship

$$J_N = (1 - \nu^2)K_I^2/E_R \tag{42}$$

is employed (where K_I is the opening-mode stress-intensity factor, E_R is Young's modulus and ν is Poisson's ratio). Recall that Eqn. (39) comes from Eqns. (18) and (19) (through the special case of Eqn. (20)) in which the portion of the contour C_2 around the tip P vanishes on account of the physical requirement of finite stresses and strains. Thus, it appears that Eqn. (18), in which Eqn. (20) is used for J_i, can be interpreted as a generalization of Barenblatt's condition to nonlinear, anisotropic, viscoelastic media with an arbitrarily large failure zone. For such a general situation, these equations may not

guarantee that the crack faces do not overlap, and thus additional analysis involving contact phenomena could be needed.

It has been shown that I_1 is a constant when $f = f(\eta)$, except for possible aging. It should be clear that this is true even when f depends also on the displacement shape function g. In this latter case one must solve simultaneously for f, g and I_1 using the dimensionless equations.

5.1 Crack Growth

The analysis in this section has so far been limited to a study of the reference elastic problem. With the addition of the superscript R to strains and displacements, they may be used with the results in Sect. 4. Equations (23) and (24) for fracture initiation were derived assuming σ_f does not vary with ξ, represented here by $f = 1$ since $\sigma_m = \sigma_f$. In this case the equations for initiation time t_i are very simple and are not limited to a small-scale failure zone. If $df/d\eta \neq 0$ it is helpful to use the results for a power law material to predict t_i. From Eqns. (40) and (14) we obtain the pseudo and viscoelastic displacements (with $g(1) = 1$),

$$\Delta u_2^R = J_s g_1 / \sigma_m I_1, \qquad \Delta u_{2a} = \{D\, d\Delta u_2^R\} \quad (43)$$

Crack initiation can be defined as σ_y at $\xi = a$ without loss of generality of the analysis. If aging is negligible, the solution in Eqn. (22) reduces to Eqn. (23) except I_1 is modified by the constant factor $I_1 g_1$.

Equation (24) for crack speed depends on the size of the failure zone. This size, now assumed small, for a power law material is given by Eqn. (39a). Consider the physical significance of this result. First, σ_m may be interpreted as a yield stress of the continuum when N is small, using $\Phi = \sigma/\Phi_y$ together with Eqn. (32) and one-dimensional or proportional loading through a stress σ, then $\varepsilon \sim \sigma^N$; hence the strain is small when $\sigma \ll \sigma_m$ and large when $\sigma \sim \sigma_m$ if $N \ll 1$. Also, σ_m may be considered the intrinsic strength if it is taken to be the maximum value (with respect to location ξ) of the failure zone stress during crack growth. Thus, the size a in Eqn. (39a) increases with increasing yield stress and is sensitive to the ratio of yield stress to intrinsic strength, given J_s. In elastoplastic fracture mechanics it is common practice to assume σ_m is proportional to the yield stress and $f = 1$; in this case, the standard result $a \sim J_s/\sigma_y$ is recovered since I_1 is a constant. More generally, σ_m may vary with a (and other parameters) so that a J_s is not necessarily constant.

The results so far have been expressed in terms of material functions for the failure zone, σ_f and Γ. These quantities may depend on a and other variables such as temperature and moisture, especially if the zone is viscoelastic. One could explicitly incorporate specific physical models of the failure zone in order to complete the formulation of the theory. Assuming the failure process for material elements on the crack plane is unaffected by stresses prior to the arrival or near arrival of the crack tip, such an analysis for a small-scale failure zone would yield a function $a = a(J_s)$, with possible dependence on physical parameters and material constants such as temperature, age and nonlinear exponent N; that the instantaneous J_s (but not past values) determines the instantaneous $\dot{a}$ follows from the fact that the crack tip neighborhood is surrounded by a stress field which is defined solely by the current value of J_s (i.e., Eqn. (41) but in terms of the dimensional physical variables), assuming J_s changes slowly enough that a is essentially constant during the failure time, $a \dot{a}$. Thus, when the dependence of $\dot{a}$ on basic material parameters is not of direct interest, one could characterize fracture behavior with the function $\dot{a} = a(J_s)$ found directly from experimental data. If theoretical investigations indicate a range exists for which $da/dJ_s < 0$, unstable crack growth (possibly in steps of stop–start behavior) may result and the intrinsic $\dot{a} - J_s$ function for slow, continuous growth could not be found experimentally. Indeed, for this case an appropriate analysis may involve initiation and dynamic arrest phenomena.

5.2 Power Law Viscoelasticity

The creep compliance for viscoelastic materials can often be expressed as a power law in time. Thus, as an important special case, consider nonaging material behavior for which $D(t - \tau) = D_1(t - \tau)^n$ (where D_1 and n are positive constants) in order to predict the form of the equation $\dot{a} = \dot{a}(J_s)$ using certain specified failure zone characteristics. A small-scale failure zone with a shape factor $f \equiv \sigma_f/\sigma_m$ that depends at most on ξ and $\eta = \xi - a$ is assumed. In general, σ_m and Γ may depend on crack speed and other parameters. If, however, σ_m and Γ are constant (so that this zone exhibits elastic-like behavior) Eqns. (29) and (39a) yield

$$\dot{a} \sim J_s^p \quad (44)$$

where $p = 1 + (1/n)$. If a (instead of σ_m) and Γ are constant, Eqn. (29) predicts $p = 1/n$. The failure zone dimensions are defined by a and crack-opening displacement Δu_2 at $\xi = a$; if these two quantities are constant, one may use Eqn. (39a) to solve for σ_m, and then use Eqn. (27) for Δu_2 and Eqn. (40) for Δu_2^R at $\eta \equiv \xi - a = 1$ to find that $p = [n(1 + N)]^{-1}$. Notice that only in this last case does the nonlinearity exponent appear in the equation for p.

Experimentally determined values of p, when compared with the results for these and other cases, may be helpful in determining failure zone characteristics and guiding theoretical model development. The values of $p = 3$ and $n = 0.5$ were obtained from experimental data on a globally linear elastomer; this is consistent with the assumption of constant Γ and

σ_∞ (Schapery 1975, pp. 549–62). Some studies of crack growth in metals undergoing secondary creep (i.e., $n = 1$) provide values of $p = 1$ (Landes and Begley 1976; Nikbin et al. 1976); since $N \ll 1$ typically, the data are consistent with the last two cases for constant values of Γ and a or Δu_{2_0} and a. It should be added that the exponent N used here pertains to nonlinear behavior of the continuum in the neighborhood of the crack tip. The relationships are valid even if nonlinearity of material far from the tip (relative to a) does not obey a power law, or is linear (i.e., $N = 1$) while its local behavior is described using $N \neq 1$. The remote nonlinear behavior does not affect the $\dot{a} - J_v$ equation, but it does affect the functional dependence of J_v on the externally applied loads.

6. *Conclusions*

Through the use of a nonlinear single-integral constitutive equation, generalized J-integral theory and certain approximations, relatively simple crack growth equations based on mechanical work for time of initiation, Eqns. (23) and (24), and speed, Eqn. (29) were derived. Only the opening mode of growth has been analyzed in detail here, but the basic relationships in Sects. 1–3 could be used for shearing and mixed-mode conditions. Rheological properties of the continuum are reflected in the creep compliance D and the generalized integral J_v. The length a of the zone of failing material at the crack tip appears in the equation for speed, and it provides a scale which determines, in effect, the magnitude of local strain rates resulting from crack growth. In general a is not constant; instead, it is related to J_v through Eqns. (18) and (20), which reduce to Eqn. (34) with power law nonlinearity.

All of these results come from an analysis of the continuum in the vicinity of the crack tip. Thus, for limited crack growth it is not necessary for the entire body to be represented by Eqn. (1) and the local creep compliance D. However, if it is, Eqn. (31) may be employed to predict J_v with an arbitrary amount of crack growth by using theoretical and experimental methods similar to those already developed for time-independent materials. In this expression P_v and J_v are defined just as for elastic materials, but displacements and strains are pseudo quantities, $u_i^R = \{E\, du_i\}$ and $\epsilon_{ij}^R = \epsilon_{ij}^e = \{E\, d\epsilon_{ij}\}$, respectively. Stresses and loads are the actual physical quantities. For example, experimentally measured displacements u_i would be converted to pseudo displacements u_i^R through Eqn. (8) before evaluating J_v from test data. The coefficient E_R is a free constant, and could be taken as the modulus or reciprocal of compliance at some specified time.

The bibliography includes publications which describe various models for characterizing and predicting crack growth in different types of materials. Several models are special cases of the general theory presented here. For secondary creep (i.e., nonlinear viscous behavior), experimental data on crack speed have been successfully correlated in terms of a C^* parameter by many investigators (e.g., Landes and Begley 1976); the function $\dot{a} = \dot{a}(C^*)$ typically obeys a power law. This characterization, whether or not the power law is obeyed, is obtained from the present theory by using the relaxation modulus $E = E_R\delta(t - \tau)$ in Eqn. (8), which reduces the pseudo variables to strain rates ($\epsilon_{ij}^R = \dot{\epsilon}_{ij}$) and velocities ($u_i^R = \dot{u}_i$); in turn, J_v becomes C^*. The use here of nonsingular strains at the crack tip, in contrast to earlier work on secondary creep, leads to a simple physical interpretation of J_v for viscous media. Specifically, from Eqn. (29) with $k = 1/3$ and $D = E_R^{-1}(t - \tau)$, corresponding to the aforestated modulus, we find $J_v = 3(2\Gamma\dot{a}/a) = 3 \times$ (mechanical power input to the failure zone per unit area). For viscoelastic materials J_v has a simple physical meaning if the continuum is essentially elastic except for a small amount of material around the crack tip. In this case J_v is approximately the energy release rate, $-\partial P_v/\partial A$, since $u_i^R \simeq u_i$; also, $\Gamma/E_R D$ in Eqn. (29) may be properly called an effective fracture energy.

Crack growth in homogeneous linear viscoelastic media has been characterized traditionally in terms of stress-intensity factors because of the many situations in which viscoelastic stresses are the same as in elastic materials. With isotropy, linearity, a constant Poisson's ratio, homogeneity and locally plane strain, it is found that Eqn. (41) (after expressing it in terms of the stress-intensity factor) and Eqn. (39a) yield Eqn. (42). Substitution of Eqn. (42) into Eqns. (24) and (29) results in the same crack growth relations derived earlier (Schapery 1975). Similar results in terms of stress-intensity factors for linear behavior exist without the restrictions of constant Poisson's ratio, isotropy and homogeneity (Brockway and Schapery 1978; Schapery 1975, 1978). This observation includes cracks between dissimilar media (i.e., adhesive fracture) if both materials are incompressible or one is relatively rigid and the other is incompressible; without the incompressible behavior, tensile and shearing stresses act simultaneously on the crack plane, and a complex mixed-mode condition generally exists at the crack tip. The nonlinear theory in Sect. 4 is applicable to adhesive fracture if the mixed-mode state does not exist and D is the same for both materials (or one is relatively rigid); Γ_i and Γ in Eqns. (24) and (29) obviously have to be interpreted as the fracture energies for the particular material combinations involved.

Primary creep of metals and ceramics is customarily represented by using a nonlinear power law model of viscous flow with strain hardening. When crack growth exists this behavior is not described by Eqn. (1), and the correspondence principle, Eqn. (13), does not apply. However, with proportional loading and a stationary crack, the strain-hardening

constitutive equation becomes identical to that of a nonlinear, aging elastic body (e.g., Riedel 1981). Equation (1) takes the appropriate form by using $E_R D = h(t)$. A suitable choice of $h(t)$ and a power law potential $\Phi(\varepsilon_{ij}^e)$, where the only time dependence is through $\varepsilon_{ij}^e = \varepsilon_{ij}/h$, yields the desired primary creep behavior as well as a singular stress field parameter C_k^* (Riedel 1981) which is identical to J_k. For a small-scale failure zone, the early stages of crack growth are determined by the stress field surrounding a stationary crack tip and therefore by J_k. However, a theory does not appear to be available for relating crack growth to a single parameter when the amount of growth becomes comparable to the scale of the initial singular stress field.

It should be observed that a different type of primary creep, such as that used to characterize polymers, is contained in Eqn (1) through the dependence of creep compliance D on $t - \tau$. Also, through the use of aging time in $\Phi = \Phi(\varepsilon_{ij}^e, t)$, one may characterize different types of nonlinear behavior at short and long times even though the creep compliance itself is not a function of stress. Thus, in spite of the apparent simplicity of Eqn. (1) compared with other available nonlinear viscoelastic constitutive equations, it is really quite general and yet permits the use of the correspondence principle with large amounts of crack growth. Nevertheless, the accuracy of Eqn (1) for many materials under various stress histories *is not yet established*.

The deformation and fracture analysis has been formulated assuming small strains and rotations for the continuum. This restriction is needed because the correspondence principle is not generally valid with nonlinear strain–displacement relations. An approximate theory with large deformations is described by Schapery (1984). Another possible complication not explicitly treated here is crack tip heating, which can be very significant in polymers because of their typically low thermal conductivity and high ultimate strains. If this heating is sufficiently localized, it could be included in the characteristics of the failure zone, and thus not complicate the continuum analysis.

The idealization of a slender failure zone is quite realistic for crack tips in many materials, as well as for craze tips in plastics. In considering the zone shape and size, it should be recalled that only the part of the body which does not obey Eqn. (15) has to be included in the failure zone. In some cases it is helpful to represent part of the failing material (such as craze) as a surface loading, consequently accounting for it in J_k. As a further generalization it is shown by Schapery (1984) that important aspects of the theory remain valid even if distributed damage, such as microcracks, is included in the mathematical model of the continuum.

Considerable progress has been made in the last twenty years in understanding effects of time-dependent rheological properties on crack growth. However, most basic experimental and theoretical investigations have been for the opening mode of cohesive fracture in essentially homogeneous materials. In this same time period, use of fiber-reinforced materials, especially plastics, in load-bearing structures has increased dramatically. Thus, considering the complex interactions which may occur at various scales and the importance of interfaces in fibrous lamina and laminates and in other multiphase materials, there is an especially important need for more basic studies on mixed-mode crack growth, adhesive cracking and the effect of nonhomogeneous time-dependent properties on all types of crack growth.

See also Time-Dependent Fracture: Mechanisms; Mechanics of Materials: An Overview.

Acknowledgement

This work was sponsored by the US Air Force Office of Scientific Research, Office of Aerospace Research.

Bibliography

Andrews E H 1974 A generalized theory of fracture mechanics. *J. Mater. Sci.* 9: 887–94

Barenblatt G I 1962 The mathematical theory of equilibrium cracks in brittle fracture. *Adv. Appl. Mech.* 7: 55–129

Brockway G S, Schapery R A 1978 Some viscoelastic crack growth relations for orthotropic and prestrained media. *Eng. Fract. Mech.* 10: 453–68

Christensen R M 1982 *Theory of Viscoelasticity: An Introduction*. 2nd edn. Academic Press, New York

Evans A G 1982 The high temperature failure of ceramics. In: Wilshire B, Owen D R J (eds.) 1982 *Recent Advances in Creep and Fracture of Engineering Materials and Structures*. Pineridge Press, Swansea, pp. 53–133

Findley W N 1981 Creep of 2618 aluminum under sidesteps of tension and torsion and stress reversal predicted by a viscous-viscoelastic model. *J. Appl. Mech.* 48: 47–54

Greenwood J A, Johnson K L 1981 The mechanics of adhesion of viscoelastic solids. *Philos. Mag. A* 43: 697–711

Kaminskii A A 1981 Investigations in the field of the mechanics of the fracture of viscoelastic bodies. *Sov. Appl. Mech.* 16: 741–59

Kinloch A J, Young R J 1983 *Fracture Behavior of Polymers*. Applied Science, Barking, UK

Lake G J 1983 Aspects of fatigue and fracture of rubber. *Prog. Rubber Technol.* 45: 89–143

Landes J D, Begley J A 1976 A fracture mechanics approach to creep crack growth. In: Rice J R, Paris P C (eds.) 1976 *Mechanics of Crack Growth*. ASTM STP 590. American Society for Testing and Materials, Philadelphia, Pennsylvania, pp. 128–48

Leckie F A, Hayhurst D R 1974 Creep rupture of structures. *Proc. R. Soc. London, Ser. A* 340: 323–47

McCartney L N 1982 On the energy balance approach to fracture in creeping materials. *Int. J. Fract. Mechan.* 19: 99–113

McClintock F. A., Bassani J. L. 1981 Problems in environmentally affected creep crack growth. In: Nemat-Nasser S. (ed.) 1981 *Three-Dimensional Constitutive Relations and Ductile Fracture*. North-Holland, Amsterdam. pp. 123–45

Morland L. W., Spring U. 1982 Single integral representations for nonlinear viscoelastic solids. *Mech. Mater.* 1: 161–70

Nikbin K. M., Webster G. A., Turner C. E. 1976 Relevance of nonlinear fracture mechanics to creep cracking. In: Swedlow J. L., Williams M. L. (eds.) 1976 *Cracks and Fracture*. ASTM STP 601. American Society for Testing and Materials, Philadelphia, Pennsylvania. pp. 47–62

Palmer A. C., Rice J. R. 1973 The growth of slip surfaces in the progressive failure of over-consolidated clay. *Proc. R. Soc. London, Ser. A* 332: 527–48

Passaglia E. 1982 Relaxation of stresses in crazes at crack tips and rate of craze extension. *Polymer* 23: 754–60

Ponter A. R. S., Hayhurst D. R. (eds.) 1981 *Creep in Structures*. Springer, Berlin

Rice J. R. 1968 A path independent integral and the approximate analysis of strain concentration by notches and cracks. *J. Appl. Mech.* 35: 379–86

Rice J. R., Rosengren G. F. 1968 Plane strain deformation near a crack tip in a power-law hardening material. *J. Mech. Phys. Solids* 16: 1–12

Riedel H. 1981 Creep deformation at crack tips in elastic-viscoplastic solids. *J. Mech. Phys. Solids* 29: 35–49

Riedel H. 1983 Crack-tip stress fields and crack growth under creep-fatigue conditions. In: Gudas J. P., Shih C. F. (eds.) 1983 *Elastic-plastic Fracture: Second Symposium. Volume I—Inelastic Crack Analysis*. ASTM STP 803. American Society for Testing and Materials, Philadelphia, Pennsylvania. pp. 505–20

Schapery R. A. 1975 A theory of crack initiation and growth in viscoelastic media. *Int. J. Fract. Mechan.* 11: 141–59, 369–88, 549–62

Schapery R. A. 1978 A method for predicting crack growth in nonhomogeneous viscoelastic media. *Int. J. Fract. Mechan.* 14: 293–309

Schapery R. A. 1981 On viscoelastic deformation and failure behavior of composite materials with distributed flaws. In: Wang S. S., Renton W. J. (eds.) 1981 *Advances in Aerospace Structures and Materials*. American Society of Mechanical Engineers, New York. pp. 5–20

Schapery R. A. 1984 Correspondence principles and a generalized *J* integral for large deformation and fracture analysis of viscoelastic media. *Int. J. Fract. Mechan.* 25: 195–223

Williams J. G. 1984 *Fracture Mechanics of Polymers*. Wiley, New York

R. A. Schapery

Time-Dependent Fracture: Mechanisms

Fracture of solids is accomplished by the formation and growth of cracks under stress. In purely elastic bodies the impending propagation of a crack is associated with a "system" instability in which ever larger amounts of elastic strain energy are released by a growing crack than is required to produce the surfaces of the cracks. Under usual conditions of applied stresses that are only a small fraction of the cohesive strength, this condition is met at such large crack levels of the cracked system that thermal motion cannot play a significant role in softening the response. Hence the only rate-dependent fractures in elastic systems at low temperatures are of the stress-corrosion cracking or static fatigue type, where slow crack growth under subcritical conditions becomes possible by rate processes of crack tip corrosion or contamination. These types of crack growth are discussed elsewhere (see *Stress Corrosion Cracking; Subcritical Crack Growth in Ceramics*).

The time-dependent fractures considered here are those which involve time-dependent quasi-homogeneous damage accumulation under stress in microscopically inhomogeneously stressed and/or homogeneously deforming solids. [illegible] not contain initial cracks or [illegible] subcritical size, the microstructural [illegible] accumulation of damage—first [illegible] more concentrated around sites of previous damage or at tips of subcritical cracks. The final and also usually time dependent growth of the cracks often takes comparatively little time. In most of these processes the time dependence largely resides in the deformation processes which chronologically order the microprocesses that build up the microstress concentrations, even in the presence of other similar processes that try to dissipate these same stress concentrations. Only rarely does the time dependence reside in true processes of decohesion on the molecular scale. The phases of the time-dependent fracture that involves crack growth in a creeping solid are dealt with elsewhere (see *Time-Dependent Fracture: Continuum Aspects of Crack Growth*).

1. Forms of Damage

1.1 Rupture versus Damage

A bar in tension, as shown in Fig. 1, capable of undergoing time-dependent deformation in steady state under a constant stress at high temperature will rupture as a result of gradually accelerating deformation when under a constant applied load as the area continuously decreases. If the steady state strain rate $\dot{\varepsilon}$ is a power function of tensile stress σ, in the form $\dot{\varepsilon} = B(T)(\sigma/\sigma_0)^m$, where $B(T)$, σ_0 and m are material parameters, the time to complete rupture is

$$t_r = 1/m\dot{\varepsilon}_i \qquad (1)$$

where $\dot{\varepsilon}_i (= B(T)(\sigma_i/\sigma_0)^m)$ is the initial creep strain rate. As Fig. 2 shows for two typical cases of $m = 5$ and $m = 8$ for engineering alloys, the acceleration of creep in the final stages is extremely rapid.

In the majority of cases where steady-state deformation is attainable only after a primary creep transient, the overall extension of the bar is somewhat

PH.D. DISSERTATION

Finite Element Analysis of Crack Growth in Inelastic Media

by

Joe Randall Weatherby

Mechanical Engineering, May 1986.

Co-Chairmen of Advisory Committee: Dr. R.A. Schapery
Dr. W.L. Bradley

ABSTRACT

In most materials, macrocrack extension is accompanied by inelastic phenomena (such as microcracking or plastic deformation) throughout a region surrounding the crack tip. Immediately ahead of the crack tip, strain localization occurs in a small volume of heavily damaged material referred to as the failure zone or fracture process zone. In this study, the failure zone and the surrounding zone of inelastic material are treated as two distinct regions. The failure zone is assumed to be thin relative to its length and is represented in a two-dimensional finite element model as tractions which act across the crack faces near the tip. An opening mode of crack tip deformation is assumed. The normal traction at any point on the crack surface in the failure zone is specified as a decreasing function of the crack opening displacement which vanishes after a critical value of displacement is reached. Two different rate-independent, inelastic continuum characterizations are used; one models metal plasticity and another represents microcracking in brittle materials. Both constitutive models allow for the definition of a generalized J-integral developed by Schapery, which has the same value for most paths around the crack tip for realistic distributions of plasticity or damage in the material surrounding a stationary or propagating

crack. This path independence is verified numerically for a crack growing under conditions of small-scale inelasticity, and the equivalence between J and the work input to the last ligament of material in the failure zone is demonstrated. Steady-state crack growth is stuided in two different specimen geometries. Simplified J integral analyses are used to estimate the work input to the failure zone for these steady-state problems. The J integral estimations are compared with finite element results to determine the accuracy of the simplified analyses.

PH.D. DISSERTATION

Techniques for Characterizing Damage Zones in Composite Materials

by

Richard Dale Tonda

Interdisciplinary Engineering, August 1987

ABSTRACT

Experimental methods for determining the existence of a work potential, useful in characterizing material response even in the presence of significant damage, are developed and described. The underlying fracture theory and motivation for the development is briefly discussed. The theory involving the work potential and the existence and use of a damage parameter is reviewed, as is the basic composite laminate theory and underlying constitutive formulation. An experimental program which addresses these factors through the biaxial loading of composite tubes is presented. The results are analyzed, incorporating viscoelasticity theory for power law time dependence of the matrix material, and it is demonstrated that the theory provides a less complicated presentation of the data by eliminating the superimposed effects of time dependent behavior.

PH.D. DISSERTATION

Finite Element Analysis of Crack Growth in Inelastic Media

by

Joe Randall Weatherby

Mechanical Engineering, May 1986.

Co-Chairmen of Advisory Committee: Dr. R.A. Schapery
Dr. W.L. Bradley

ABSTRACT

In most materials, macrocrack extension is accompanied by inelastic phenomena (such as microcracking or plastic deformation) throughout a region surrounding the crack tip. Immediately ahead of the crack tip, strain localization occurs in a small volume of heavily damaged material referred to as the failure zone or fracture process zone. In this study, the failure zone and the surrounding zone of inelastic material are treated as two distinct regions. The failure zone is assumed to be thin relative to its length and is represented in a two-dimensional finite element model as tractions which act across the crack faces near the tip. An opening mode of crack tip deformation is assumed. The normal traction at any point on the crack surface in the failure zone is specified as a decreasing function of the crack opening displacement which vanishes after a critical value of displacement is reached. Two different rate-independent, inelastic continuum characterizations are used; one models metal plasticity and another represents microcracking in brittle materials. Both constitutive models allow for the definition of a generalized J-integral developed by Schapery, which has the same value for most paths around the crack tip for realistic distributions of plasticity or damage in the material surrounding a stationary or propagating

crack. This path independence is verified numerically for a crack growing under conditions of small-scale inelasticity, and the equivalence between J and the work input to the last ligament of material in the failure zone is demonstrated. Steady-state crack growth is stuided in two different specimen geometries. Simplified J integral analyses are used to estimate the work input to the failure zone for these steady-state problems. The J integral estimations are compared with finite element results to determine the accuracy of the simplified analyses.

PH.D. DISSERTATION

Techniques for Characterizing Damage Zones in Composite Materials

by

Richard Dale Tonda

Interdisciplinary Engineering, August 1987

ABSTRACT

Experimental methods for determining the existence of a work potential, useful in characterizing material response even in the presence of significant damage, are developed and described. The underlying fracture theory and motivation for the development is briefly discussed. The theory involving the work potential and the existence and use of a damage parameter is reviewed, as is the basic composite laminate theory and underlying constitutive formulation. An experimental program which addresses these factors through the biaxial loading of composite tubes is presented. The results are analyzed, incorporating viscoelasticity theory for power law time dependence of the matrix material, and it is demonstrated that the theory provides a less complicated presentation of the data by eliminating the superimposed effects of time dependent behavior.

END

DATE

3-88

DTIC